FACULTY OF SCIENCES

• DEPARTMENT OF PHYSICS AND ASTRONOMY

Elastic and inelastic neutrino-nucleus scattering in the low energy regime

Natalie Jachowicz, K. Niewczas, A. Nikolakopoulos, V. Pandey, P. Vancraeyveld, N. Van Dessel, K. Vantournhout

GHENT UNIVERSITY

Neutrinos .....

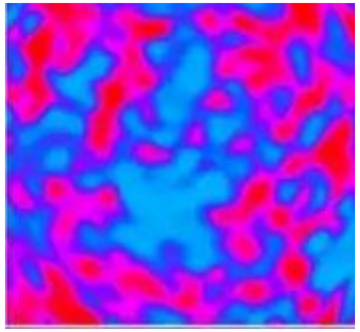

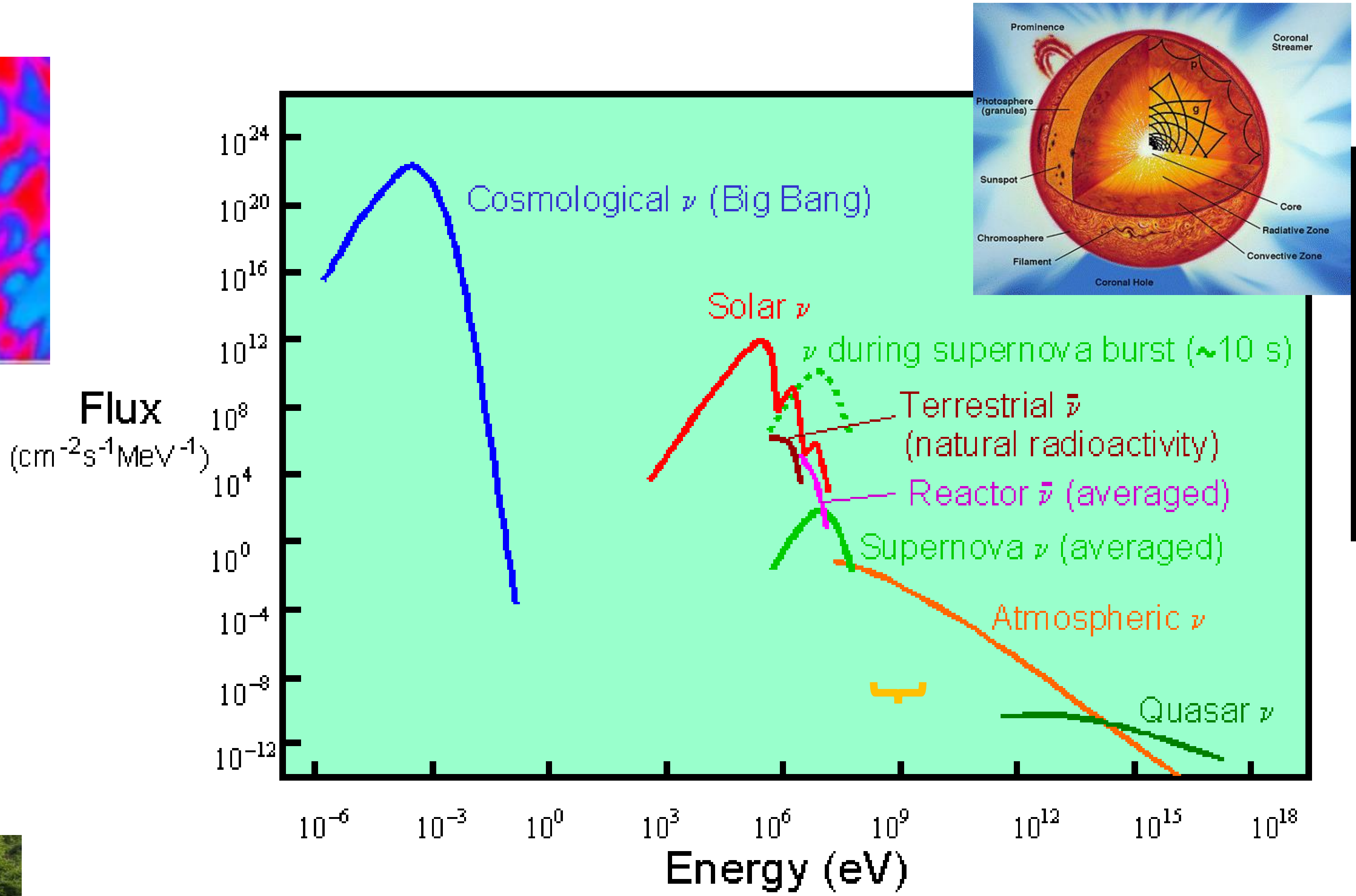

Flux on earth of neutrinos from various sources, in function of energy

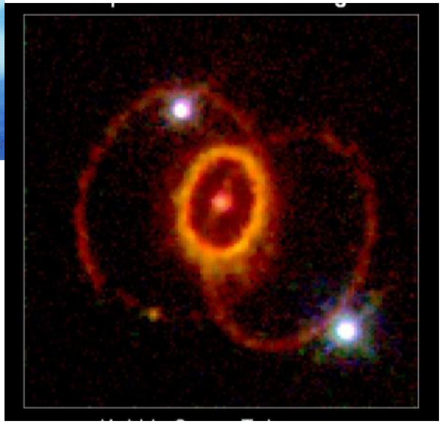

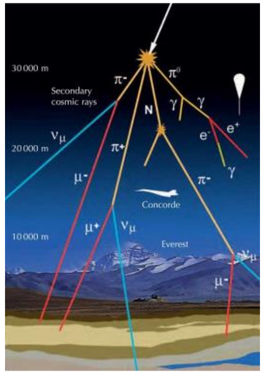

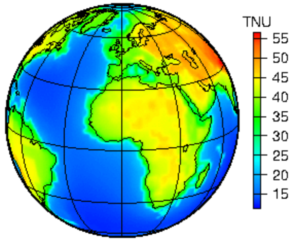

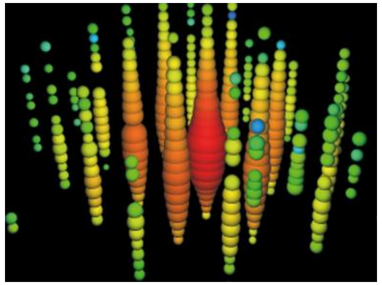

Neutrinos .....

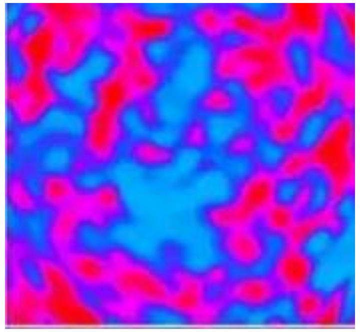

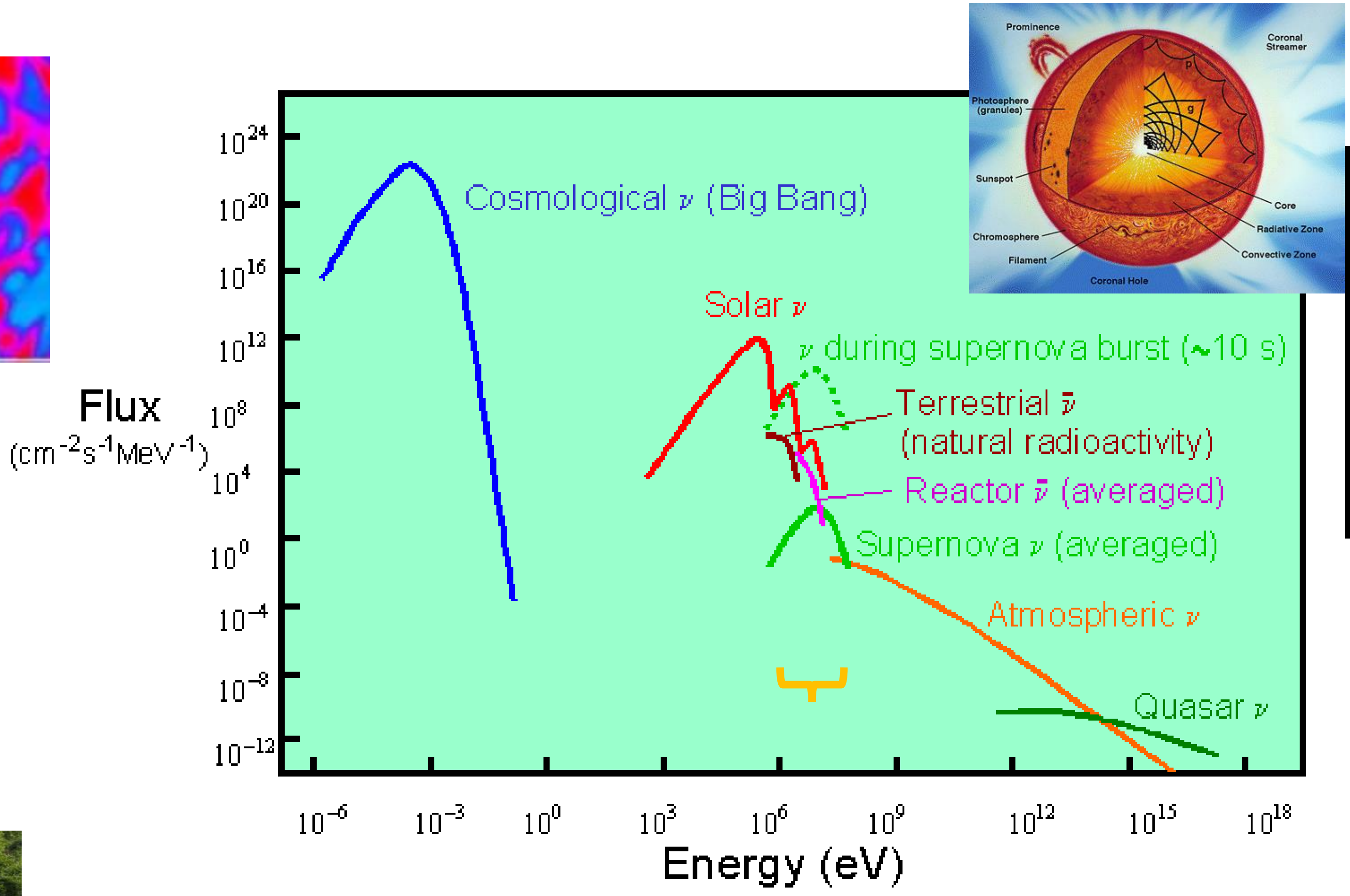

Flux on earth of neutrinos from various sources, in function of energy

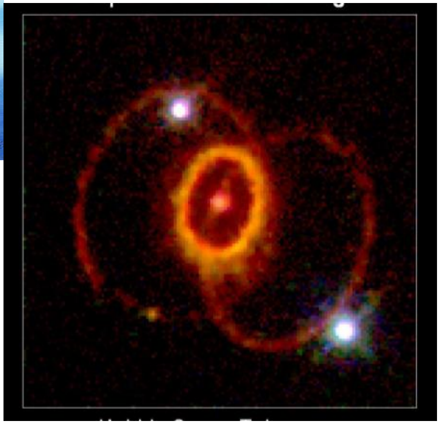

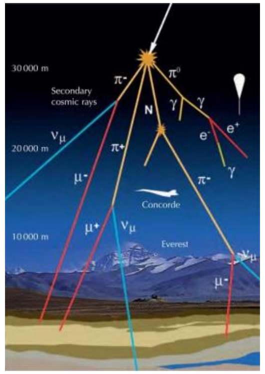

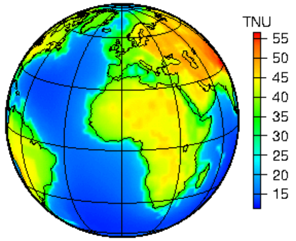

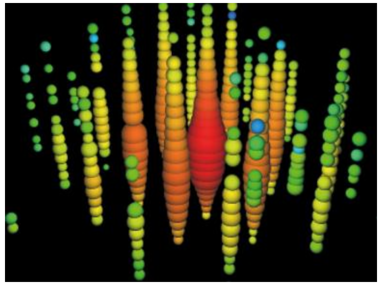

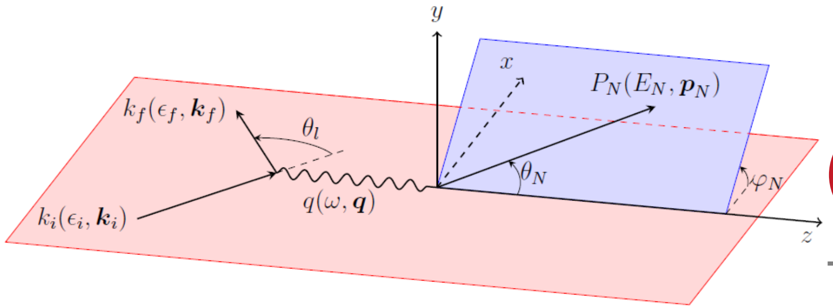

CEvNS

multinucleon mechanisms and 2-nucleon knockout processes in the dip region

Low-energy processes

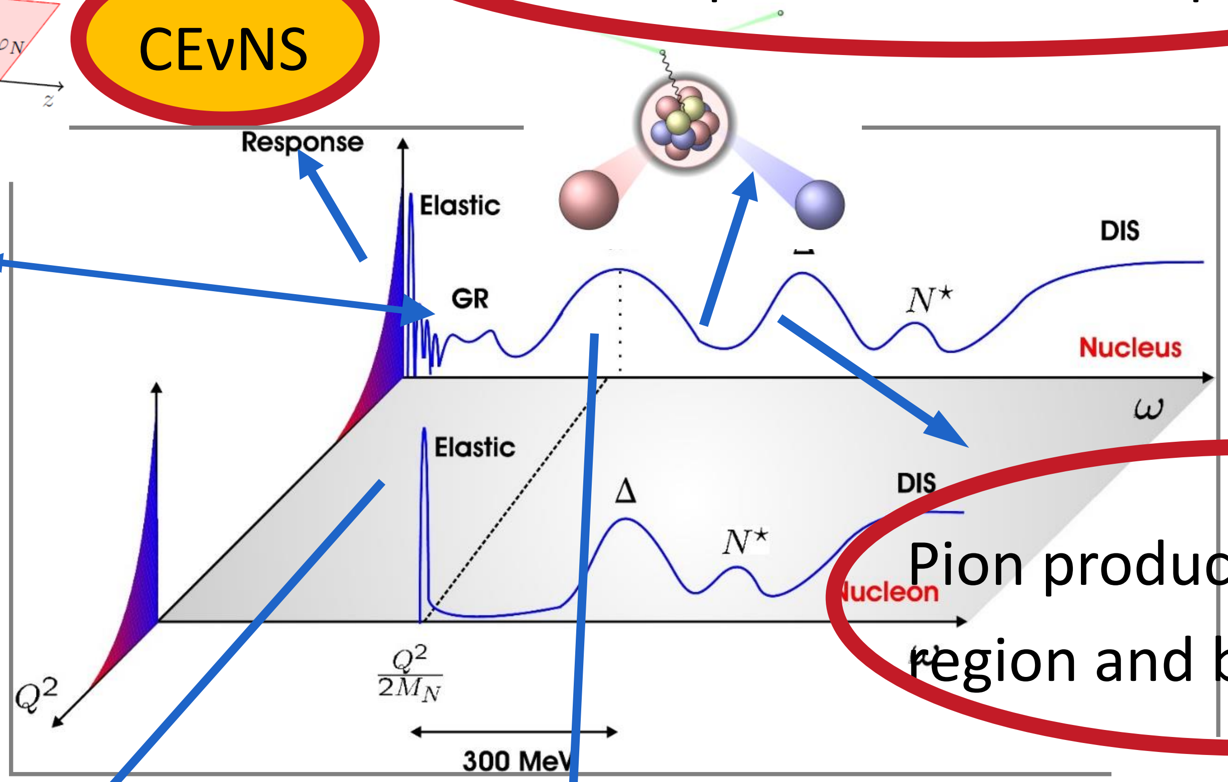

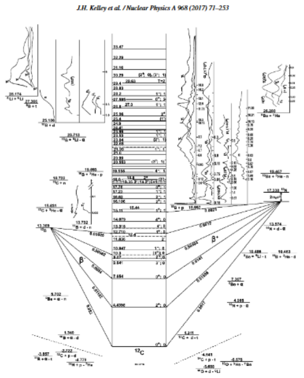

Pion production in the delta region and beyond

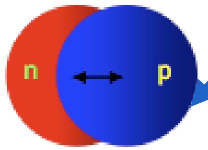

Quasi-elastic processes

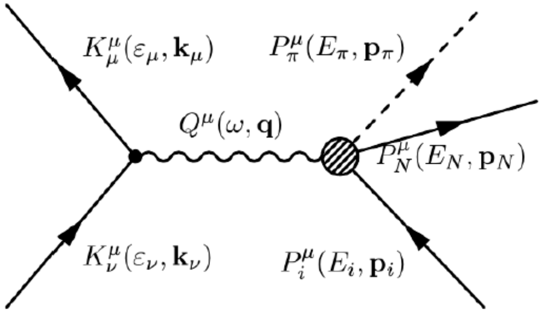

Low energy collective excitations

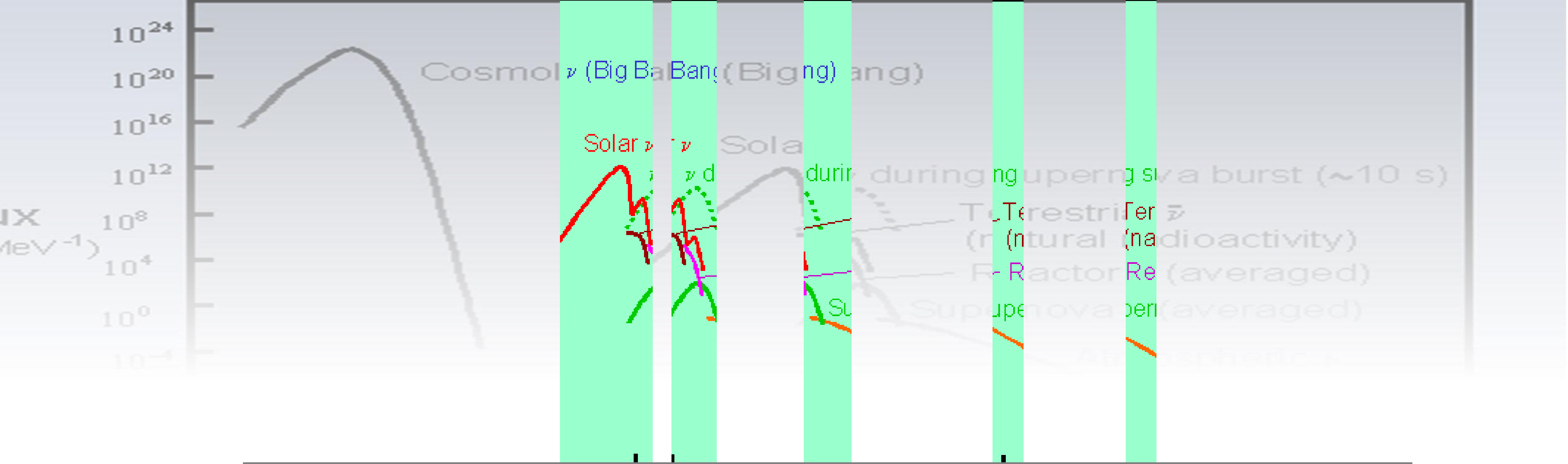

10^{24}
10^{20}
10^{16}
10^{12}
10^{8}
10^{4}
10^{0}
Solar ν
Reactor
Terrestrial ν̄
(natural radioactivity)
(averaged)
during a supernova burst (~10 s)

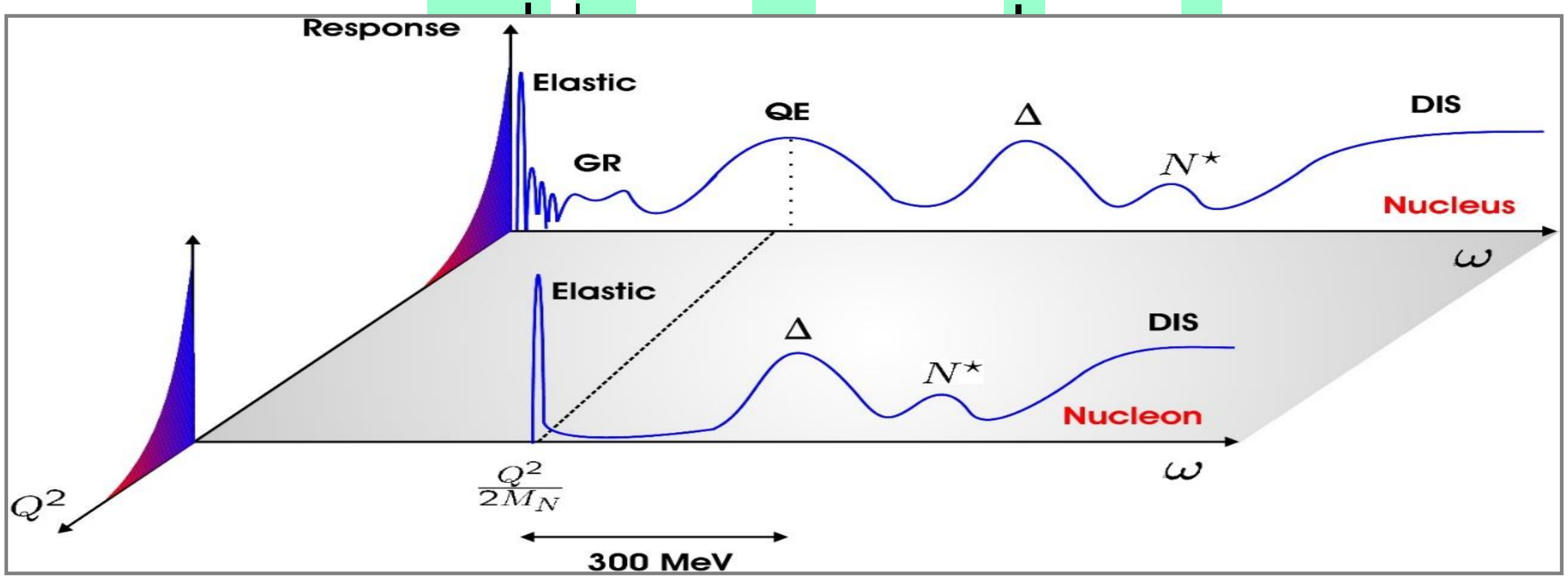

Response
Elastic
GR
QE
Δ
$N^{\star}$
DIS
Nucleus
ω
Elastic
Δ
$N^{\star}$
DIS
Nucleon
ω
Q^2
$\frac{Q^2}{2M_N}$
300 MeV

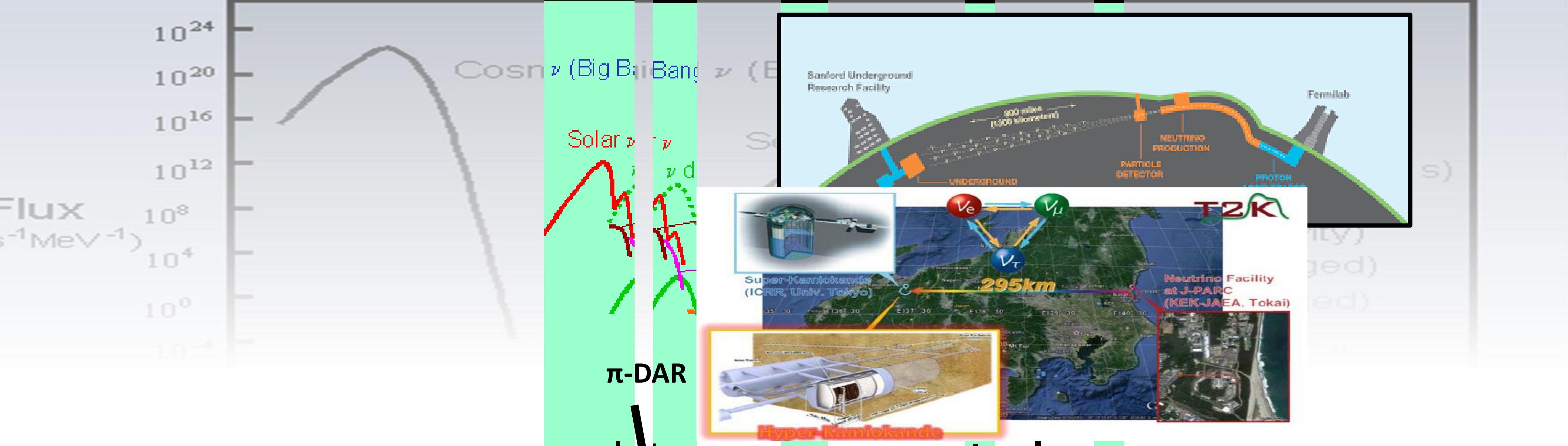
Flux
Solar ν
Sanford Underground Research Facility
Fermilab
NEUTRINO PRODUCTION
PARTICLE DETECTOR
UNDERGROUND
PROTON ACCELERATOR
T2K
295km
Super-Kamiokande (ICRR, Univ. Tokyo)
Neutrino Facility at J-PARC (KEK-JAEA, Tokai)
Hyper-Kamiokande

π-DAR

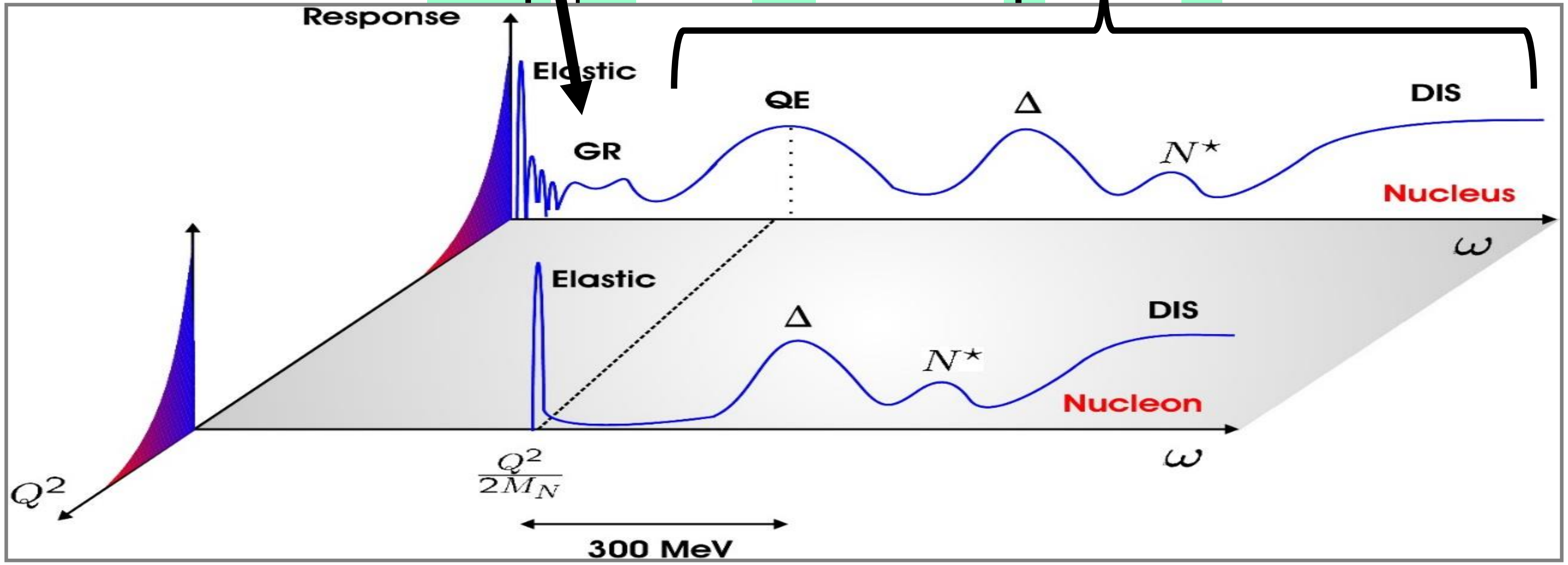
Response
Elastic
GR
QE
Δ
$N^\star$
DIS
Nucleus
ω
Elastic
Δ
$N^\star$
DIS
Nucleon
ω
Q^2
$\frac{Q^2}{2M_N}$
300 MeV

Neutrinos .....

What can we learn from low energy neutrinos ?

- Nuclear structure information
- Electroweak tests
- Neutrino oscillations
- Astrophysical neutrinos : a.o. core-collapse supernovae
- Neutrinonucleosynthesis
- BSM physics

How can we learn from these neutrinos ?

- Study their interactions : theory + experiment
- Detect them
  - Neutrino-electron scattering
  - Neutrino-hadron scattering

Neutrinos .....

Neutrino-hadron scattering ?

- little experimental data is available
  - small cross sections
  - (almost) no monochromatic neutrino beams

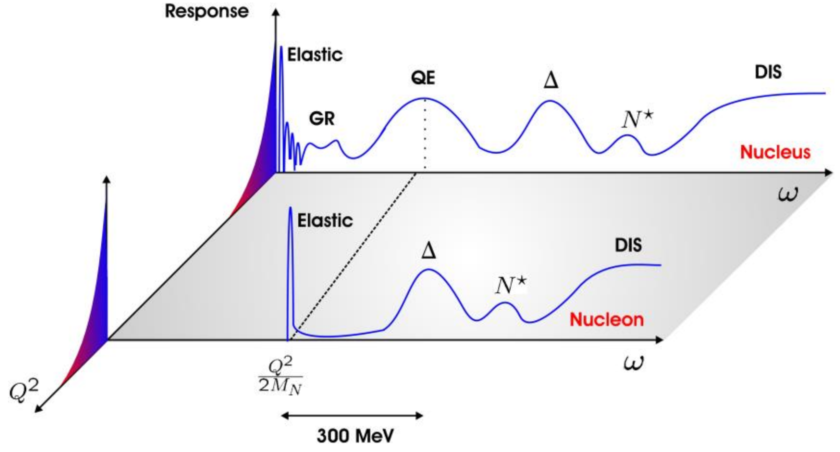

Uncertainties :

- one has to rely on theoretical predictions,
- uncertainties induced by model dependence
- and more fundamental uncertainties …

	$B(GT^-)$
HF+CRPA	8.8
GXPF1J	9.5
DD–ME2	11.3
SGII	12.3
SLy5	14.0
Exp.	9.9 ± 2.5

TABLE II. The total ^{56}Fe $B(GT^-)$ strength, tabulated for various models from Ref. [36].

^{208}Pb

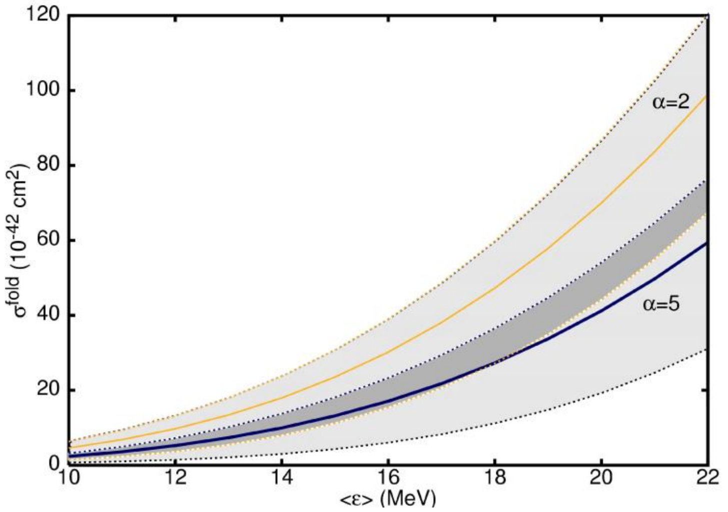

N.J. et al, PRC66, 065501 (2002) ;
E. Kolbe et al, PRC63, 025802 (2001) ;
J. Engel et al, PRD67, 013005 (2001)

	$\langle\sigma_{DAR}\rangle$ (10^{-42}cm^2)
HF+CRPA	212.9
G–Matrix QRPA [35]	173.5
Phenomenological [47]	214
Hybrid [29]	240
Hybrid [36]	259
RHB+RQRPA [36]	263
LFG+RPA [38]	277
QRPA [64]	352
Exp. (KARMEN) [30]	$256 \pm 108 \pm 43$

TABLE I. The total charged–current (ν_e, ^{56}Fe) cross section value, folded with a DAR electron neutrino spectrum, tabulated for various models.

Neutrinos .....

Neutrino-hadron scattering ?

- little experimental data is available
  - small cross sections
  - (almost) no monochromatic neutrino beams

Uncertainties :

- one has to rely on theoretical predictions,
- uncertainties induced by model dependenc
- and more fundamental uncertainties …

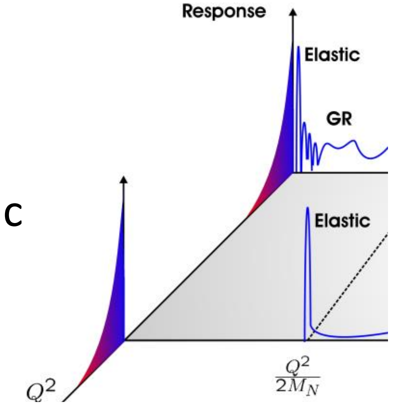

Coherent Collaboration, arXiv2212.11295

Measurement of ^{nat}Pb(ν_e,Xn) production with a stopped-pion neutrino source

smearing in arrival time. The inferred NIN rate is $> 4\sigma$ lower than expectations from the MARLEY prediction.

Channel	Cross section ($\times 10^{-40}$cm^2)
^{208}Pb(ν_e, X)	42.1
^{208}Pb($\nu_e, e^- + n$)^{207}Bi	31.6
^{208}Pb($\nu_e, e^- + 2n$)^{206}Bi	7.7
^{208}Pb($\nu_e, e^- + 3n$)^{205}Bi	0.4

Coherent Collaboration, arXiv2305.19594

Measurement of the inclusive electron-neutrino charged-current cr with the COHERENT NaIνE detector

Conclusion: COHERENT has measured the inclusive ν_eCC-^{127}I cross section on ^{127}I between 10 and 55 MeV to be $(9.2^{+2.1}_{-1.8}) \times 10^{-40}$ cm^2. This measurement is roughly 41% of the nominal cross section from MARLEY. To date, this is the heaviest nucleus to have its inelastic neu-

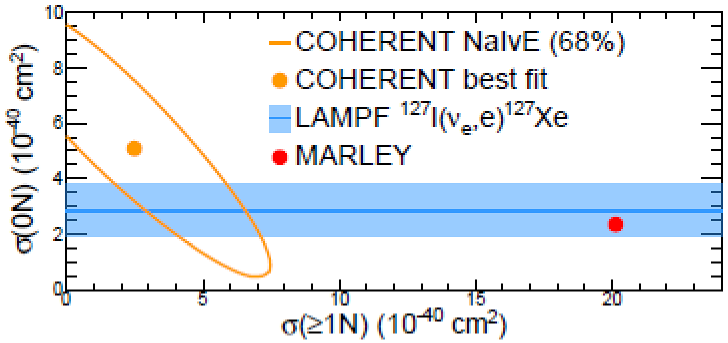

FIG. 6. Measurement (1σ) of the ν_eCC-^{127}I cross section separated into $0n$ and $\geq 1n$ channels compared to the MARLEY prediction and Ref. [12], measuring the $0n$ cross section.

-current cross sections for neutrinos with MARLEY om reference [32]. Inter- produce a final-state neu- ν_e,X) value. For lead of dances, imposing $N - Z$ -averaged cross section of

Modeling low-energy inelastic neutrino-nucleus scattering

$$\frac{d^2\sigma}{d\Omega\, d\omega} = (2\pi)^4\, k_f \varepsilon_f \sum_{s_f, s_i} \frac{1}{2J_i + 1} \sum_{M_f, M_i} \left| \left\langle f \left| \widehat{H}_W \right| i \right\rangle \right|^2$$

$$\widehat{H}_W = \frac{G}{\sqrt{2}} \int d\vec{x}\, \hat{J}_{\mu,lepton}(\vec{x})\, \hat{J}^{\mu,hadron}(\vec{x})$$

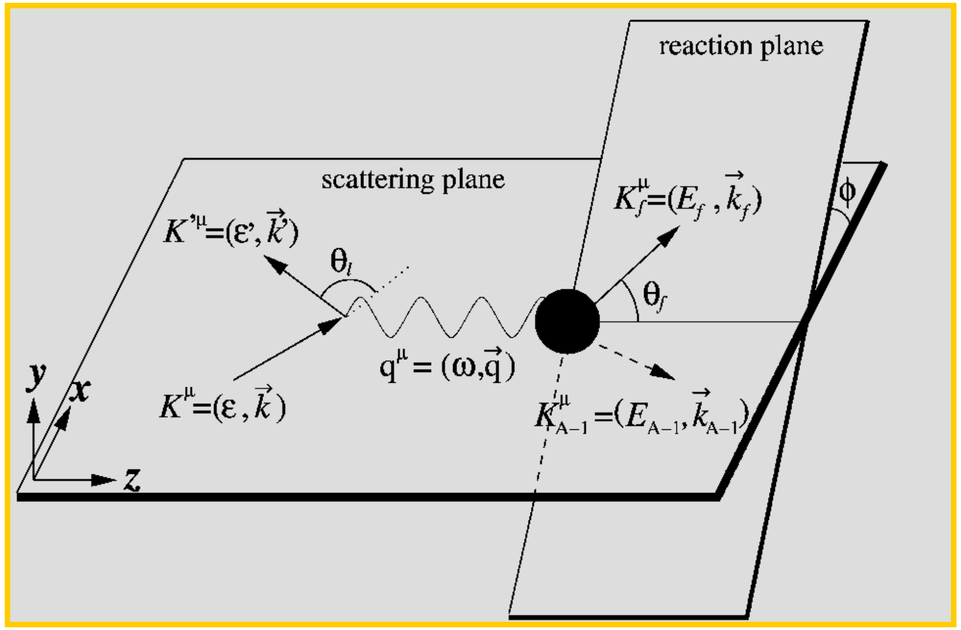

Hadron current

$$J^{\mu} = F_1(Q^2)\gamma^{\mu} + i\frac{\kappa}{2M_N}F_2(Q^2)\sigma^{\mu\nu}q_{\nu} + G_A(Q^2)\gamma^{\mu}\gamma_5 + \frac{1}{2M_N}G_P(Q^2)q^{\mu}\gamma_5$$

Lepton tensor

$$l_{\alpha\beta} \equiv \overline{\sum_{s,s'}}[\overline{u}_l\gamma_{\alpha}(1-\gamma_5)u_l]^{\dagger}[\overline{u}_{\nu}\gamma_{\beta}(1-\gamma_5)u_{\nu}]$$

Neutrino-nucleus cross sections

$$\vec{J}_V^{\alpha}(\vec{x}) = \vec{J}^{\alpha}_{convection}(\vec{x}) + \vec{J}^{\alpha}_{magnetization}(\vec{x})$$

with
$$\vec{J}_c^{\alpha}(\vec{x}) = \frac{1}{2Mi}\sum_{i=1}^{A} G_E^{i,\alpha}\left[\delta(\vec{x}-\vec{x}_i)\overrightarrow{\nabla}_i - \overleftarrow{\nabla}_i\,\delta(\vec{x}-\vec{x}_i)\right],$$

$$\vec{J}_m^{\alpha}(\vec{x}) = \frac{1}{2M}\sum_{i=1}^{A} G_M^{i,\alpha}\,\overrightarrow{\nabla}\times\vec{\sigma}_i\,\delta(\vec{x}-\vec{x}_i),$$

$$\vec{J}_A^{\alpha}(\vec{x}) = \sum_{i=1}^{A} G_A^{i,\alpha}\,\vec{\sigma}_i\,\delta(\vec{x}-\vec{x}_i),$$

$$J_V^{0,\alpha}(\vec{x}) = \rho_V^{\alpha}(\vec{x}) = \sum_{i=1}^{A} G_E^{i,\alpha}\,\delta(\vec{x}-\vec{x}_i),$$

$$J_A^{0,\alpha}(\vec{x}) = \rho_A^{\alpha}(\vec{x}) = \frac{1}{2Mi}\sum_{i=1}^{A} G_A^{i,\alpha}\,\vec{\sigma}_i\cdot\left[\delta(\vec{x}-\vec{x}_i)\overrightarrow{\nabla}_i - \overleftarrow{\nabla}_i\,\delta(\vec{x}-\vec{x}_i)\right]$$

$$J_P^{0,\alpha}(\vec{x}) = \rho_P^{\alpha}(\vec{x}) = \frac{m_\mu}{2M}\sum_{i=1}^{A} G_P^{i,\alpha}\,\vec{\nabla}\cdot\vec{\sigma}_i\,\delta(\vec{x}-\vec{x}_i)$$

for NC reactions

$$G_E^{V,o} = \left(\frac{1}{2}-\sin^2\theta_W\right)\tau_3 - \sin^2\theta_W,$$

$$G_M^{V,o} = \left(\frac{1}{2}-\sin^2\theta_W\right)(\mu_p-\mu_n)\,\tau_3 - \sin^2\theta_W\,(\mu_p+\mu_n)$$

$$G^{A,0} = g_a\,\frac{\tau_3}{2} = -\,\frac{1.262}{2}\,\tau_3$$

for CC reactions

$$G_E^{V,\pm} = \tau_\pm$$

$$G_M^{V,\pm} = (\mu_p-\mu_n)\,\tau_\pm$$

$$G^{A,\pm} = g_a\,\tau_\pm = -1.262\,\tau_\pm$$

$G = (1+Q^2/M^2)^{-2}$ Q^2 dependence : dipole or BBBA parametrization :

Neutrino-nucleus cross sections

$$\left(\frac{d^2\sigma}{d\omega d\Omega}\right)_\nu = \frac{G_F^2\ \cos^2\theta_c}{(4\pi)^2}\left(\frac{2}{2J_i+1}\right)\varepsilon_f\kappa_f\ \ \zeta^2\left(Z',\varepsilon_f,|q|\right)\left[\sum_{J=0}^{\infty}\sigma_{CL,\nu}^J+\sum_{J=1}^{\infty}\sigma_{T,\nu}^J\right]$$

$$\sigma_{CL,\nu}^J = \left[v_\nu^{\mathcal{M}}R_\nu^{\mathcal{M}}+v_\nu^{\mathcal{L}}R_\nu^{\mathcal{L}}+\ 2\,v_\nu^{\mathcal{ML}}R_\nu^{\mathcal{ML}}\right],$$

$$\sigma_{T,\nu}^J = \left[v_\nu^{T}R_\nu^{T}\pm 2\,v_\nu^{TT}R_\nu^{TT}\right],$$

Neutrino-nucleus cross sections

$$\left(\frac{d^2\sigma}{d\omega d\Omega}\right)_\nu = \frac{G_F^2 \cos^2\theta_c}{(4\pi)^2}\left(\frac{2}{2J_i+1}\right)\varepsilon_f\kappa\ \zeta^2(Z',\varepsilon_f,|q|)\left[\sum_{J=0}^{\infty}\sigma_{CL,\nu}^J+\sum_{J=1}^{\infty}\sigma_{T,\nu}^J\right]$$

$$v_\nu^{\mathcal{M}} = \left[1+\frac{\kappa_f}{\varepsilon_f}\cos\theta\right],$$

$$v_\nu^{\mathcal{L}} = \left[1+\frac{\kappa_f}{\varepsilon_f}\cos\theta-\frac{2\varepsilon_i\varepsilon_f}{|\vec{q}|^2}\left(\frac{\kappa_f}{\varepsilon_f}\right)^2\sin^2\theta\right],$$

$$v_\nu^{\mathcal{ML}} = \left[\frac{\omega}{|\vec{q}|}\left(1+\frac{\kappa_f}{\varepsilon_f}\cos\theta\right)+\frac{m_l^2}{\varepsilon_f|\vec{q}|}\right],$$

$$v_\nu^{T} = \left[1-\frac{\kappa_f}{\varepsilon_f}\cos\theta+\frac{\varepsilon_i\varepsilon_f}{|\vec{q}|^2}\left(\frac{\kappa_f}{\varepsilon_f}\right)^2\sin^2\theta\right],$$

$$v_\nu^{TT} = \left[\frac{\varepsilon_i+\varepsilon_f}{|\vec{q}|}\left(1-\frac{\kappa_f}{\varepsilon_f}\cos\theta\right)-\frac{m_l^2}{\varepsilon_f|\vec{q}|}\right],$$

$$[v_\nu^{\mathcal{M}}R_\nu^{\mathcal{M}}+v_\nu^{\mathcal{L}}R_\nu^{\mathcal{L}}$$

$$= [v_\nu^T R_\nu^T \pm 2$$

$$R_\nu^{\mathcal{M}} = |\langle J_f||\widehat{\mathcal{M}}_J^\nu(|\vec{q}|)||J_i\rangle|^2,$$

$$R_\nu^{\mathcal{L}} = |\langle J_f||\widehat{\mathcal{L}}_J^\nu(|\vec{q}|)||J_i\rangle|^2,$$

$$R_\nu^{\mathcal{ML}} = \mathcal{R}\left[\langle J_f||\widehat{\mathcal{L}}_J^\nu(|\vec{q}|)||J_i\rangle\langle J_f||\widehat{\mathcal{M}}_J^\nu(|\vec{q}|)||J_i\rangle^*\right],$$

$$R_\nu^{T} = \left[|\langle J_f||\widehat{\mathcal{J}}_J^{mag,\nu}(|\vec{q}|)||J_i\rangle|^2+|\langle J_f||\widehat{\mathcal{J}}_J^{el,\nu}(|\vec{q}|)||J_i\rangle|^2\right],$$

$$R_\nu^{TT} = \mathcal{R}\left[\langle J_f||\widehat{\mathcal{J}}_J^{mag,\nu}(|\vec{q}|)||J_i\rangle\langle J_f||\widehat{\mathcal{J}}_J^{el,\nu}(|\vec{q}|)||J_i\rangle^*\right].$$

Neutrino-nucleus cross sections

$$\widehat{\mathcal{M}}_{JM}(\kappa) = \int d\vec{x}\ \left[j_J\ (\kappa r)\ Y_J^M\ (\Omega_x)\right]\ \hat{J}_0(\vec{x})\quad ,$$

$$\widehat{\mathcal{L}}_{JM}(\kappa) = \frac{i}{\kappa}\ \int d\vec{x}\ \left[\vec{\nabla}\left(j_J\ (\kappa r)\ Y_J^M\ (\Omega_x)\right)\right]\ \cdot\ \widehat{\vec{J}}(\vec{x})\quad ,$$

$$\widehat{\mathcal{J}}_{JM}^{el}(\kappa) = \frac{1}{\kappa}\ \int d\vec{x}\ \left[\vec{\nabla}\ \times\ \left(j_J\ (\kappa r)\ \vec{\mathcal{Y}}_{J,J}^M\ (\Omega_x)\right)\right]\ \cdot\ \widehat{\vec{J}}(\vec{x})\quad ,$$

$$\widehat{\mathcal{J}}_{JM}^{mag}(\kappa) = \int d\vec{x}\ \left[j_J\ (\kappa r)\ \vec{\mathcal{Y}}_{J,J}^M\ (\Omega_x)\right]\ \cdot\ \widehat{\vec{J}}(\vec{x})\quad .$$

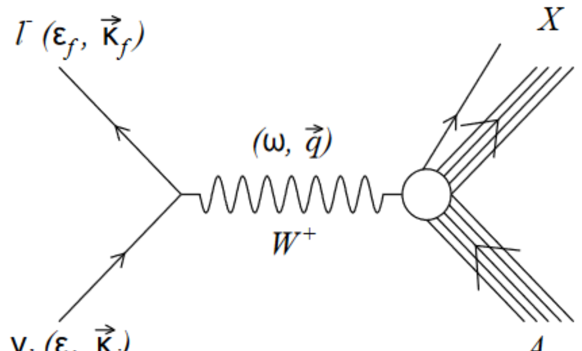

(b)

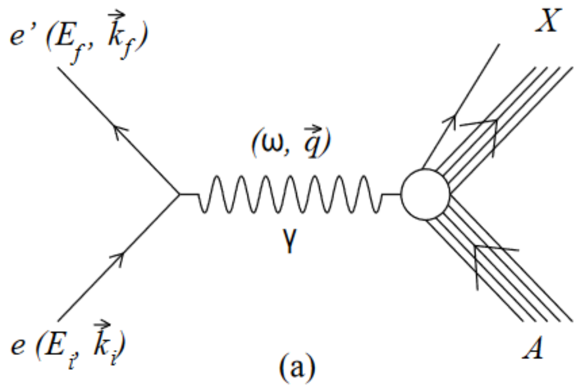

(a)

Neutrino-nucleus cross sections

$$\widehat{\mathcal{M}}_{JM}(\kappa) = \int d\vec{x} \; [j_J\,(\kappa r)\; Y_J^M\;(\Omega_x)]\;\; \hat{J}_0(\vec{x}) \;\;,$$

$$\widehat{\mathcal{L}}_{JM}(\kappa) = \frac{i}{\kappa}\; \int d\vec{x}\; \left[\vec{\nabla}\left(j_J\,(\kappa r)\; Y_J^M\;(\Omega_x)\right)\right] \;\cdot\; \widehat{\vec{J}}(\vec{x}) \;\;,$$

$$\widehat{\mathcal{J}}^{el}_{JM}(\kappa) = \frac{1}{\kappa}\; \int d\vec{x}\; \left[\vec{\nabla} \;\times\; \left(j_J\,(\kappa r)\; \vec{\mathcal{Y}}^M_{J,J}\;(\Omega_x)\right)\right] \;\cdot\; \widehat{\vec{J}}(\vec{x}) \;\;,$$

$$\widehat{\mathcal{J}}^{mag}_{JM}(\kappa) = \int d\vec{x}\; \left[j_J\,(\kappa r)\; \vec{\mathcal{Y}}^M_{J,J}\;(\Omega_x)\right] \;\cdot\; \widehat{\vec{J}}(\vec{x}) \;\;.$$

$$\langle a||\widehat{\mathcal{M}}^{Coul}_J\,[\widehat{\rho}_V]\,||b\rangle = G_E(Q^2) \int \mathrm{d}r\; \langle a||\tau_\pm j_J(qr) Y_J(\Omega_1)||b\rangle_r$$

$$\langle a||\widehat{\mathcal{M}}^{Coul}_J\,[\widehat{\rho}_A]\,||b\rangle = \frac{G_A(Q^2)}{2m_N i} \int \mathrm{d}r\; \langle a||\tau_\pm j_J(qr) Y_J(\Omega_1)\,\boldsymbol{\sigma}_1 \cdot \left(\overrightarrow{\boldsymbol{\nabla}}_1 - \overleftarrow{\boldsymbol{\nabla}}_1\right)||b\rangle_r$$

$$\langle a||\widehat{\mathcal{O}}^\lambda_J\left[\widehat{J}_{conv}\right]||b\rangle = \frac{G_E(Q^2)}{2m_N i} \int \mathrm{d}r\; \langle a||\tau_\pm j_{J+\lambda}(qr) \times \left[Y_{J+\lambda}(\Omega_1) \otimes \left(\overrightarrow{\boldsymbol{\nabla}}_1 - \overleftarrow{\boldsymbol{\nabla}}_1\right)\right]_J ||b\rangle_r$$

$$\langle a||\widehat{\mathcal{O}}^\lambda_J\left[\widehat{J}_{magn}\right]||b\rangle = i\sqrt{6}q\frac{G_M(Q^2)}{2m_N} \int \mathrm{d}r \sum_{\eta=\pm 1} \sqrt{J+\lambda+\delta_{\eta,+1}} \times \begin{Bmatrix} J & J+\lambda & 1 \\ 1 & 1 & J+\lambda+\eta \end{Bmatrix} \times \langle a||\tau_\pm j_{J+\lambda+\eta}(qr)\left[Y_{J+\lambda+\eta}(\Omega_1)\otimes\boldsymbol{\sigma}_1\right]_J ||b\rangle_r$$

$$\langle a||\widehat{\mathcal{O}}^\lambda_J\left[\widehat{J}_A\right]||b\rangle = G_A(Q^2) \int \mathrm{d}r\; \langle a||\tau_\pm j_{J+\lambda}(qr)\left[Y_{J+\lambda}(\Omega_1)\otimes\boldsymbol{\sigma}_1\right]_J ||b\rangle_r$$

A model for the nucleus

- Nuclear radius $\approx 1.2A^{\frac{1}{3}}$ fm
- Nucleon is a diffuse system
  - Hard core (repulsion) ≈ 0.5 fm
  - RMS charge radius from (e,e') $= 0.897(18)$ fm
- $0.07 \lesssim \text{NPF} \lesssim 0.42$
  - closest packing fraction of spheres ≈ 0.74
  - packing fraction of Argon liquid ≈ 0.032
  - packing fraction of Argon gas $\approx 3.75 \cdot 10^{-5}$
- The nuclear medium is a rather **dense quantum liquid**

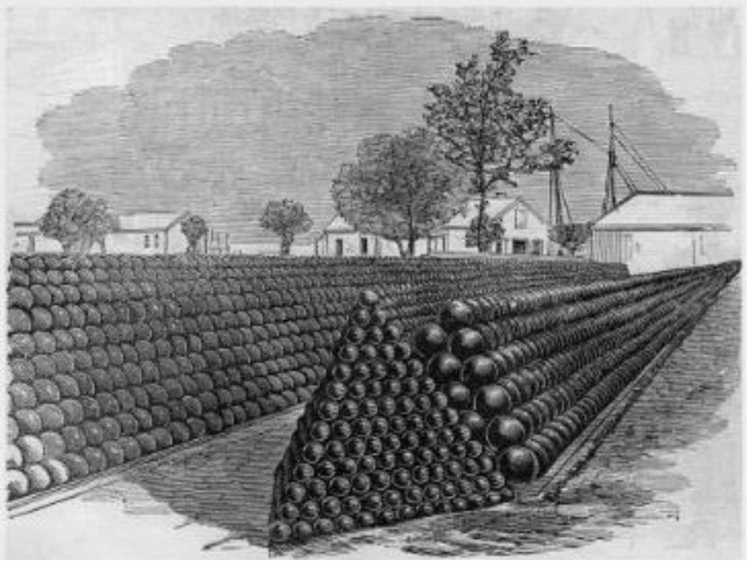

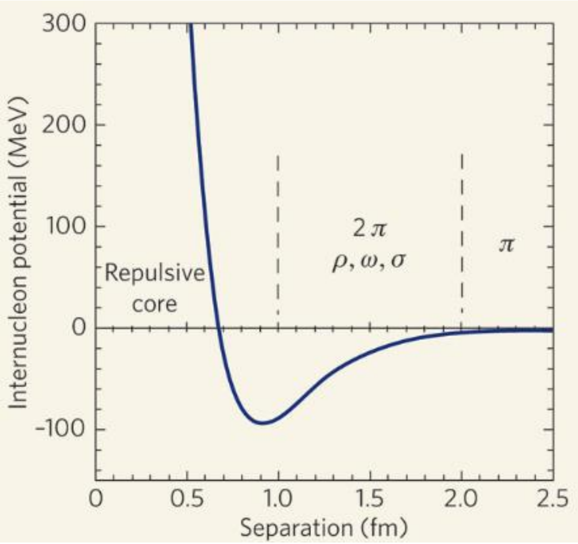

C. Colle, PhD, UGent 2017

→ Identify the right degrees of freedom and main effects for each kinematic region
→ Identify the relevant corrections, correlations to be taken into account

A model for the nucleus

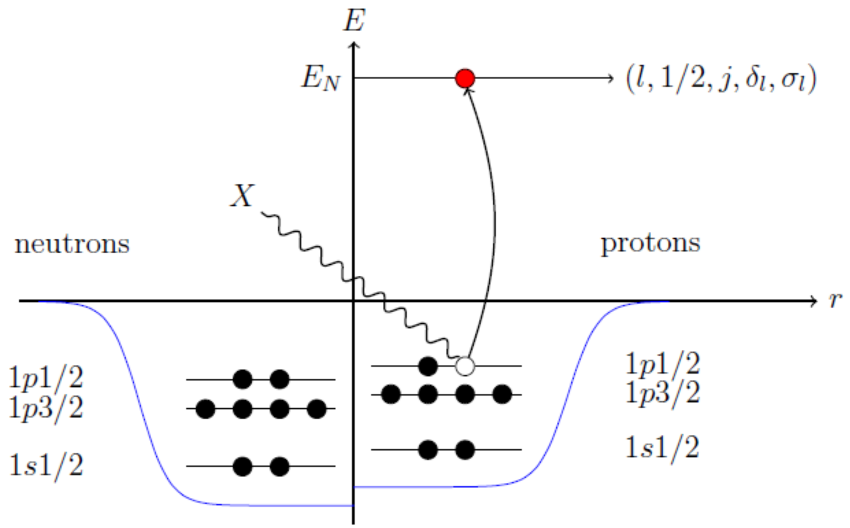

- Starting point : mean-field nucleus with Hartree-Fock single-particle wave functions
- Skyrme SkE2 force used to build the potential
- Pauli blocking
- binding

Hartree-Fock mean field

$$G^{HF}(\alpha,\beta;E) = G^{(0)}(\alpha,\beta;E) + \sum_{\gamma,\delta} G^{(0)}(\alpha,\gamma;E)\Sigma^{HF}(\gamma,\delta)G^{HF}(\delta,\beta;E)$$

- Mean field already contains correlations !
- Nucleons feel the presence of the others through the averaged field

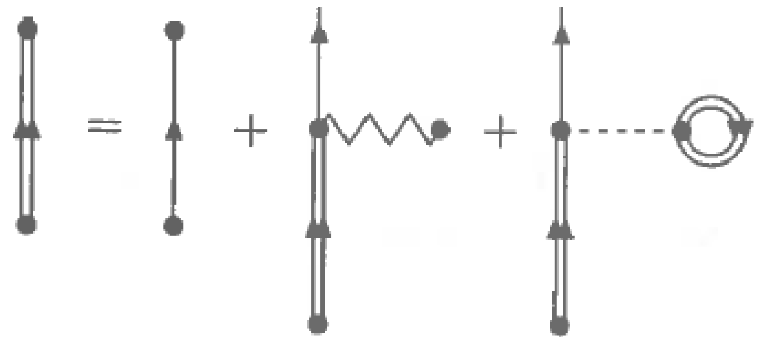

$$\Sigma^{HF}(\gamma,\delta;E) = -\langle\gamma|\,U\,|\delta\rangle - i\int \frac{dE'}{2\pi} \sum_{\mu\nu} \langle\gamma\mu|\,V\,|\delta\nu\rangle\, G^{HF}(\nu\mu;E')$$

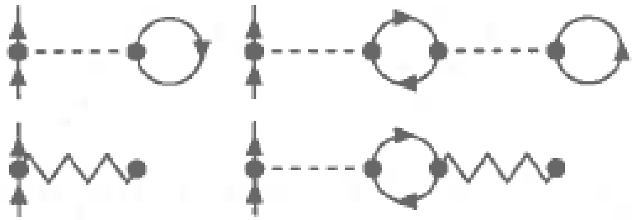

Long-range RPA correlations

- Correlations over the whole size of the nucleus
- Redistribute the incoming energy transfer to the nucleus over all the nuclear constituents.
- They manifest themselves in collective excitations such as giant resonances

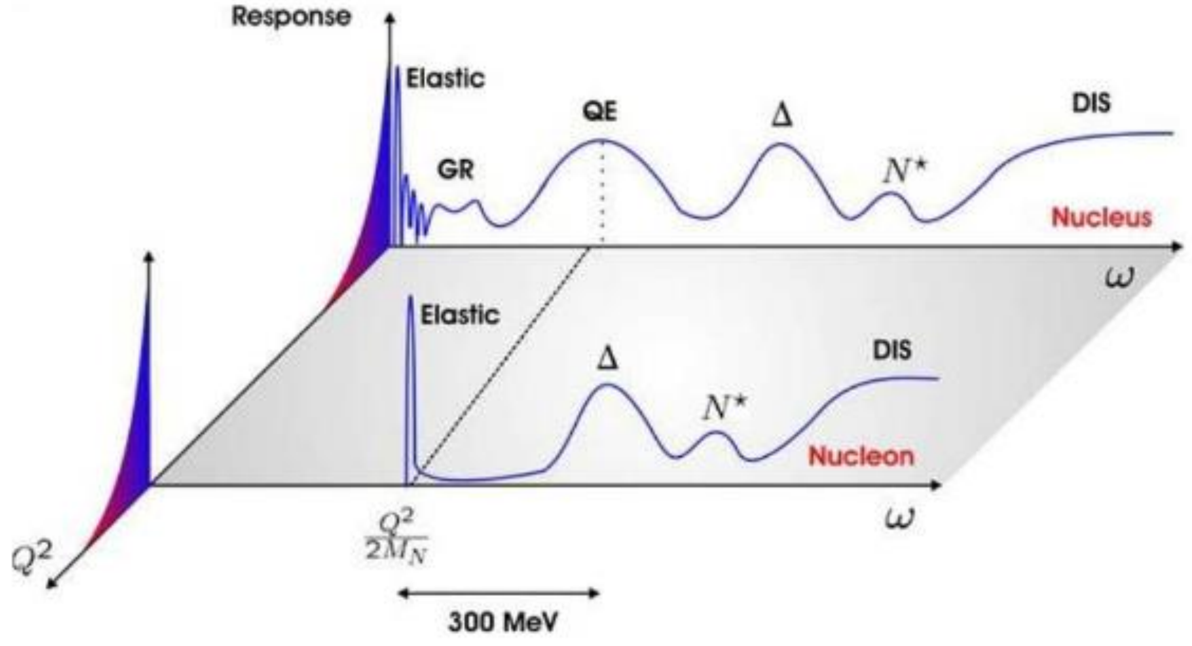

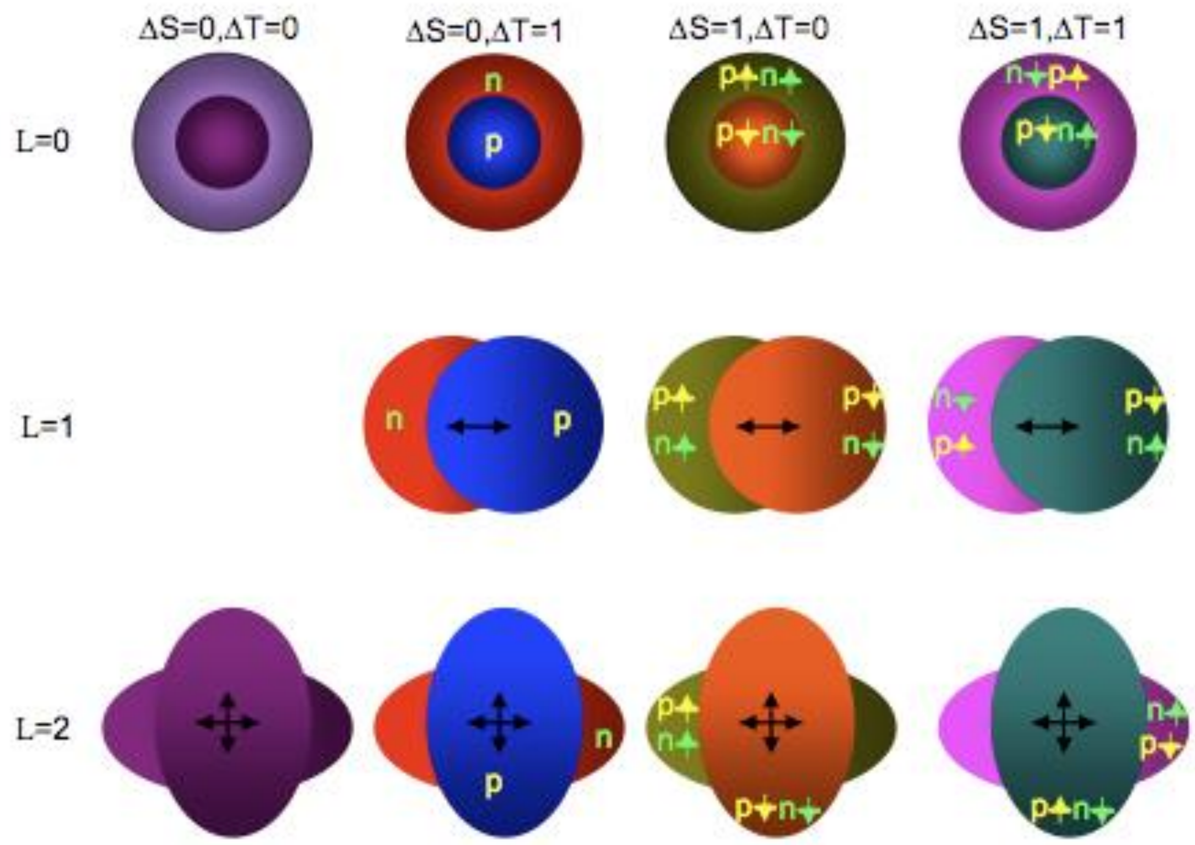

https://cyclotron.tamu.edu/research/nuclear-structure/

Long-range RPA correlations

- Green's function approach
- Skyrme SkE2 residual interaction
- self-consistent calculations

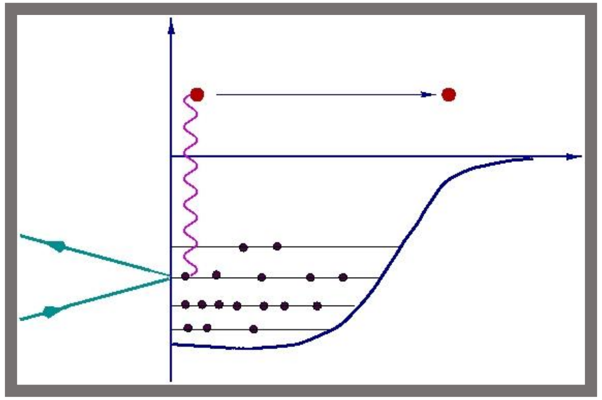

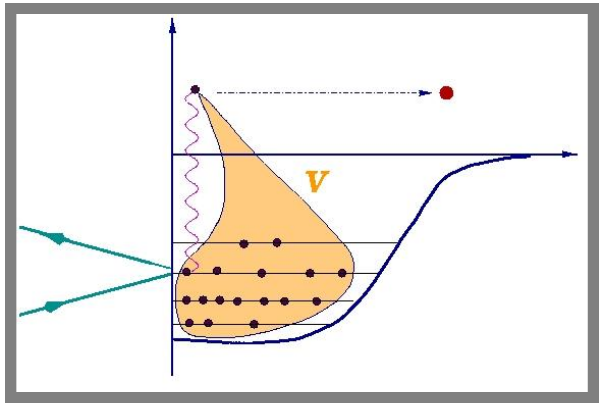

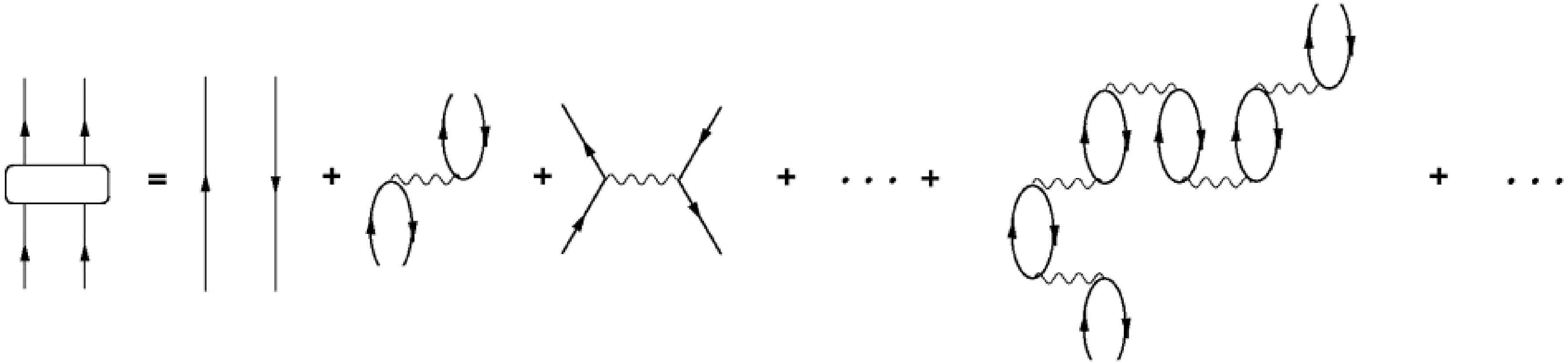

$$|\Psi_{RPA}\rangle = \sum_c \left\{ X_{(\Psi,C)} \left|ph^{-1}\right\rangle - Y_{(\Psi,C)} \left|hp^{-1}\right\rangle \right\}$$

$$\Pi^{(RPA)}(x_1,x_2;\omega) = \Pi^{(0)}(x_1,x_2;\omega) + \frac{1}{\hbar}\int dx \int dx' \; \Pi^{(0)}(x_1,x;\omega)\,\widetilde{V}(x,x')\,\Pi^{(RPA)}(x',x_2;\omega)$$

Hartree-Fock-CRPA

Solving the RPA equations in coordinate space

$$|\Psi_C(E)\rangle = \left|ph^{-1}(E)\right\rangle + \int dx_1 \int dx_2 \; \widetilde{V}(x_1,x_2)$$

$$\sum_{c'} \mathcal{P} \int d\varepsilon_{p'} \left[\frac{\psi_{h'}(x_1)\psi^{\dagger}_{p'}(x_1,\varepsilon_{p'})}{E-\varepsilon_{p'h'}} \left|p'h'^{-1}(\varepsilon_{p'h'})\right\rangle \right.$$

$$\left. - \frac{\psi^{\dagger}_{h'}(x_1)\psi_{p'}(x_1,\varepsilon_{p'})}{E+\varepsilon_{p'h'}} \left|h'p'^{-1}(-\varepsilon_{p'h'})\right\rangle \right] \left\langle \Psi_0 \left| \hat{\psi}^{\dagger}(x_2)\hat{\psi}(x_2) \right| \Psi_C(E) \right\rangle$$

What we really need is transition densities :

$$\langle \Psi_0 || X_{\eta J} || \Psi_C(J;E)\rangle_r = -\langle h || X_{\eta J} || p(\varepsilon_{ph})\rangle_r$$

$$+ \sum_{\mu,\nu} \int dr_1 \int dr_2 \; U^J_{\mu\nu}(r_1,r_2) \; \mathcal{R}\left(R^{(0)}_{\eta\mu;J}(r,r_1;E)\right) \; \langle \Psi_0 || X_{\nu J} || \Psi_C(J;E)\rangle_{r_2}$$

$$\int dr \int dr' \; R^{(0)}_{\eta\mu;JM}(r,r';E) = \frac{1}{\hbar} \int dx \int dx' \;\; X_{\eta JM}(x) \;\; \Pi^{(0)}(x,x';\omega) \;\; X^{\dagger}_{\eta' JM}(x')$$

So in the end we have to solve a set of coupled equations, that after discretizing on a mesh in coordinate space, translates into a matrix inversion :

$$\rho^{RPA}_C = -\frac{1}{1-R\,U}\;\rho^{HF}_C$$

Hartree-Fock-CRPA

- Final state interactions :

-taken into account through the calculations of the wave function of the outgoing nucleon in the (real) nuclear potential generated using the Skyrme force

-influence of the spreading width of the particle states is implemented through a folding procedure

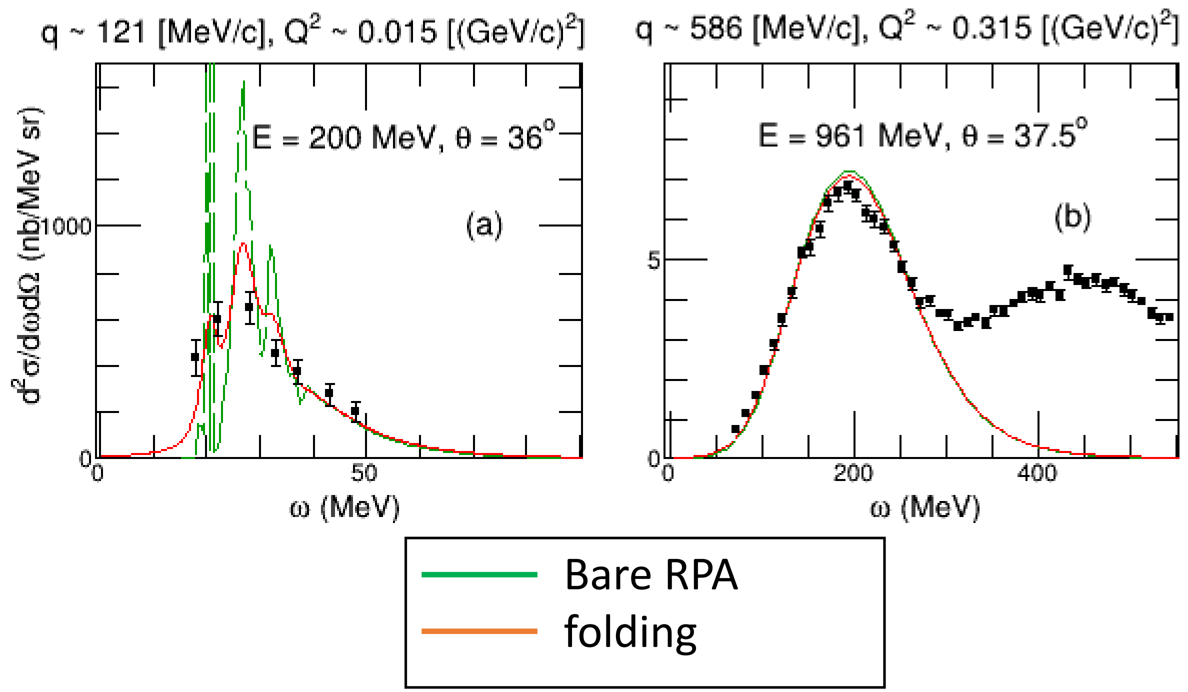

$$R'(q,\omega') = \int_{-\infty}^{\infty} d\omega \; R(q,\omega) \; L(\omega,\omega'),$$

$$L(\omega,\omega') = \frac{1}{2\pi}\left[\frac{\Gamma}{(\omega-\omega')^2 + (\Gamma/2)^2}\right].$$

Hartree-Fock-CRPA

•Coulomb correction for the outgoing lepton in charged-current interactions :

- ✓ Low energies : Fermi function

$$F(Z', E) = \frac{2\pi\eta}{1 - e^{-2\pi\eta}} \qquad \eta \sim \mp Z'\alpha$$

- ✓ High energies : modified effective momentum approximation (J. Engel, PRC57,2004

$$q_{eff} = q + 1.5 \left(\frac{Z'\alpha\hbar c}{R} \right),$$

$$\Psi_l^{eff} = \zeta(Z', E, q)\ \Psi_l\ ,$$

$$\zeta(Z', E, q) = \sqrt{\frac{q_{eff} E_{eff}}{qE}}$$

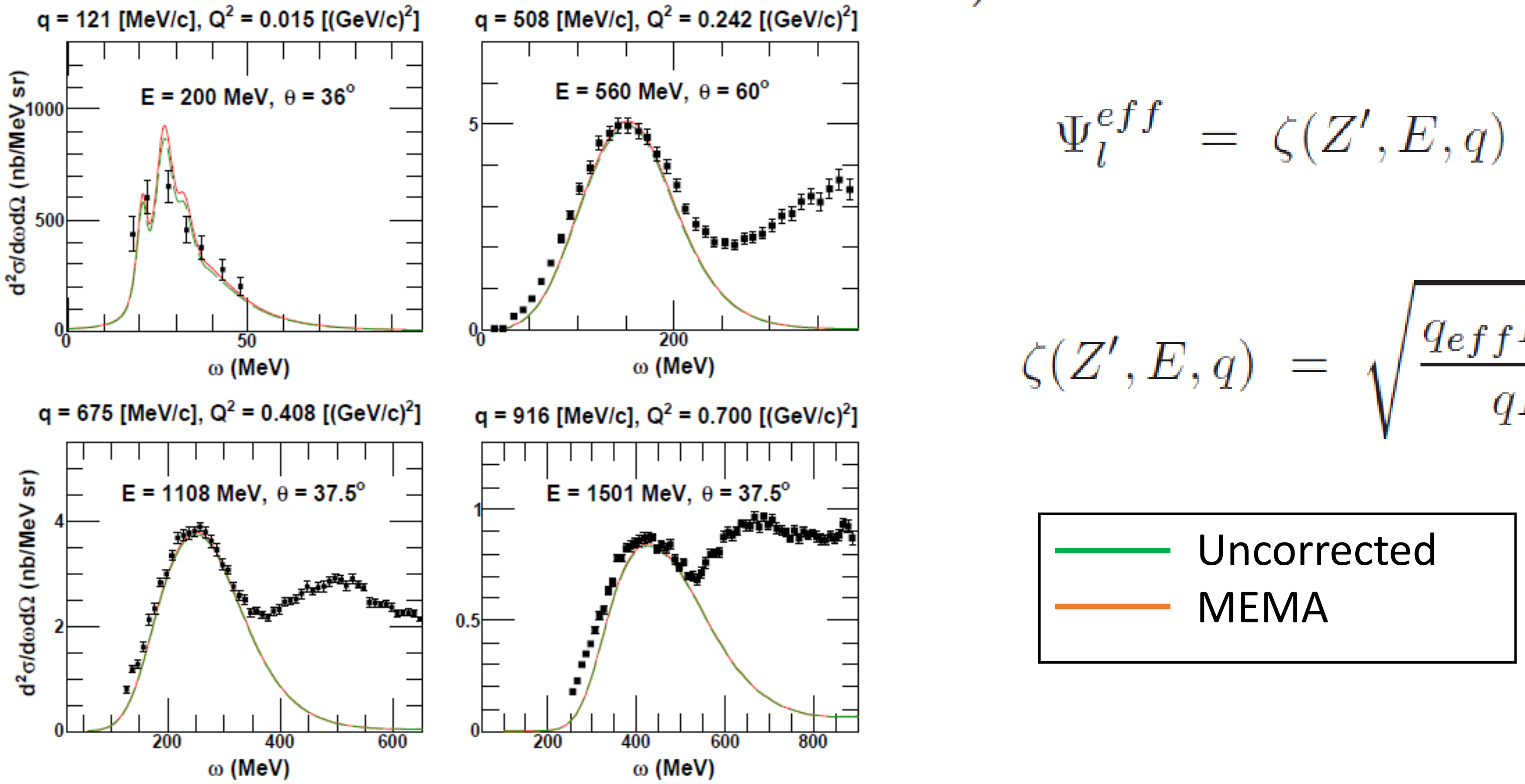

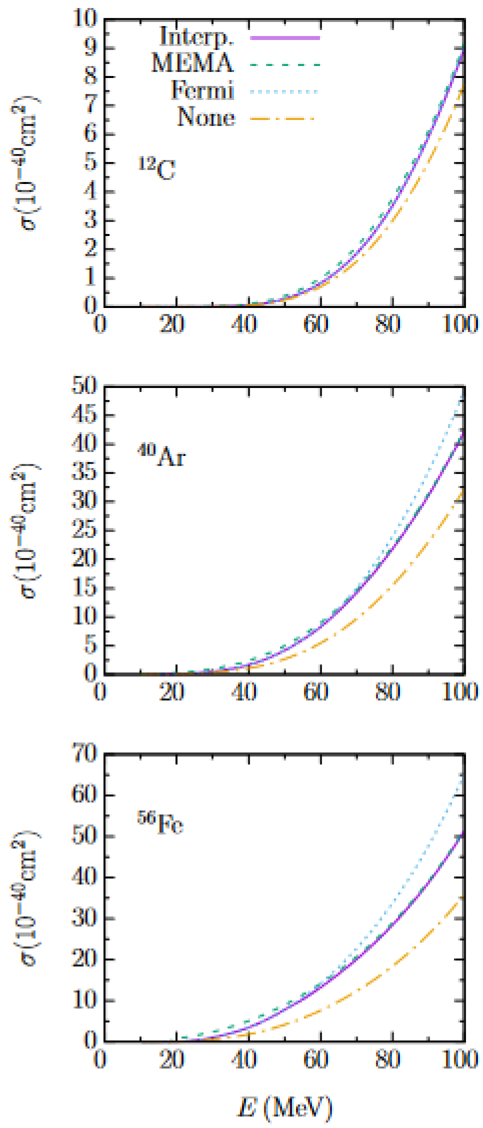

Comparison with electron scattering data

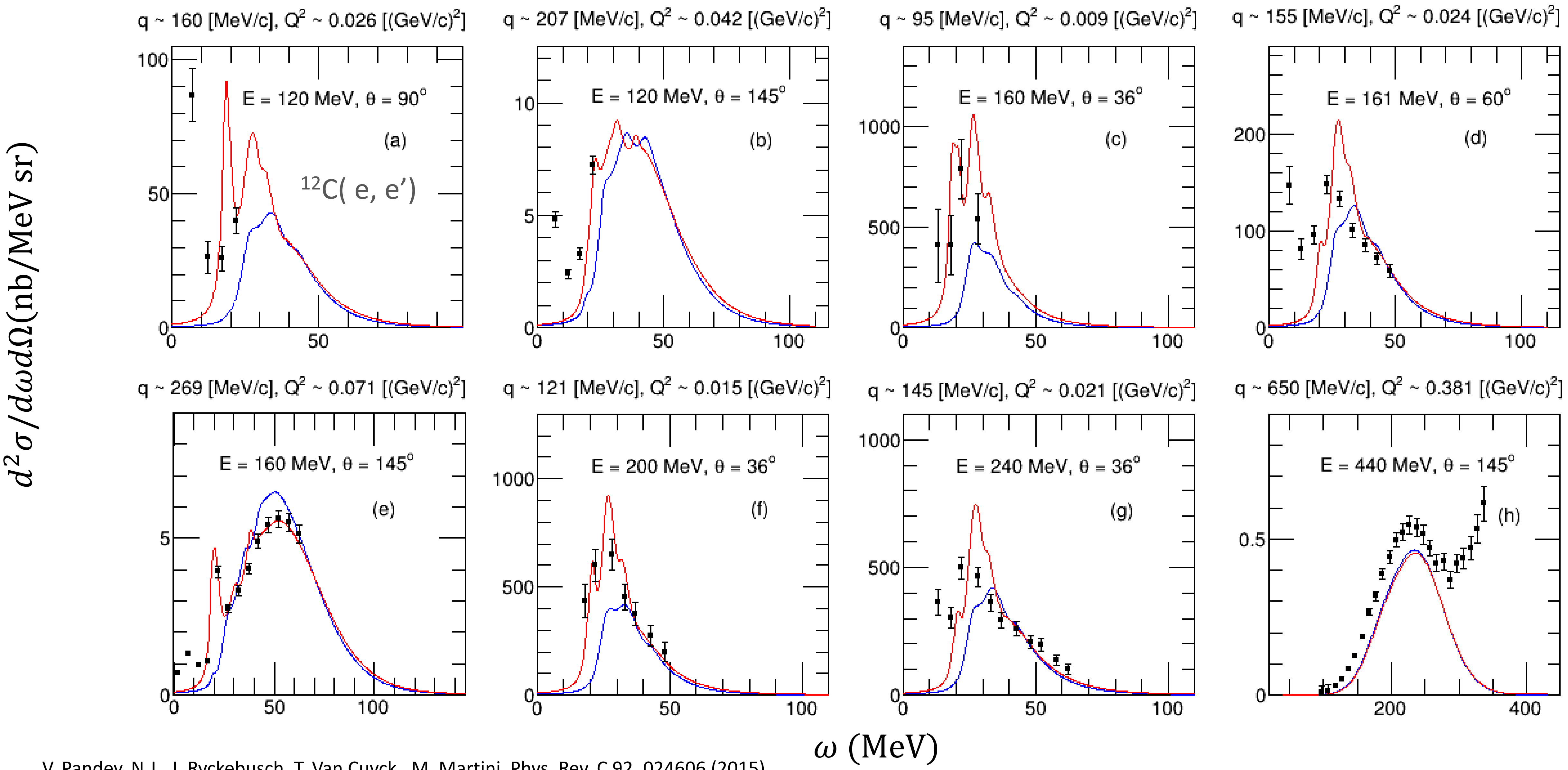

V. Pandey, N.J., J. Ryckebusch, T. Van Cuyck , M. Martini, Phys. Rev. C 92, 024606 (2015)

Inelastic neutrino cross sections

^{16}**O, 50** MeV, NC

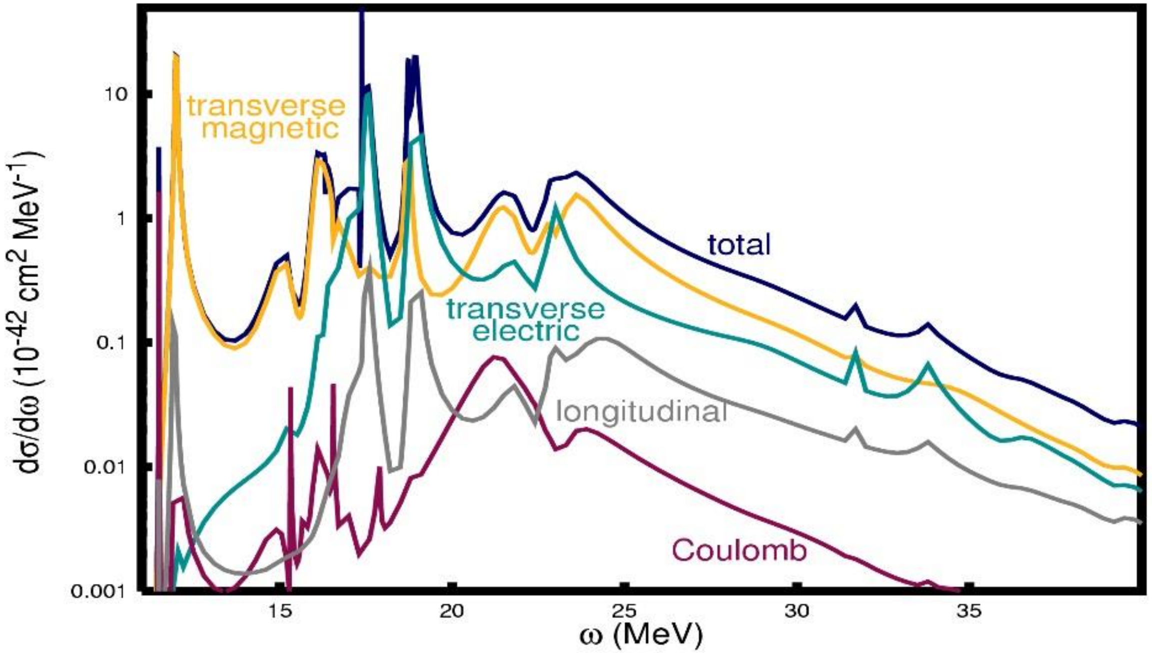

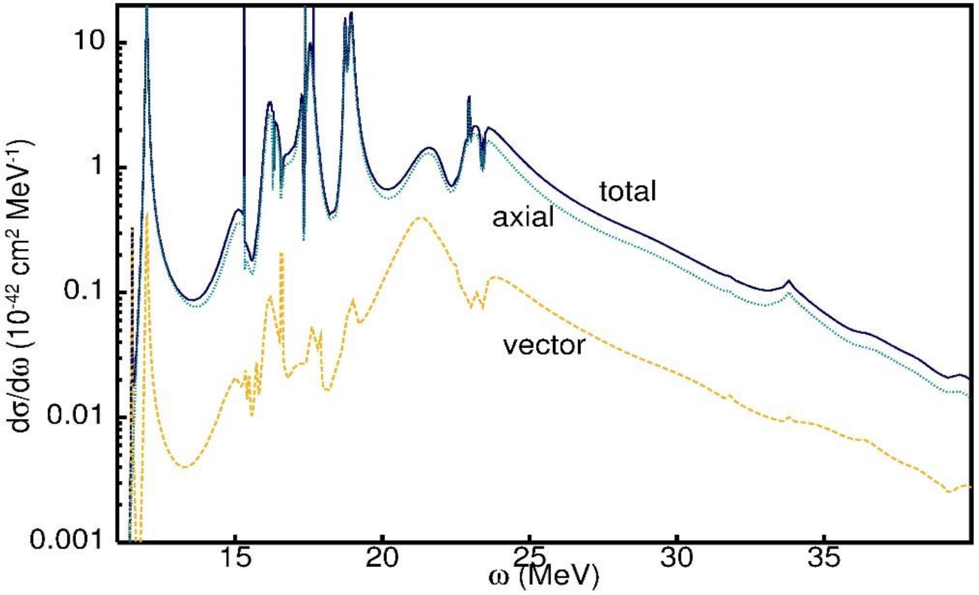

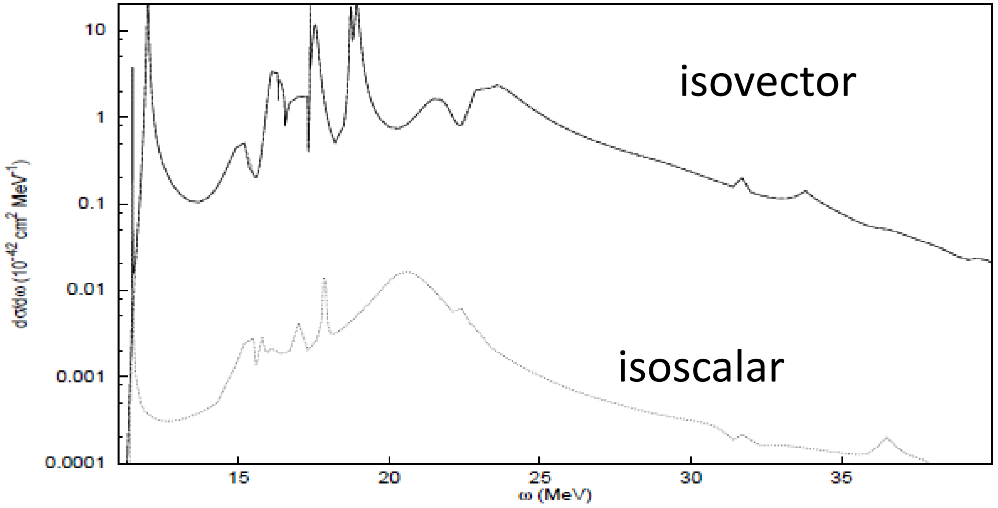

Inelastic neutrino cross sections

Contribution of different single-particle channels in ^{12}C

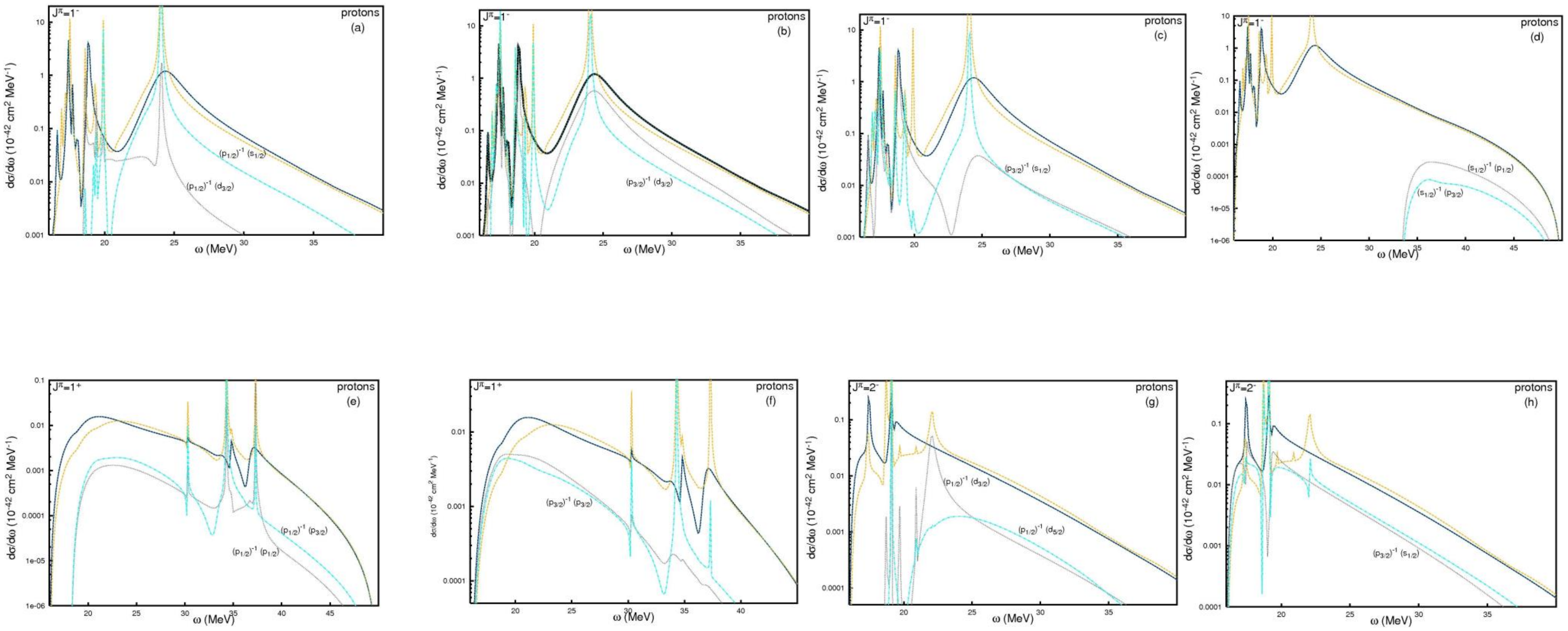

Inelastic neutrino cross sections

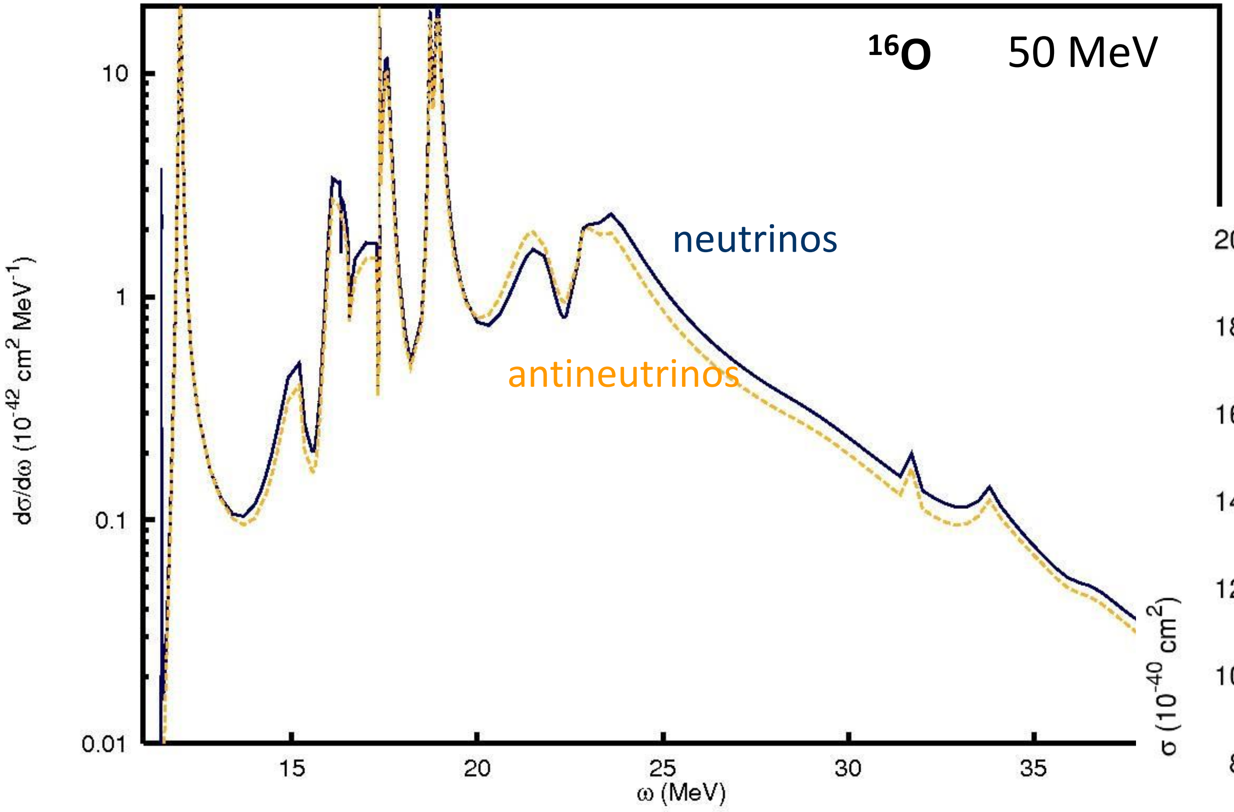

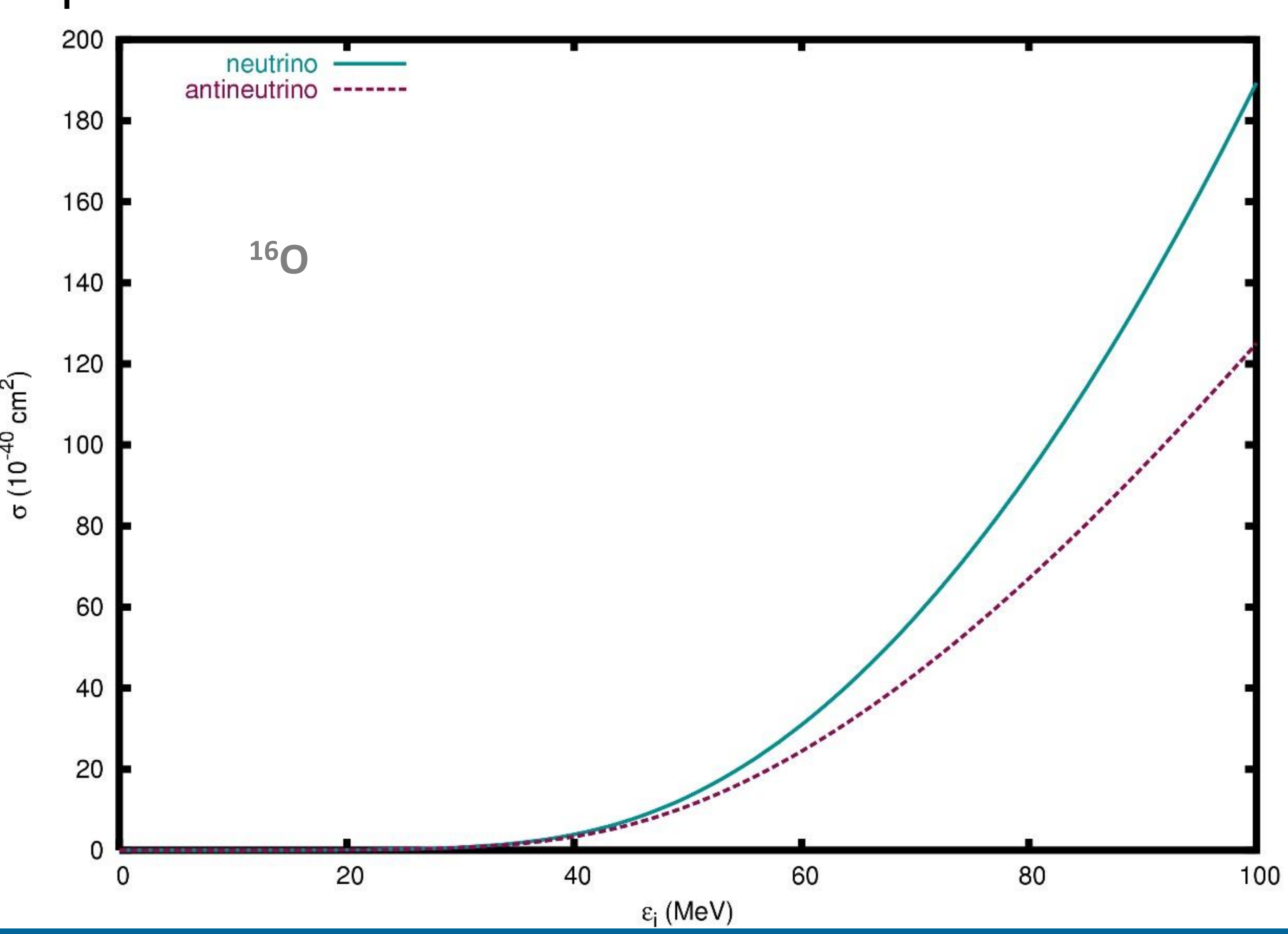

Inelastic neutrino cross sections

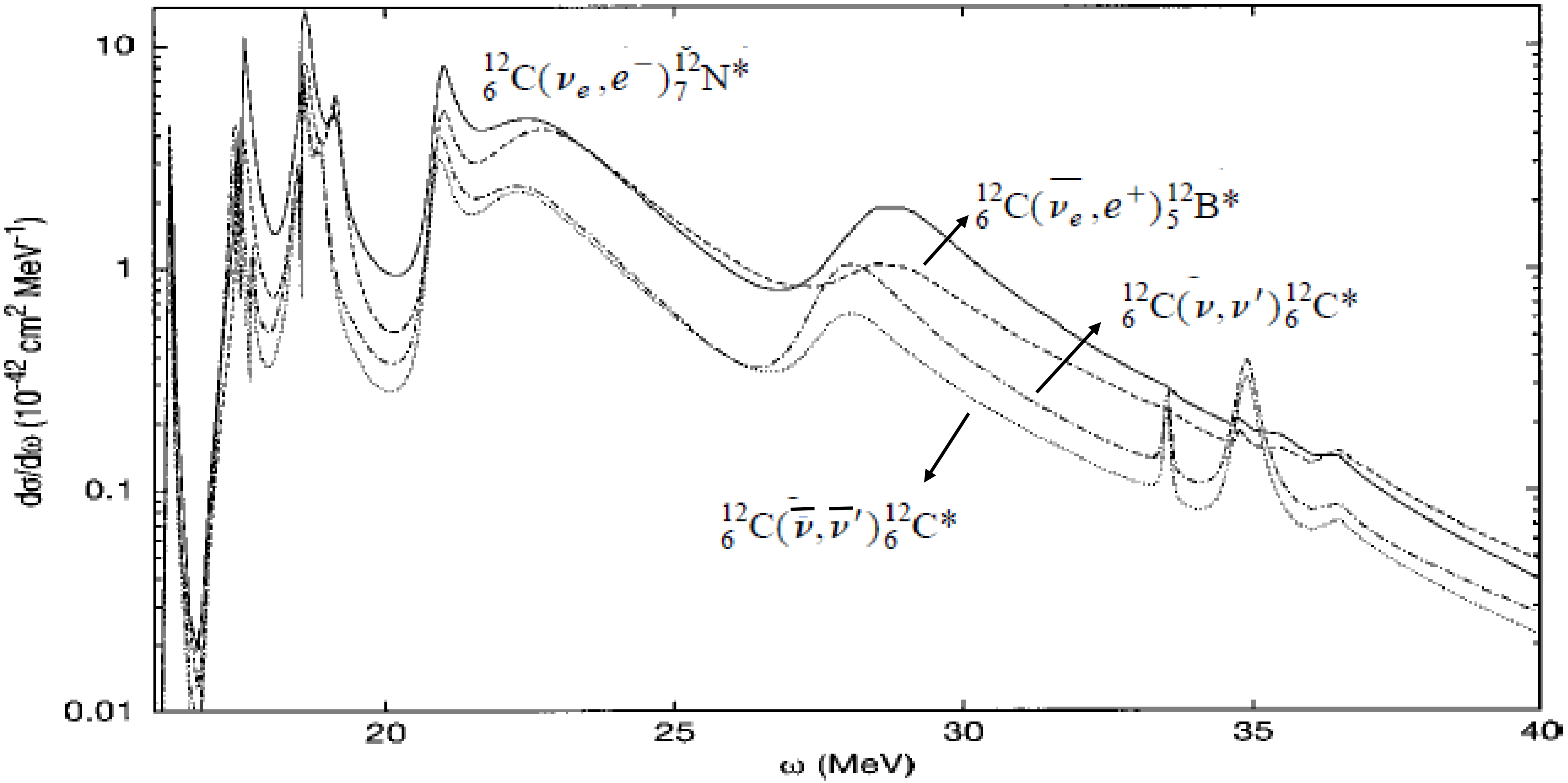

Multipole decomposition

Higher order multipoles important :

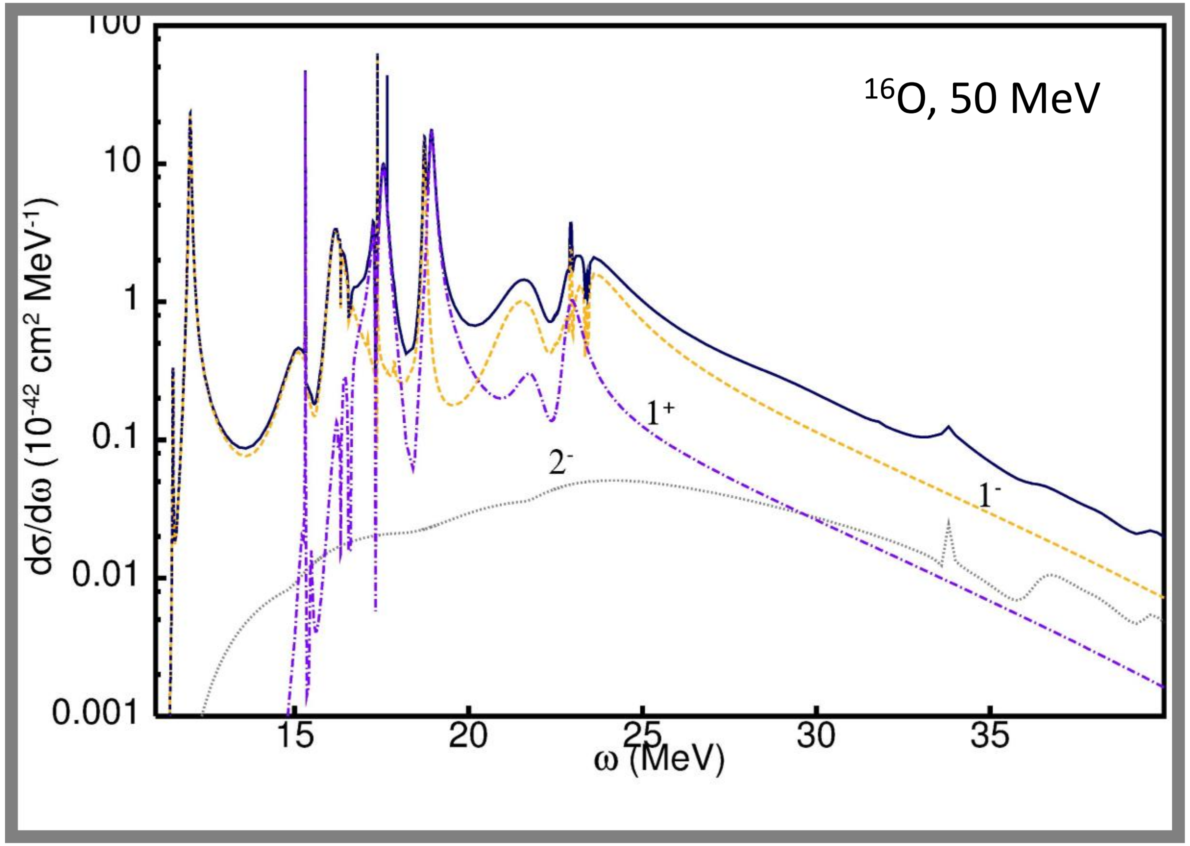

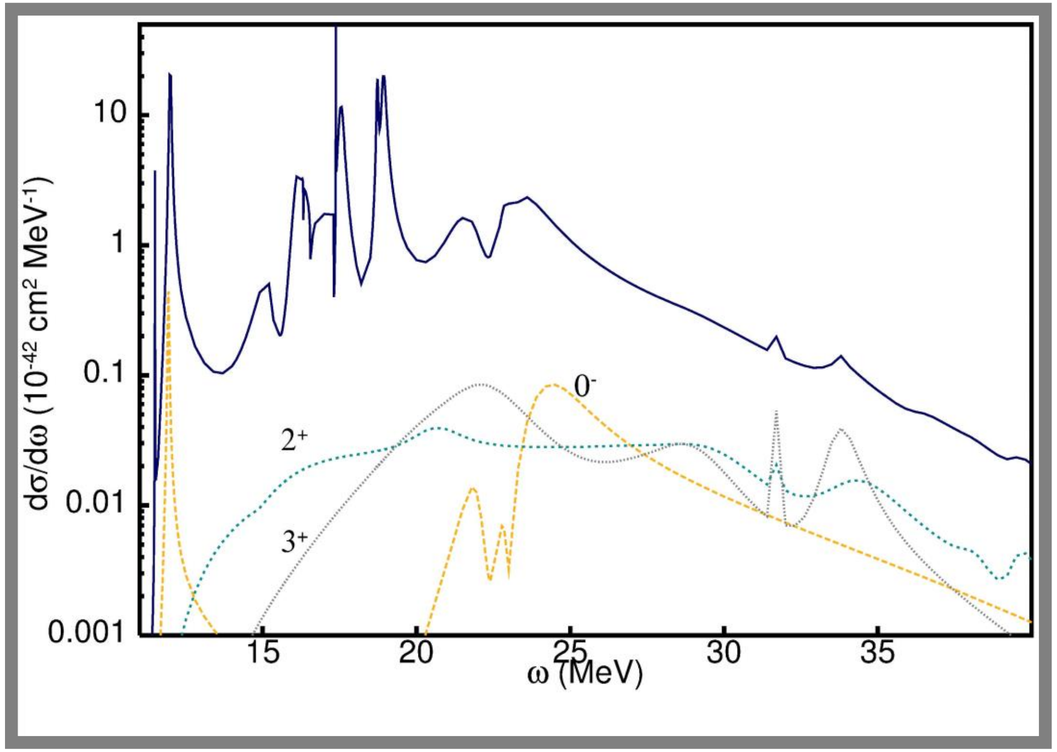

Multipole decomposition

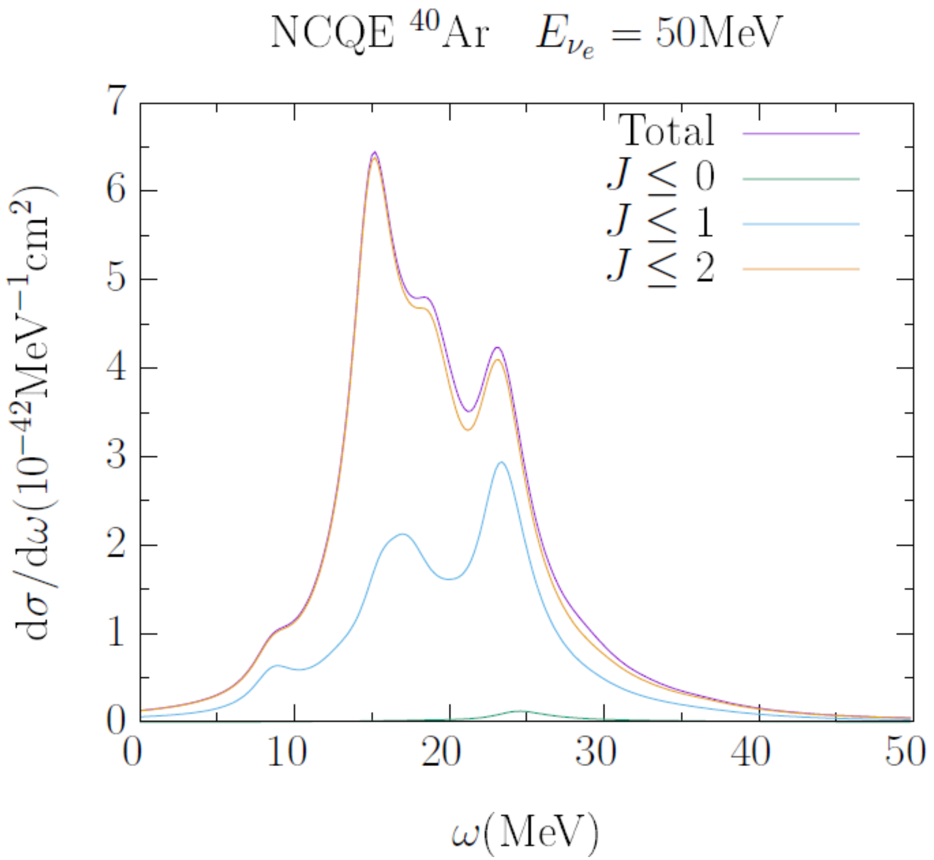

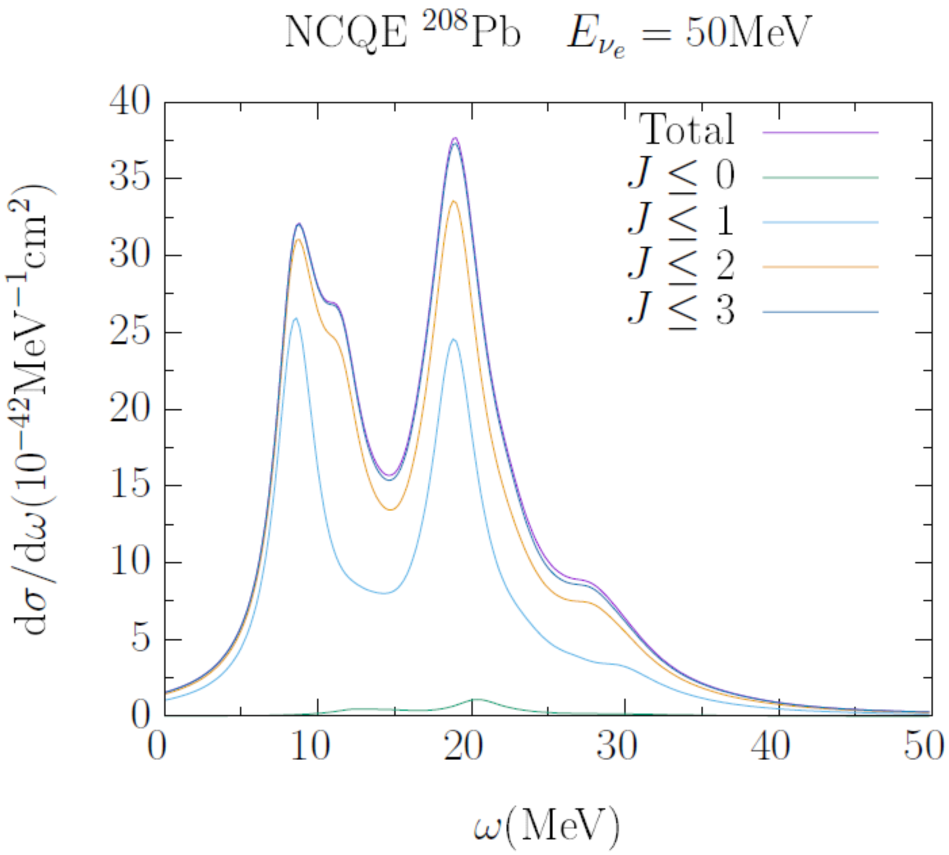

Multipole decomposition

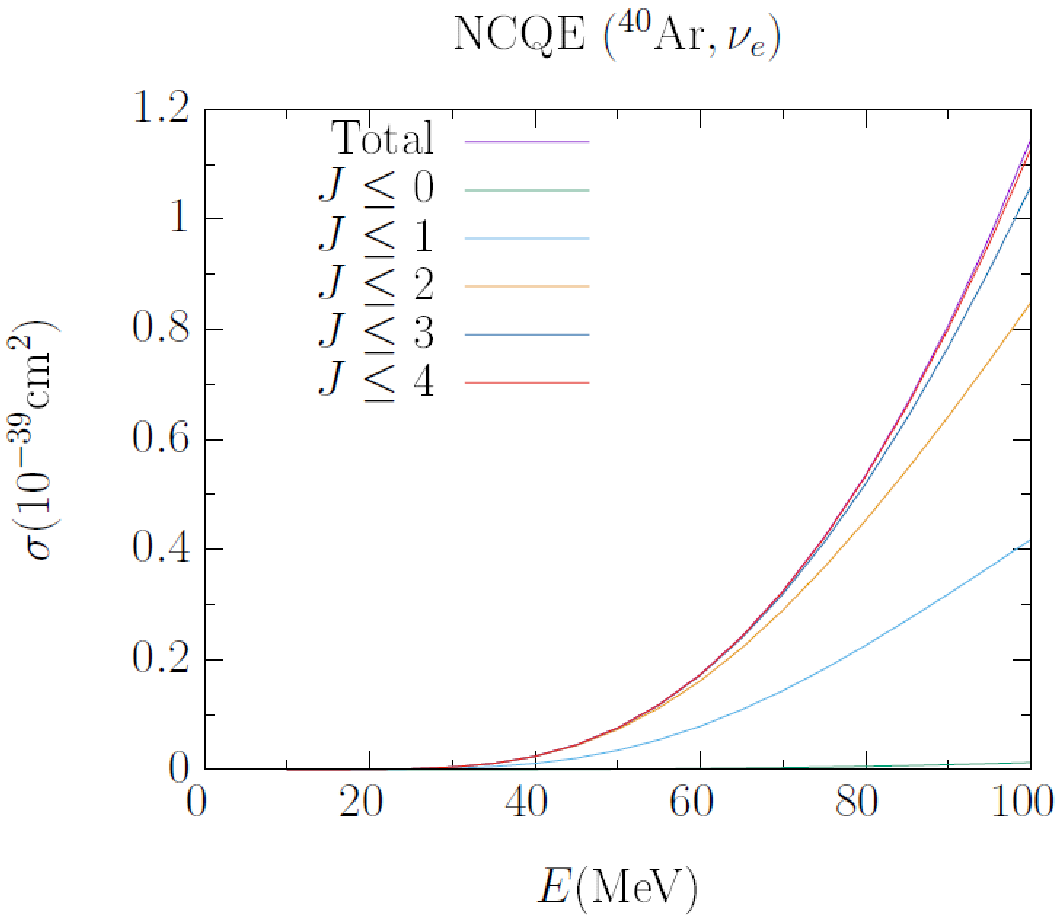

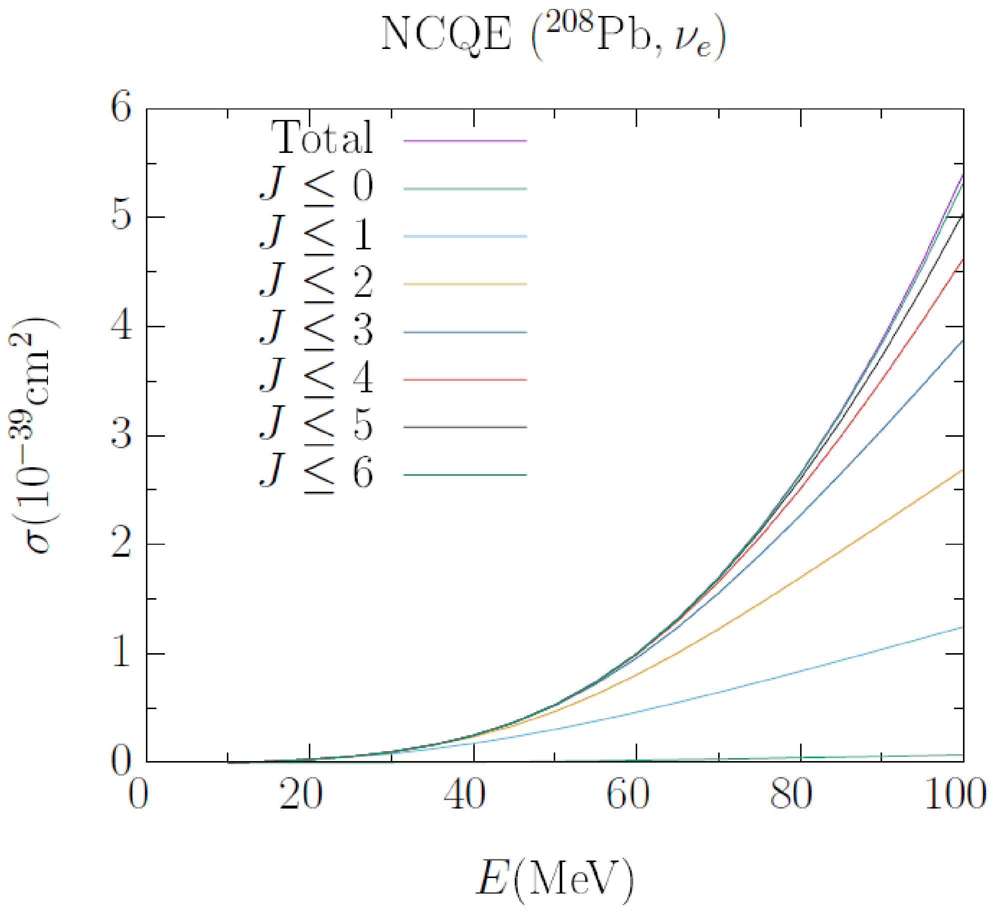

Angular dependence

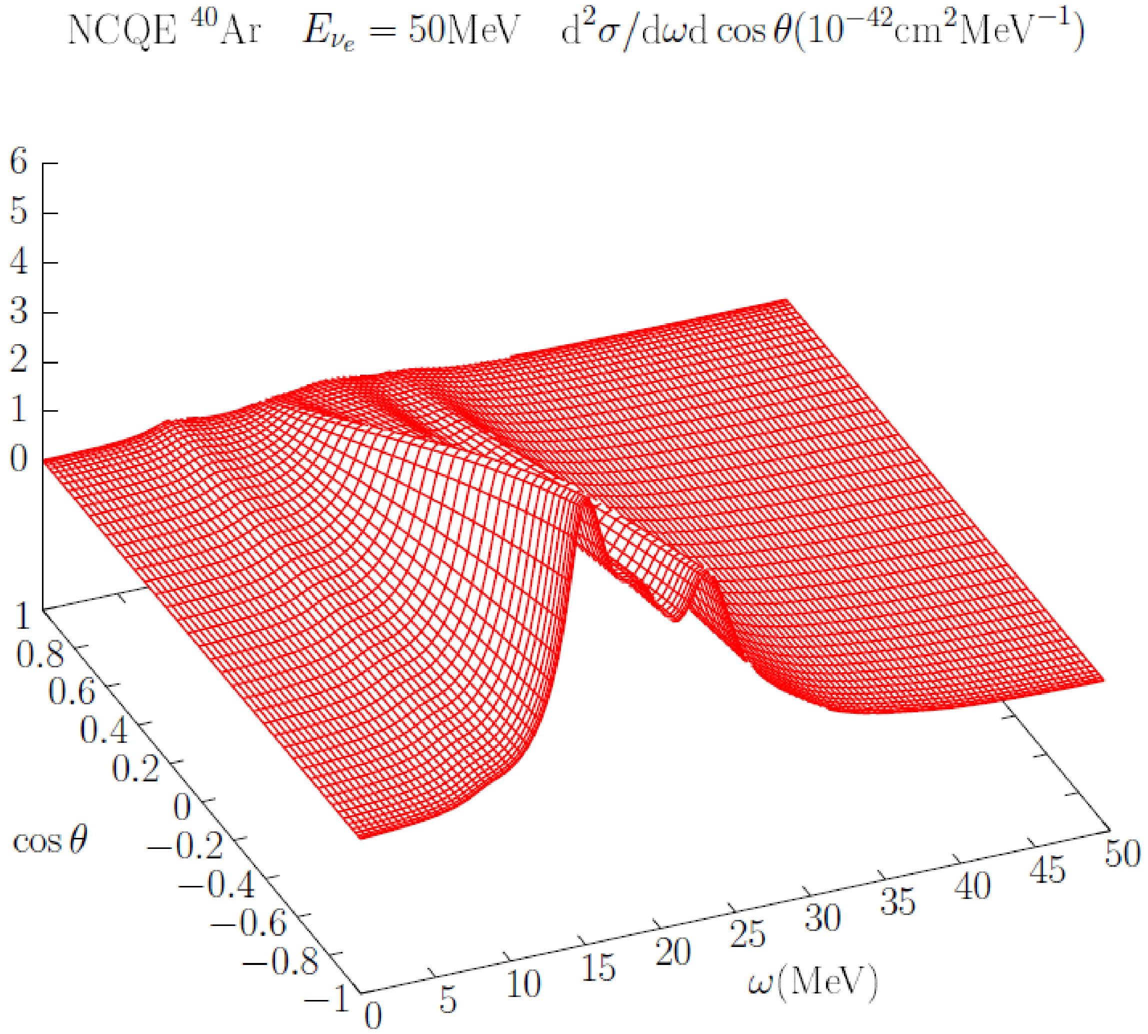

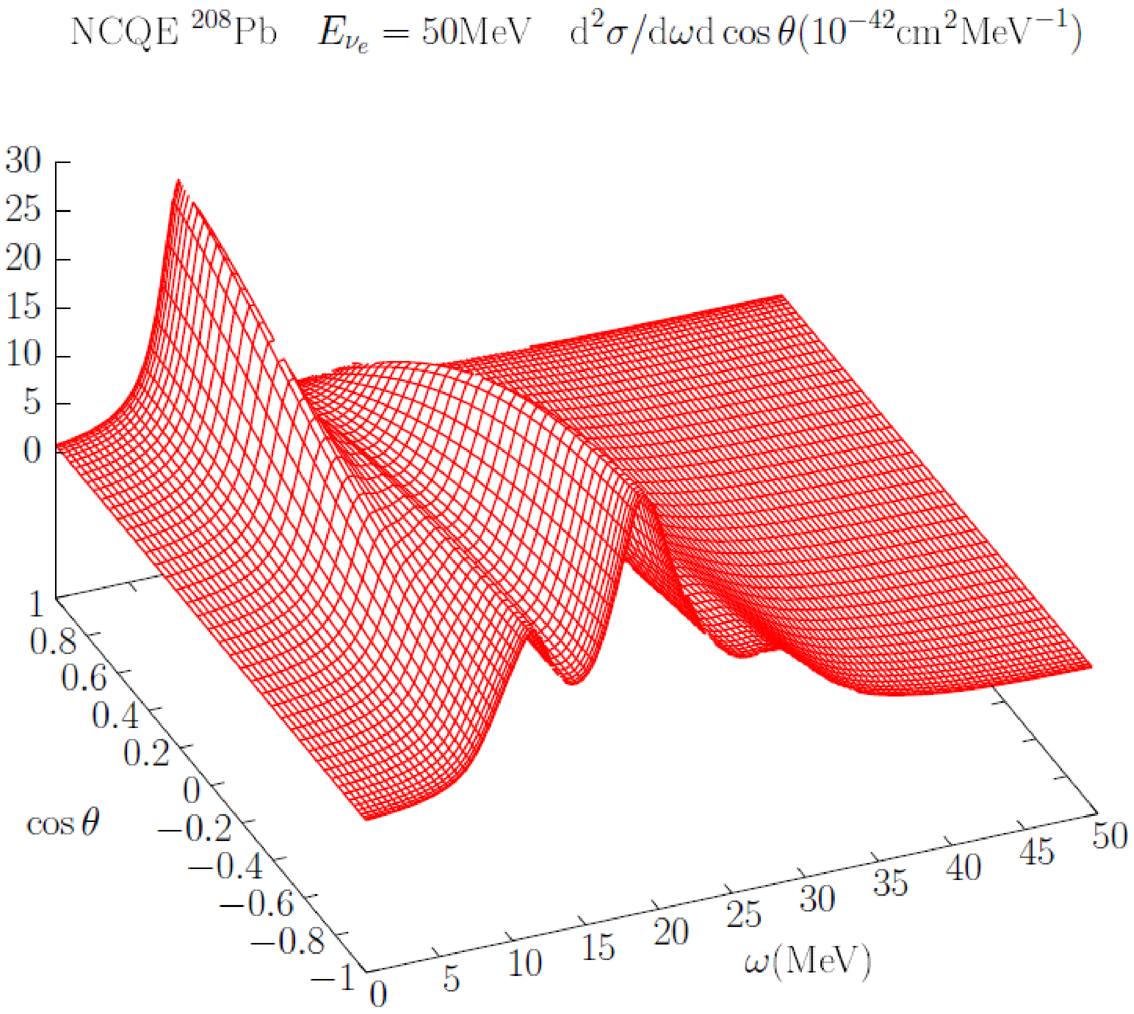

Angular dependence

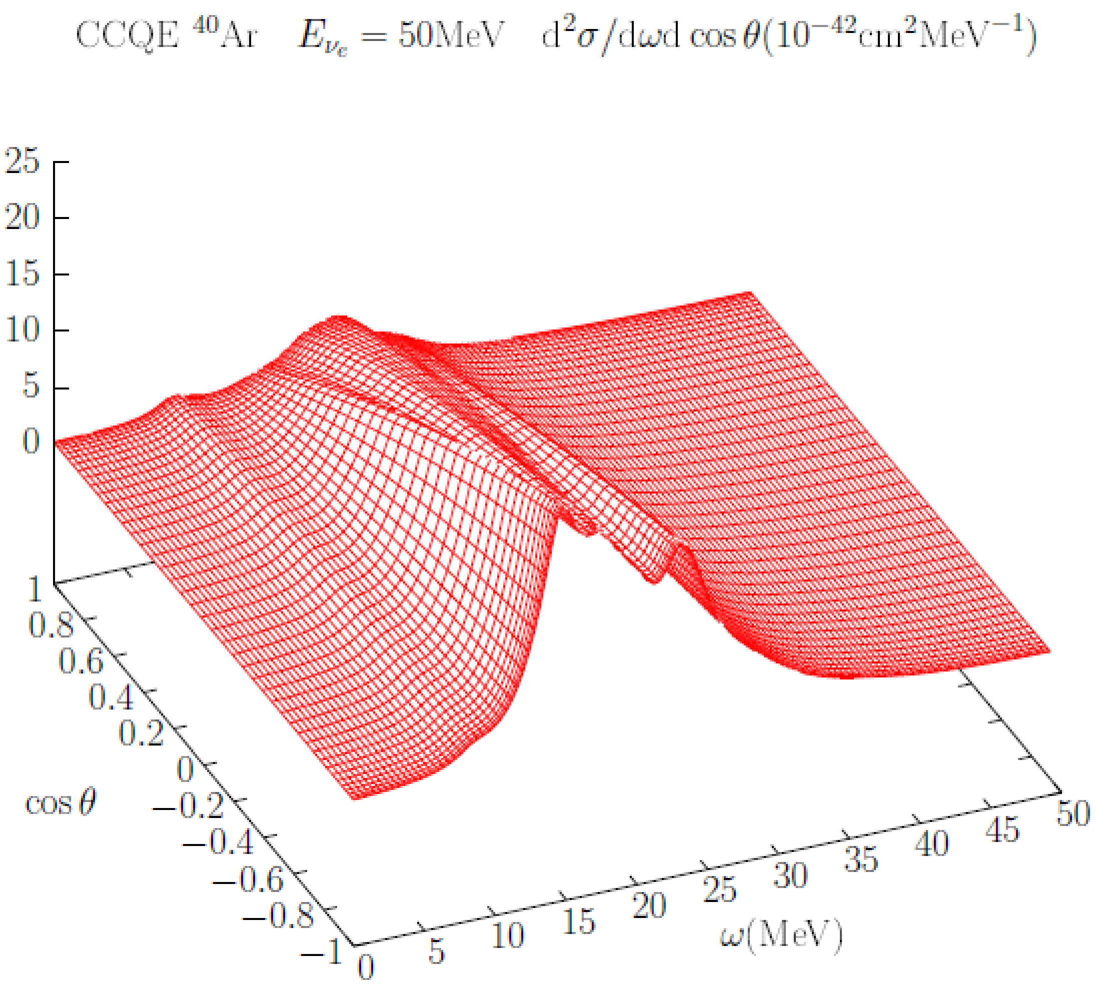

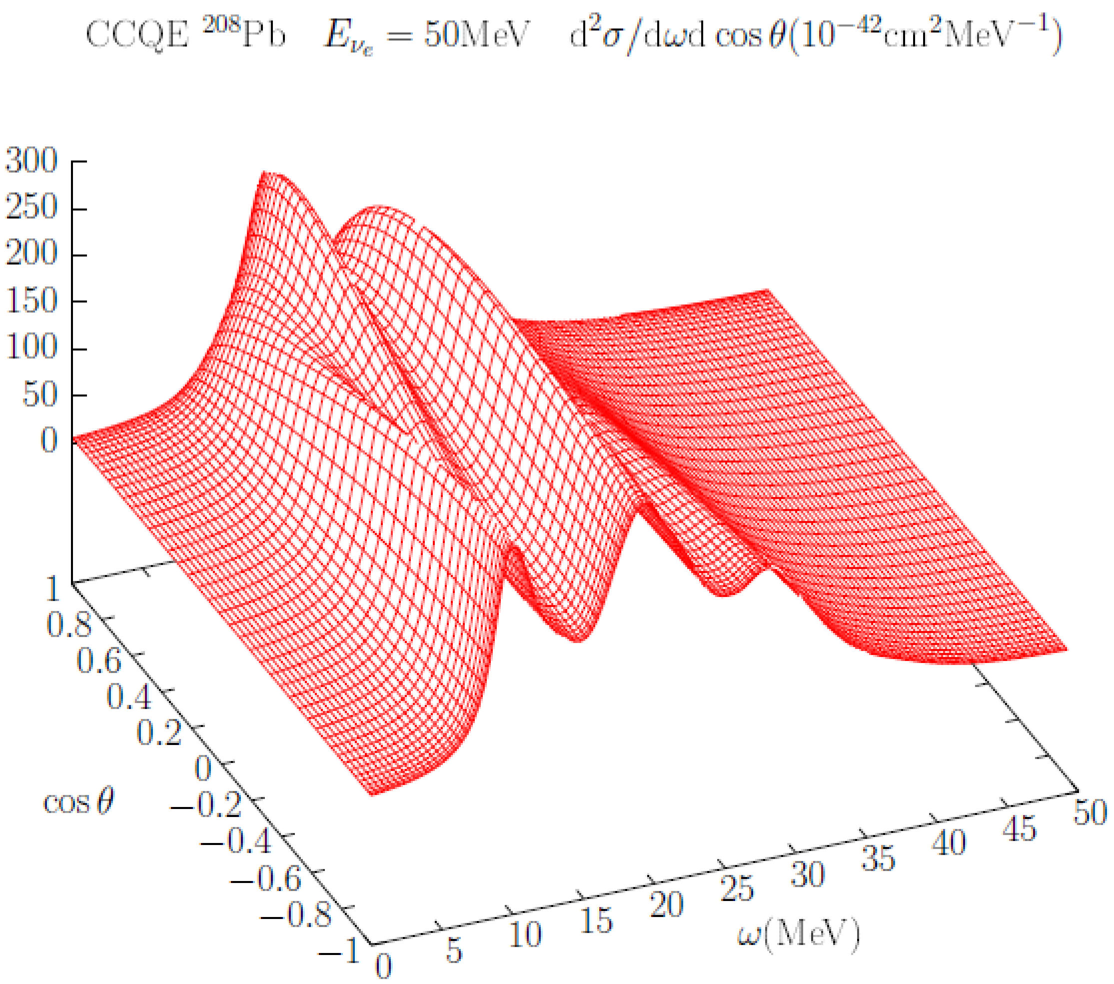

Angular dependence

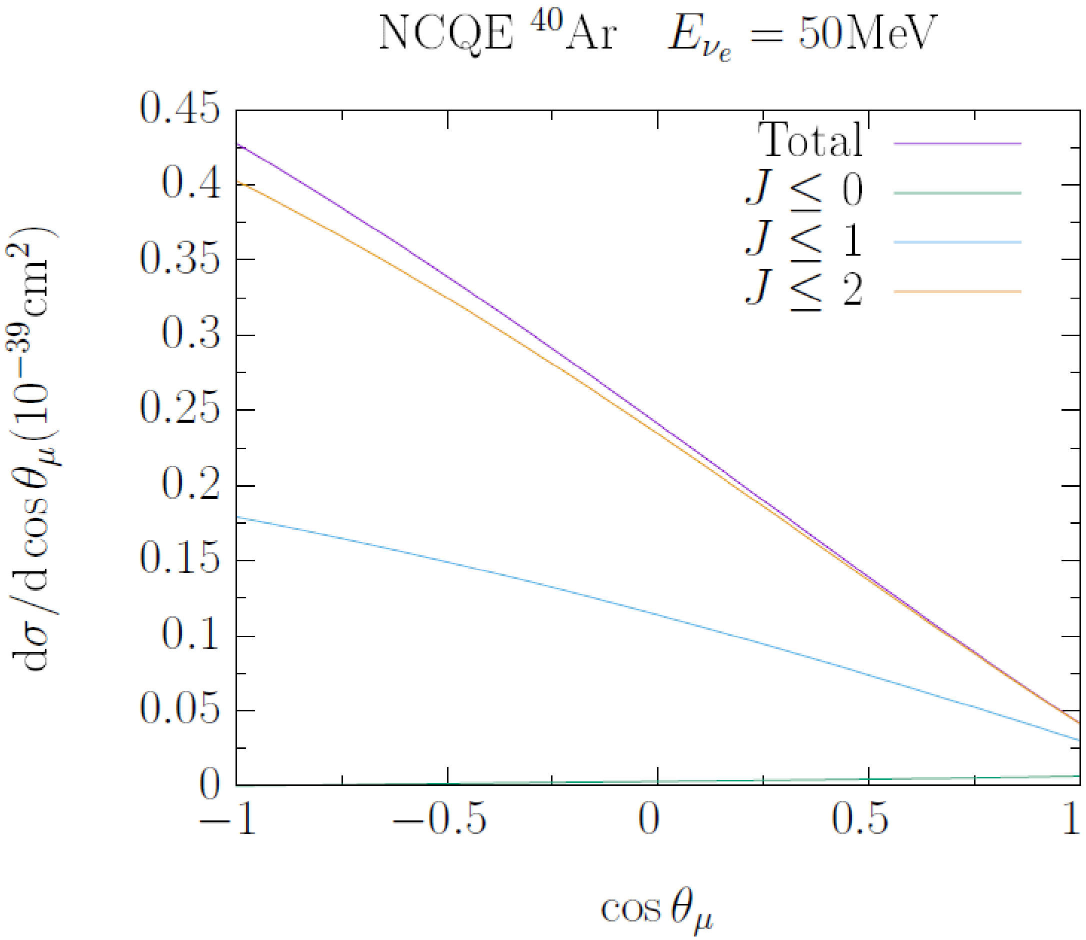

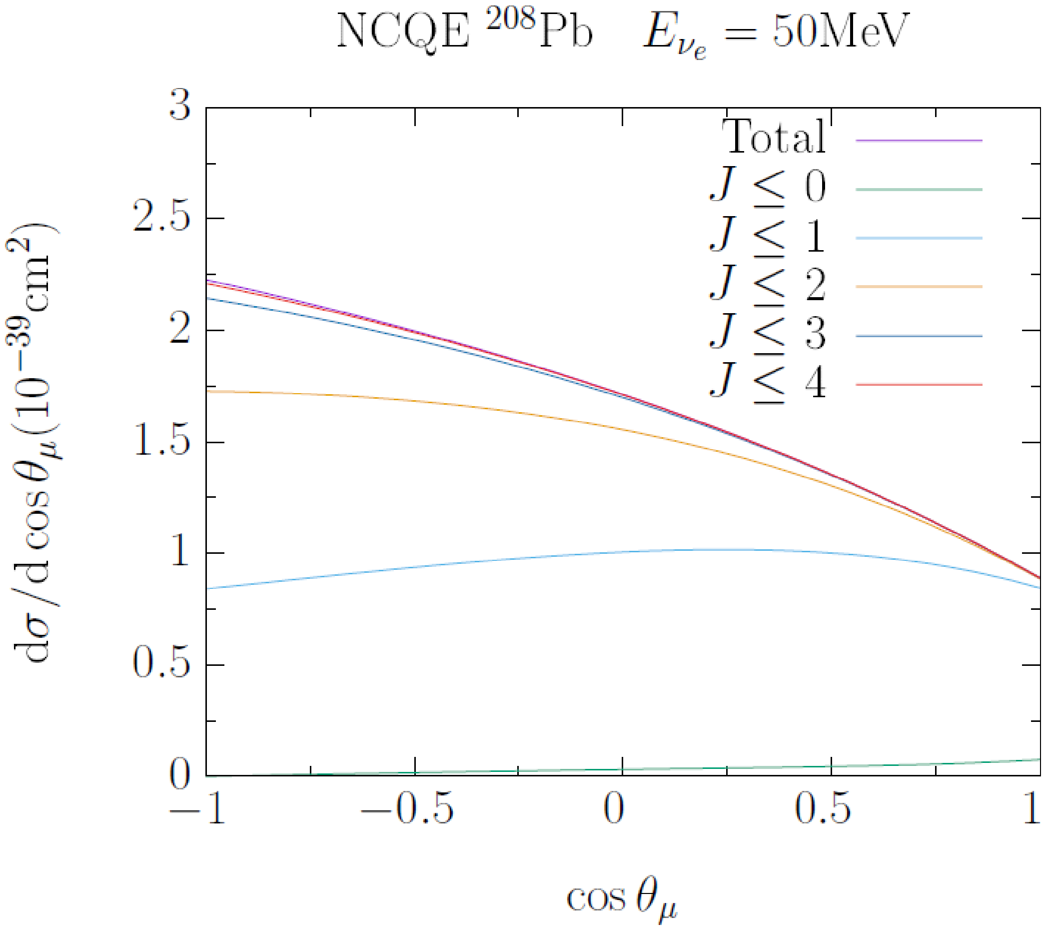

Supernovaneutrinos

Core-collapse supernova

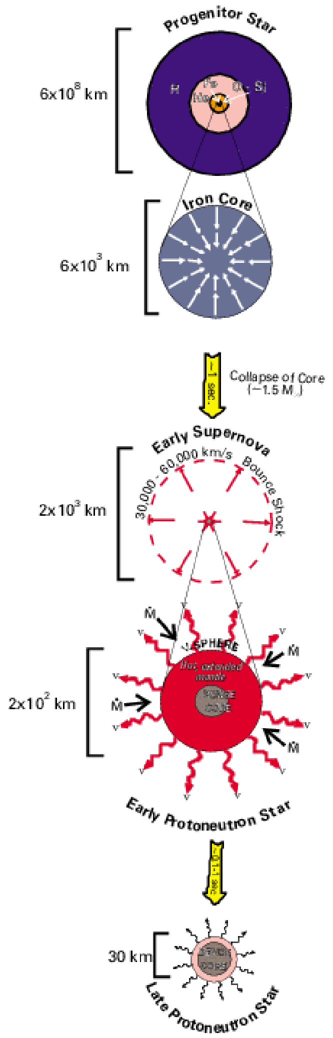

- weak interactions are important
- neutrinos are produced in the neutronization processes characterizing the gravitational collapse
- neutrinos are responsible for the cooling of the proto-neutron star
- neutrinonucleosynthesis
- energy deposition by neutrinos might reheat the stalled shock wave and cause a delayed explosion
- terrestrial detection of supernova neutrinos

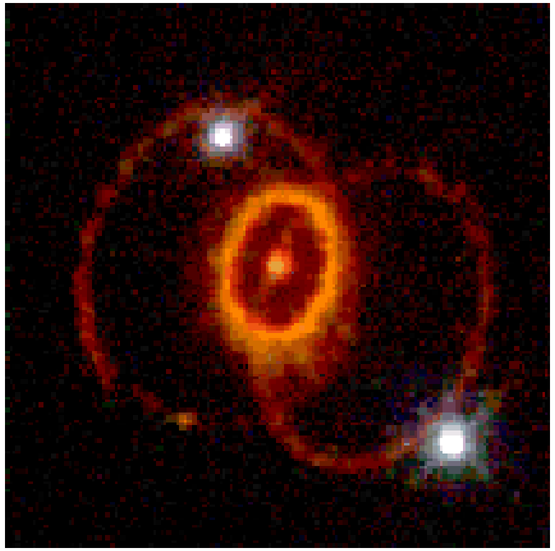

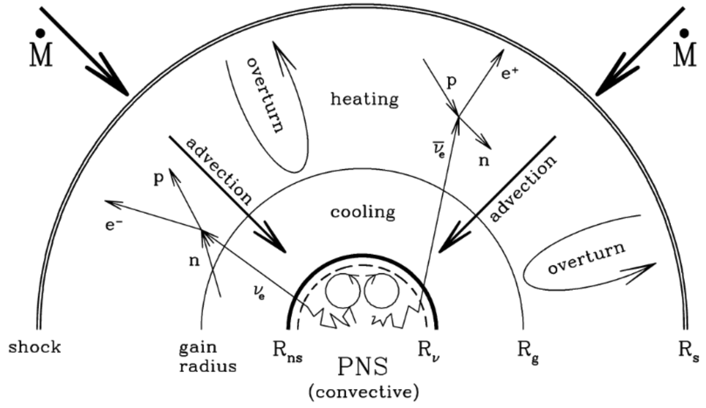

H.-T. Janka astro-ph/0008432

Supernovaneutrino : Energy spectra

$$n_{SN[\langle\varepsilon\rangle,\alpha]}(\varepsilon) = \left(\frac{\varepsilon}{\langle\varepsilon\rangle}\right)^{\alpha} e^{-(\alpha+1)\frac{\varepsilon}{\langle\varepsilon\rangle}}$$

Fermi-Dirac spectra

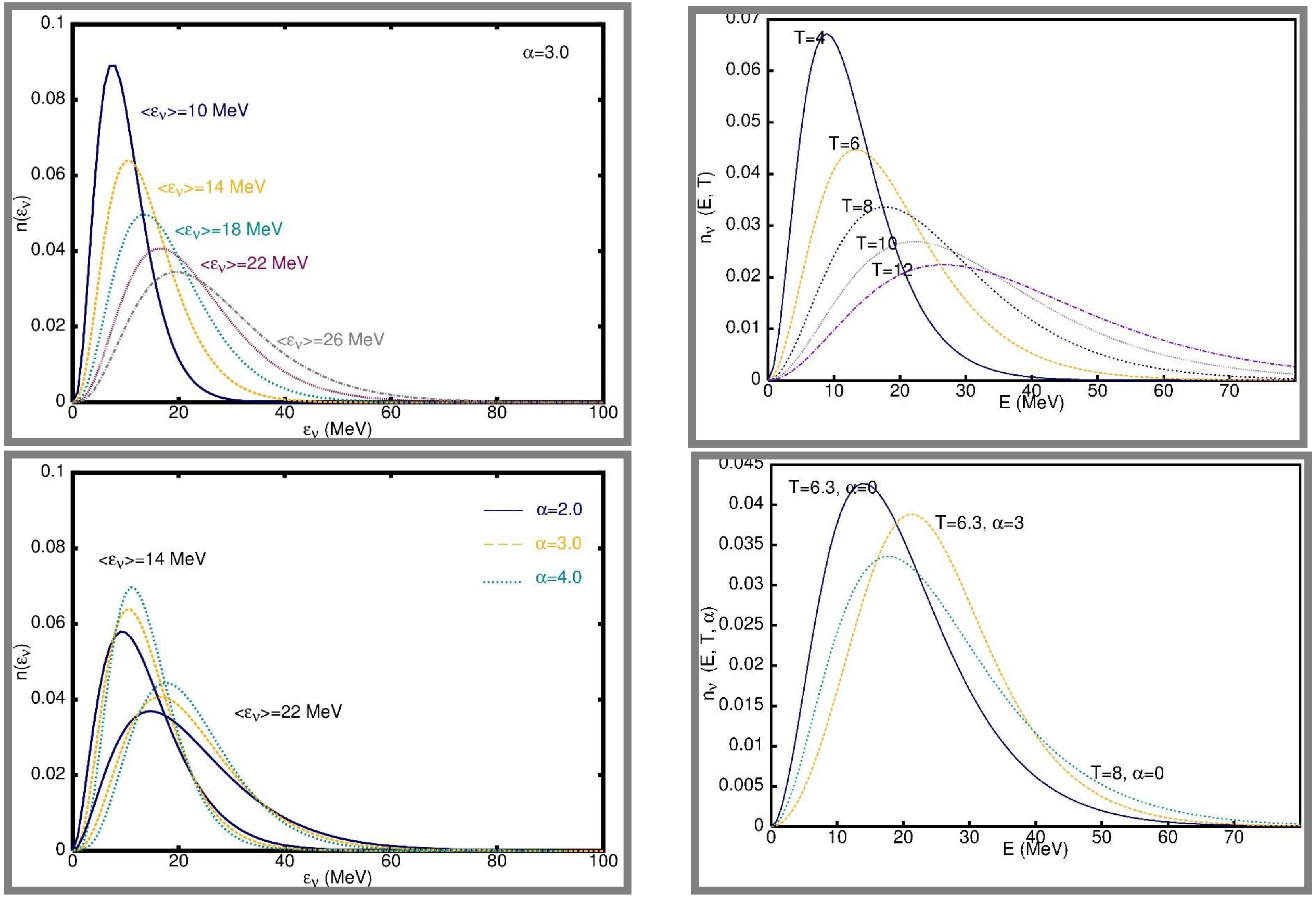

Supernovaneutrino : Energy spectra

Supernova neutrino spectra :

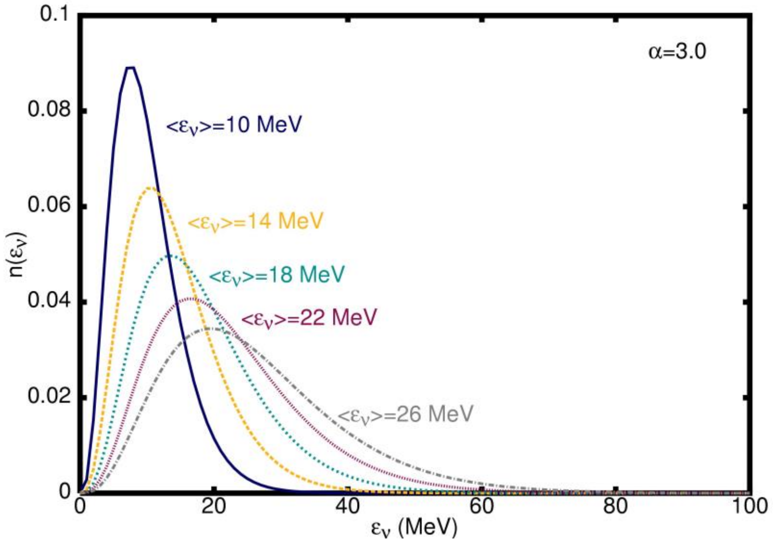

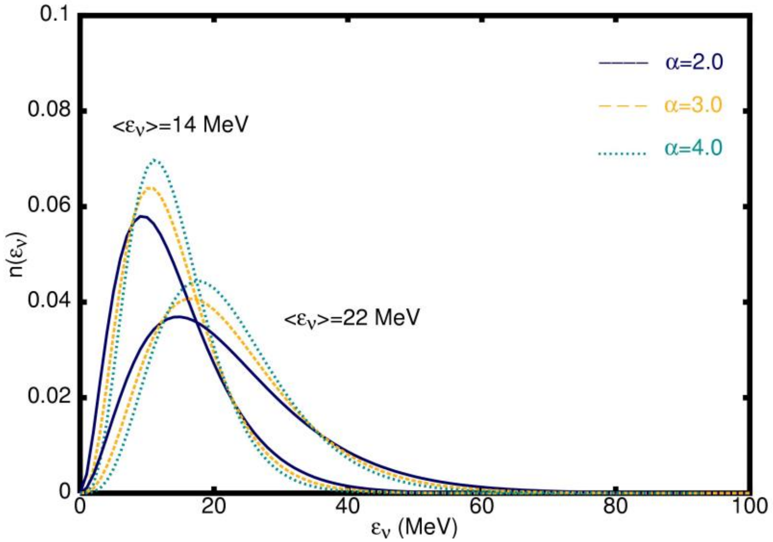

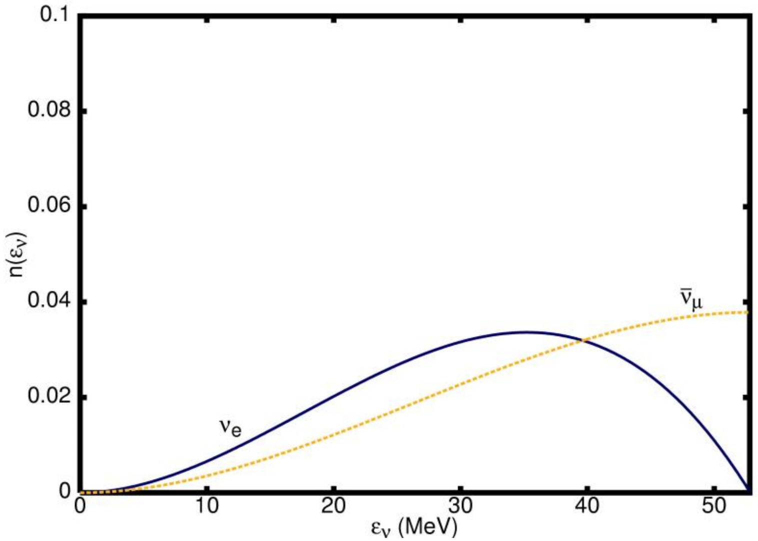

Michel spectra :

$$n(E_{\nu_e}) = \frac{96E_{\nu_e}^2}{m_\mu^4}(m_\mu - 2E_{\nu_e}),$$

$$n(E_{\bar{\nu}_\mu}) = \frac{32E_{\bar{\nu}_\mu}^2}{m_\mu^4}\left(\frac{3}{2}m_\mu - 2E_{\bar{\nu}_\mu}\right)$$

Supernovaneutrino cross sections

Folded cross sections supernova neutrino spectra :

→strong dependence on average energy of the spectrum

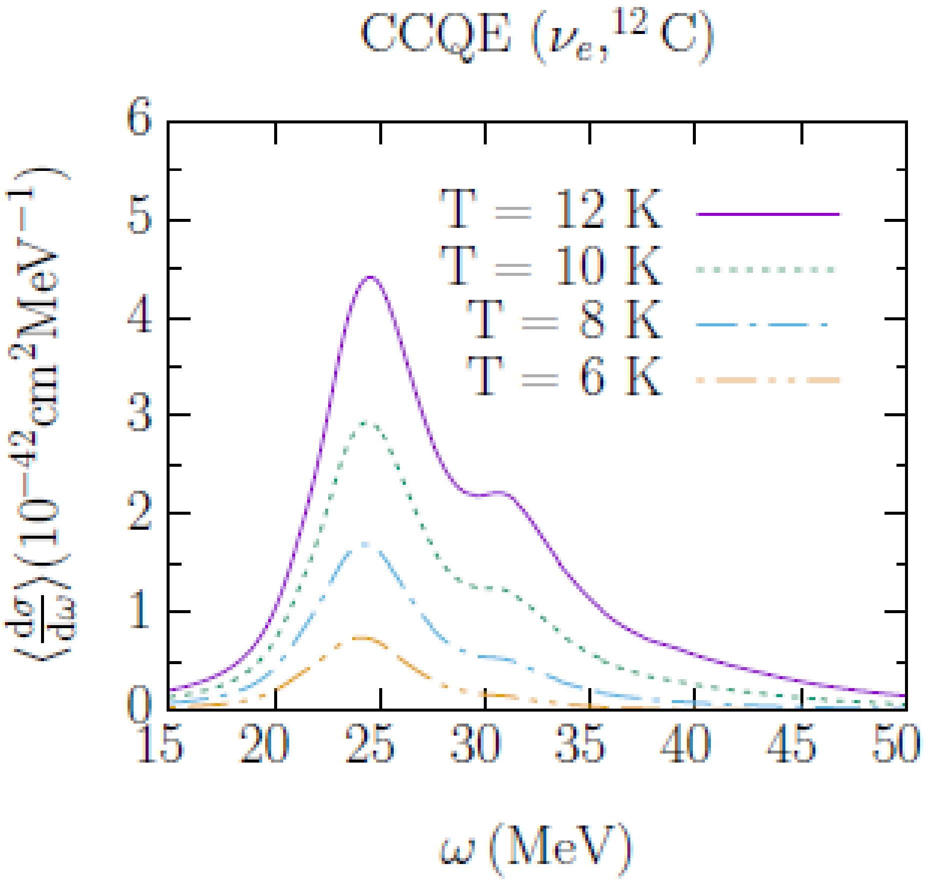

Supernovaneutrino cross sections

Cumulative folded cross sections:

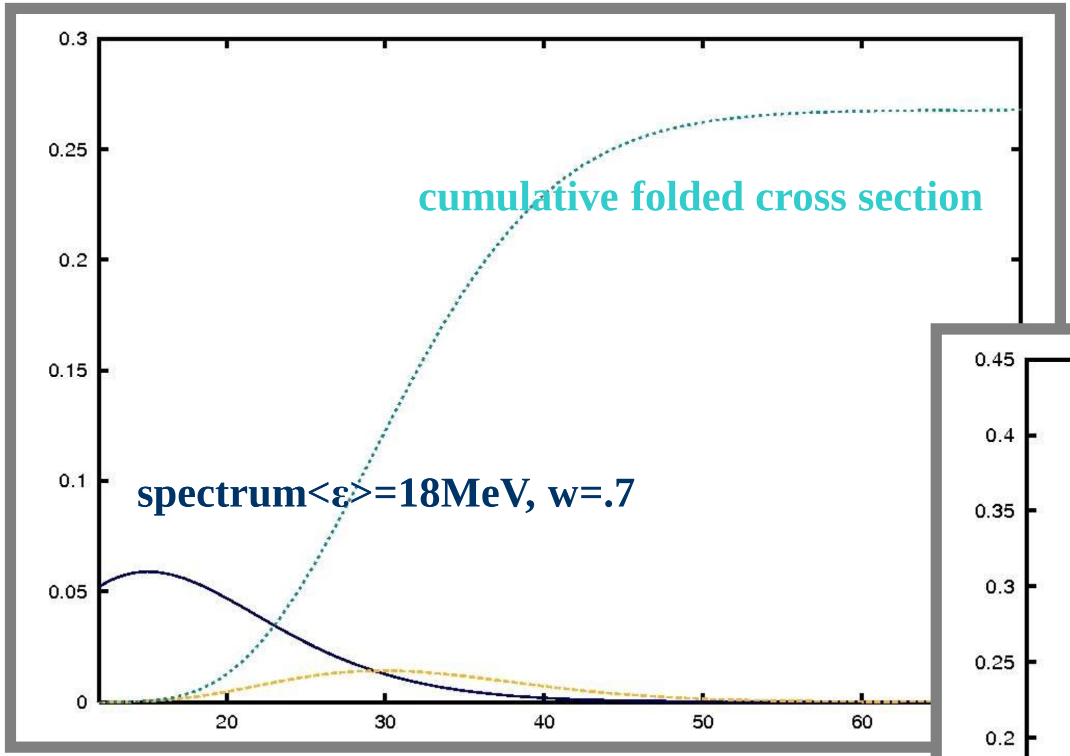

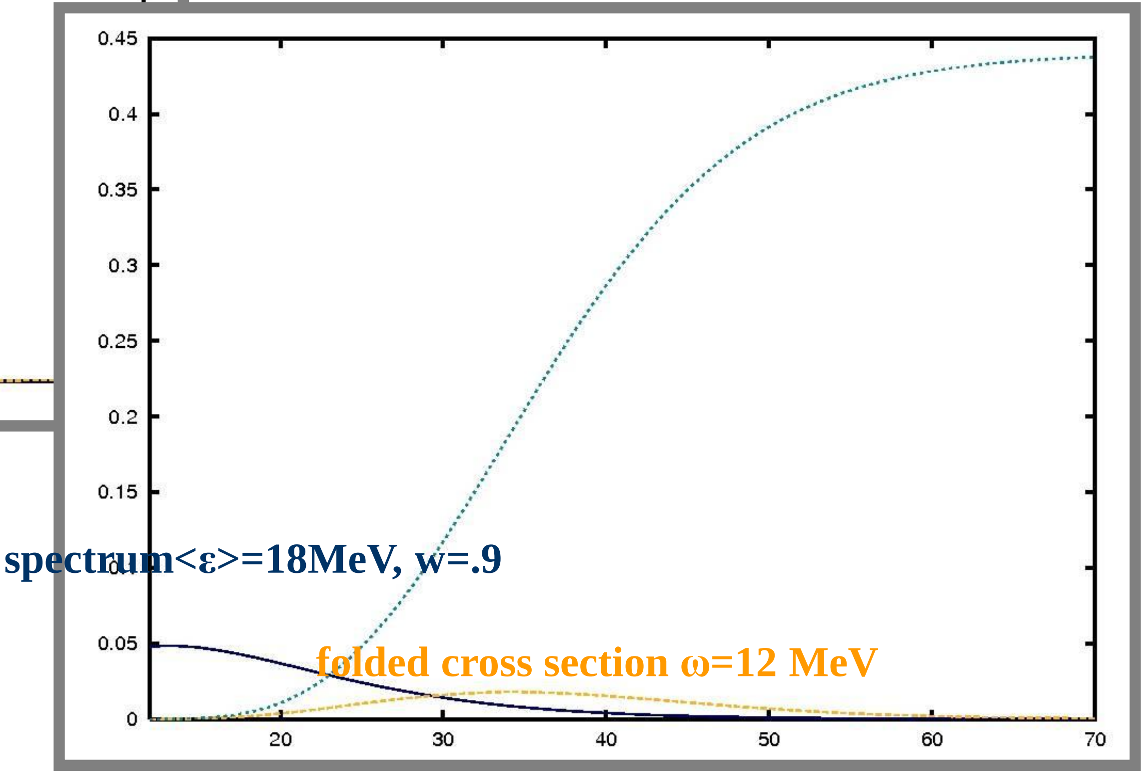

Monochromatic KDAR neutrinos @ 236 MeV

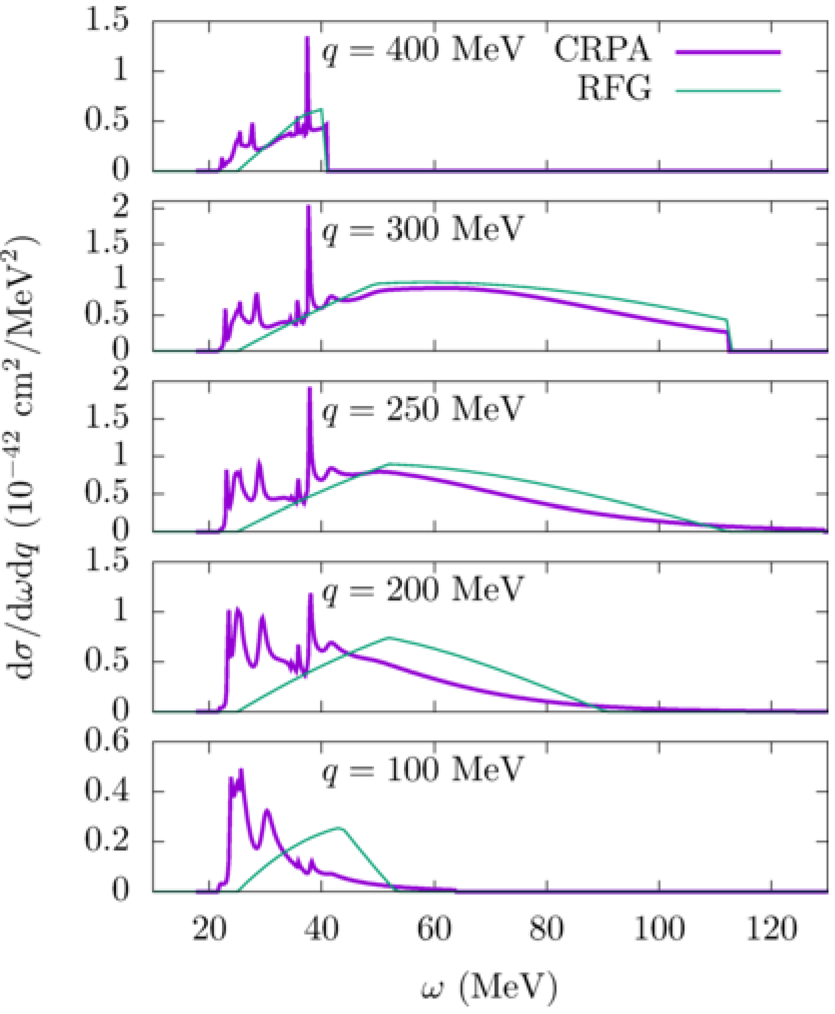

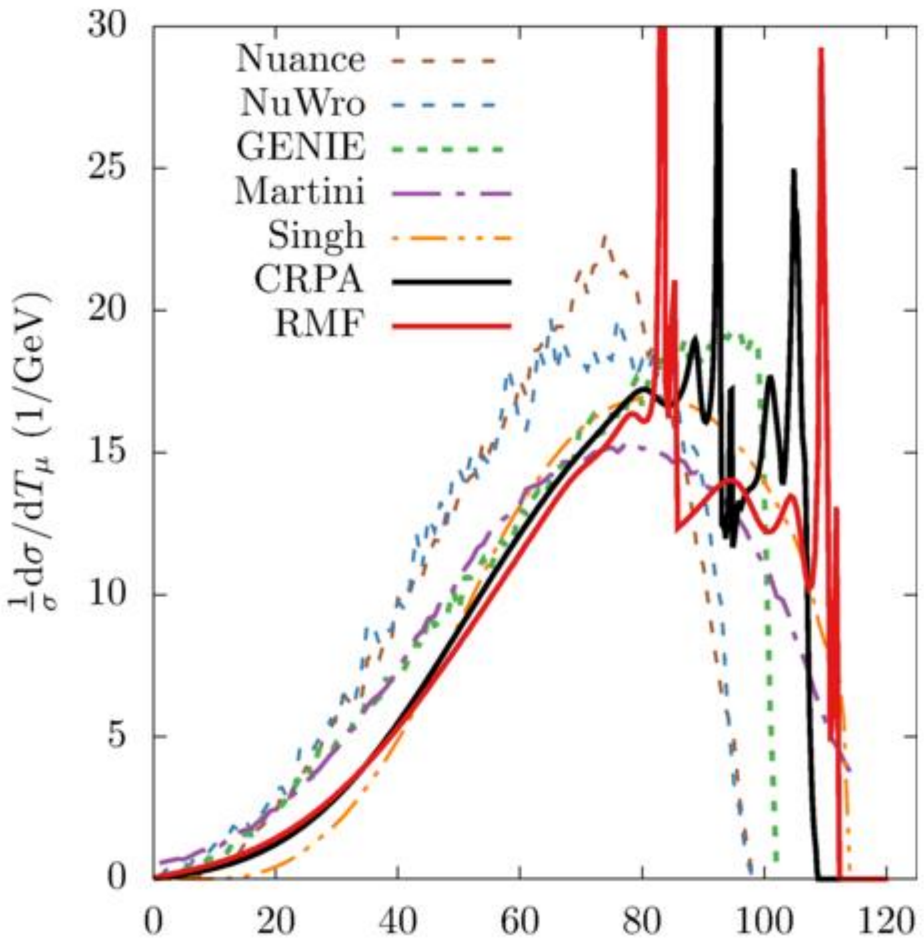

A. Nikolakopoulos, V. Spitz, V. Pandey, NJ, PRC103, 064603(2021)

Monochromatic KDAR neutrinos @ 236 MeV

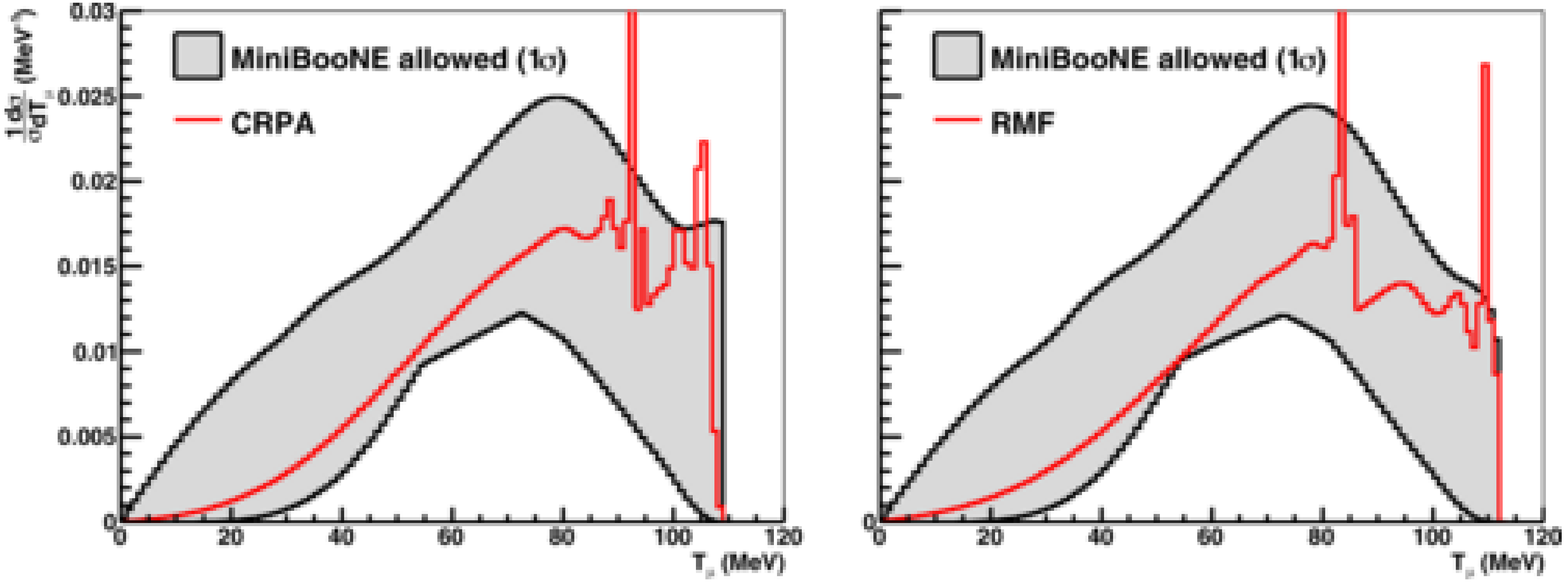

A. Nikolakopoulos, V. Spitz, V. Pandey, NJ, PRC103, 064603(2021)

Axial form factor

Axial form factor :

$$G_A(Q^2) = -\frac{(\tau_3 g_A - g_A^s)}{2} G(Q^2), \qquad g_A = 1.262$$

$$G(Q^2) = (1 + Q^2/M^2)^{-2}, \qquad M = 1.032$$

Q^2 dependence axial form factor :

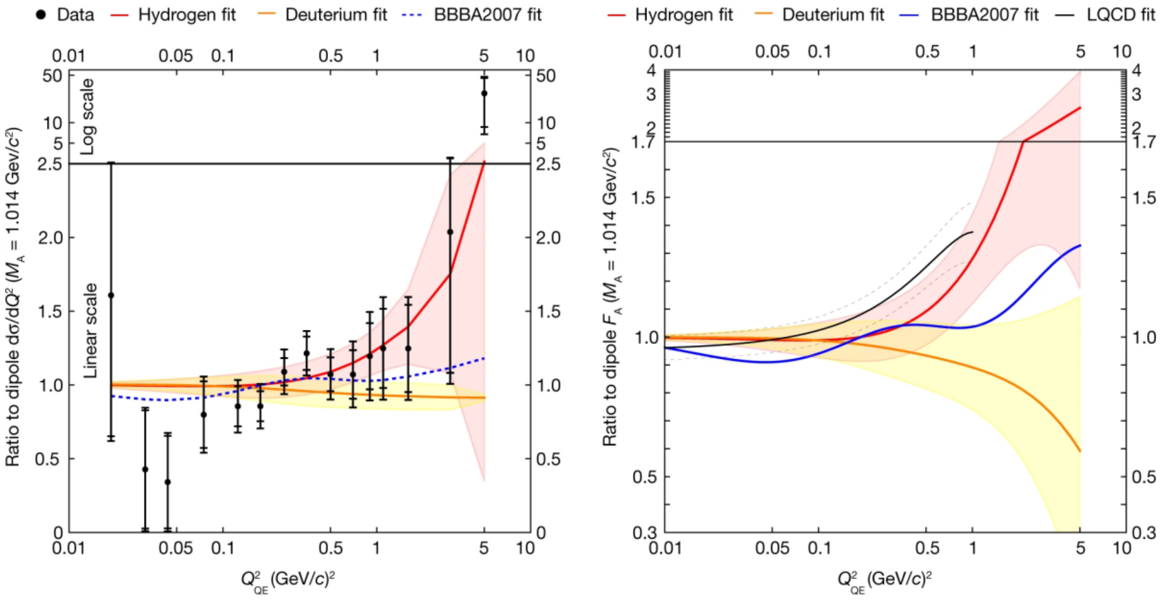

T. Cai et al, Nature 64 (2023)

Axial Form Factor

Axial form factor :

$$G_A(Q^2) = -\frac{(\tau_3 g_A - g_A^s)}{2} G(Q^2), \qquad g_A = 1.262$$

$$G(Q^2) = (1 + Q^2/M^2)^{-2}, \qquad M = 1.032$$

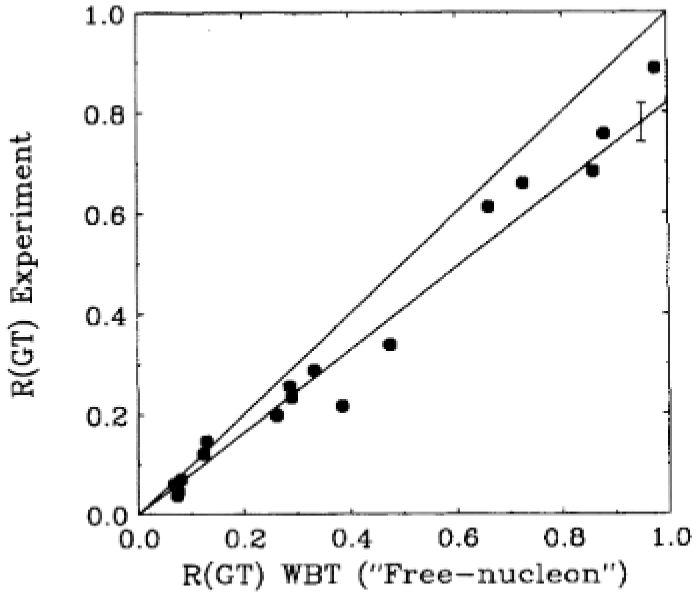

FIG. 1. Comparison of the experimental and "free nucleon" values of R(GT) for 16 0p-shell decays. A diagonal line passing through the (x,y) point (1,1) represents perfect agreement. The "best fit" line through the 16 points passes through (1,0.82). The error bar is the theoretical uncertainty Δ_{th} which is assumed independent of R(GT) and is discussed in the text.

Quenching

W.T. Chou, E.K. Warburton, B.A. Brown, PRC47,163 (1993)

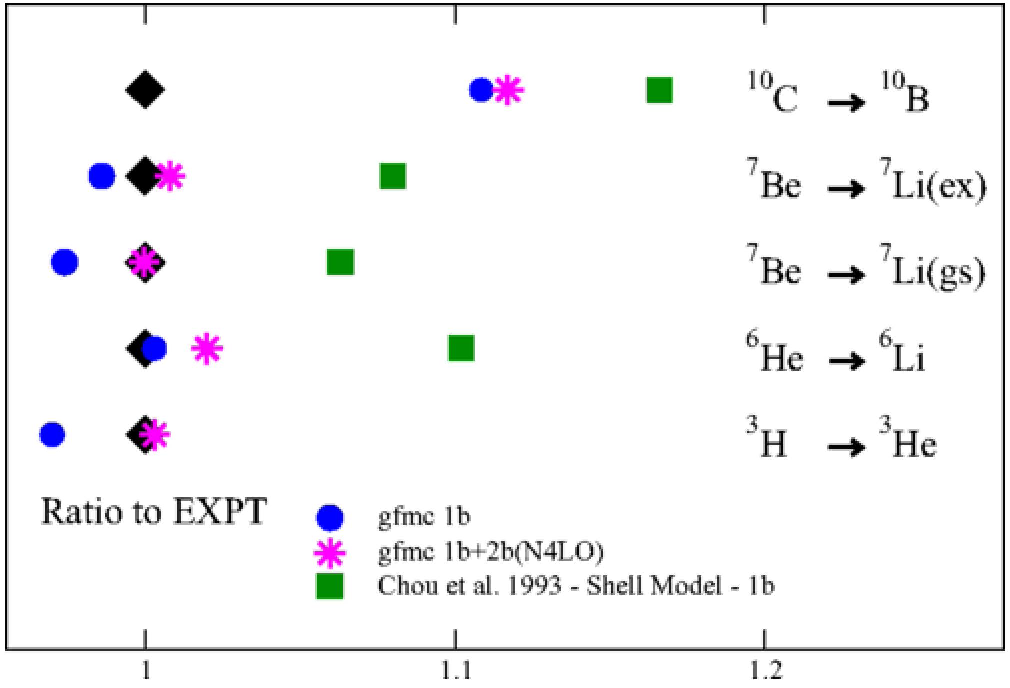

S. Pastore et al., PRC97,022501 (2018)

Strangeness

Axial form factor :

$$G_A(Q^2) = -\frac{(\tau_3 g_A - g_A^s)}{2} G(Q^2), \qquad g_A = 1.262$$

$$G(Q^2) = (1 + Q^2/M^2)^{-2}, \qquad M = 1.032$$

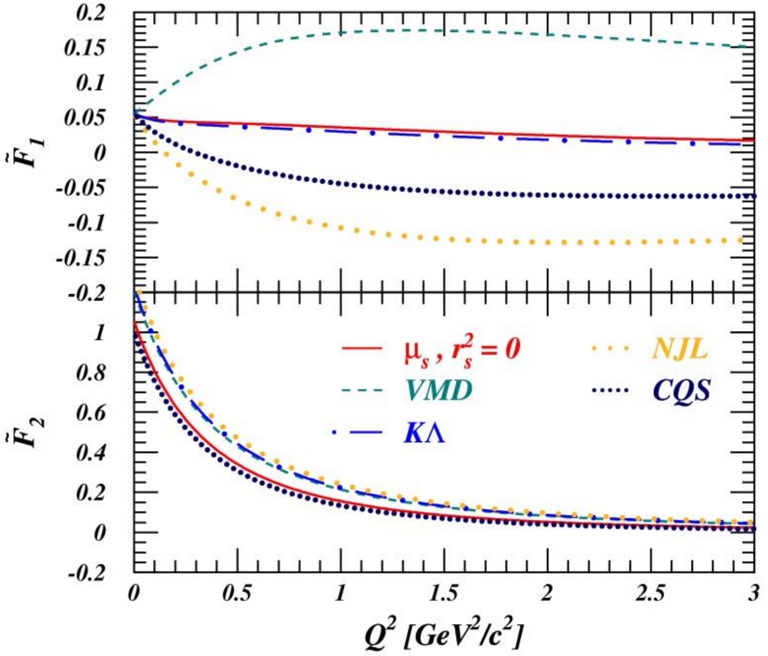

Model	$\mu_s(\mu_N)$	$r_s^2(\text{fm}^2)$
VMD	-0.31	0.16
$K\Lambda$	-0.35	-0.007
NJL	-0.45	-0.17
CQS (K)	0.115	-0.095

Weak vector form factors :

$$F_1^s = \frac{1}{6} \frac{-r_s^2 Q^2}{(1 + Q^2/M_1^2)^2}, \qquad M_1 = 1.3$$

$$F_2^s = \frac{\mu_s}{(1 + Q^2/M_2^2)^2}, \qquad M_2 = 1.26$$

T Cai et a;. Nature 614, 48

Parity violating electron scattering

Using polarized electrons, one gets access to parity violating electron scattering (HAPPEX, G0, SAMPLE, A4)

- Axial-vector interference terms
- Information about axial vector form factor
- Information about strangeness in the nucleon in the vector as well as axial sector
- Larger cross sections
- Prone to radiative corrections

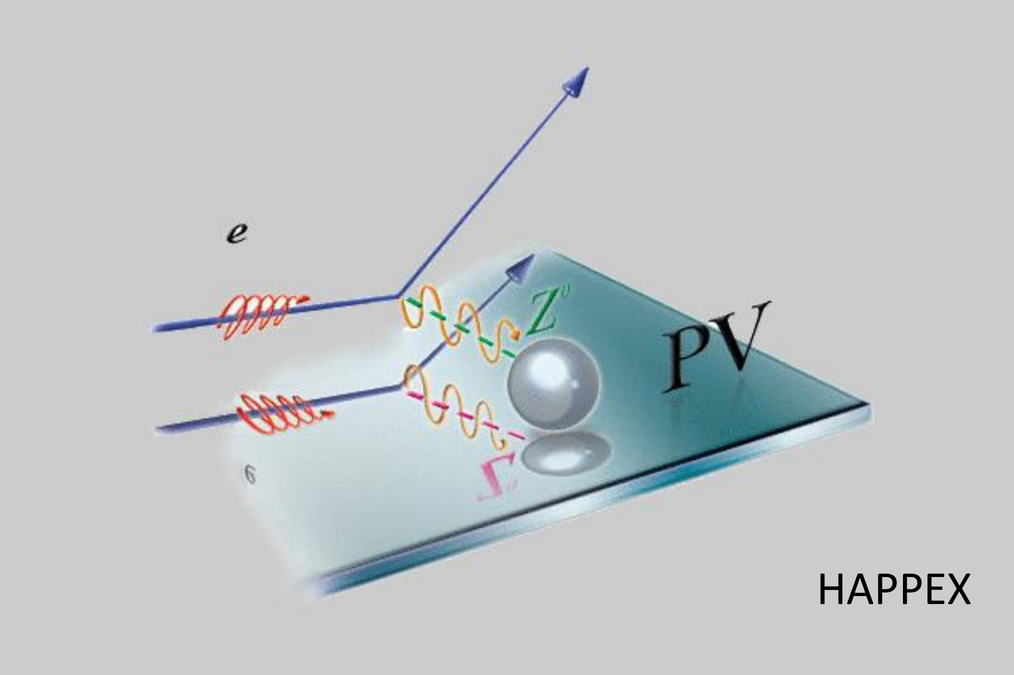

Parity violating asymmetry :

$$A^{PV} = \frac{d\sigma_R - d\sigma_L}{d\sigma_R + d\sigma_L}$$

Strangeness

Traditionally :

- strangeness contribution to the ***weak vector formfactors*** : Parity Violating Electron Scattering (Sample, HAPPEX, G0, …)

- strangeness contribution to the ***axial current*** : neutrino scattering

  -vector current contributions are suppressed

  -no radiative corrections

Strangeness

Traditionally :

- strangeness contribution to the ***weak vector formfactors*** : Parity Violating Electron Scattering (Sample, HAPPEX, G0, …)

Correlated !

- strangeness contribution to the ***axial current*** : neutrino scattering

-vector current contributions are suppressed

-no radiative corrections

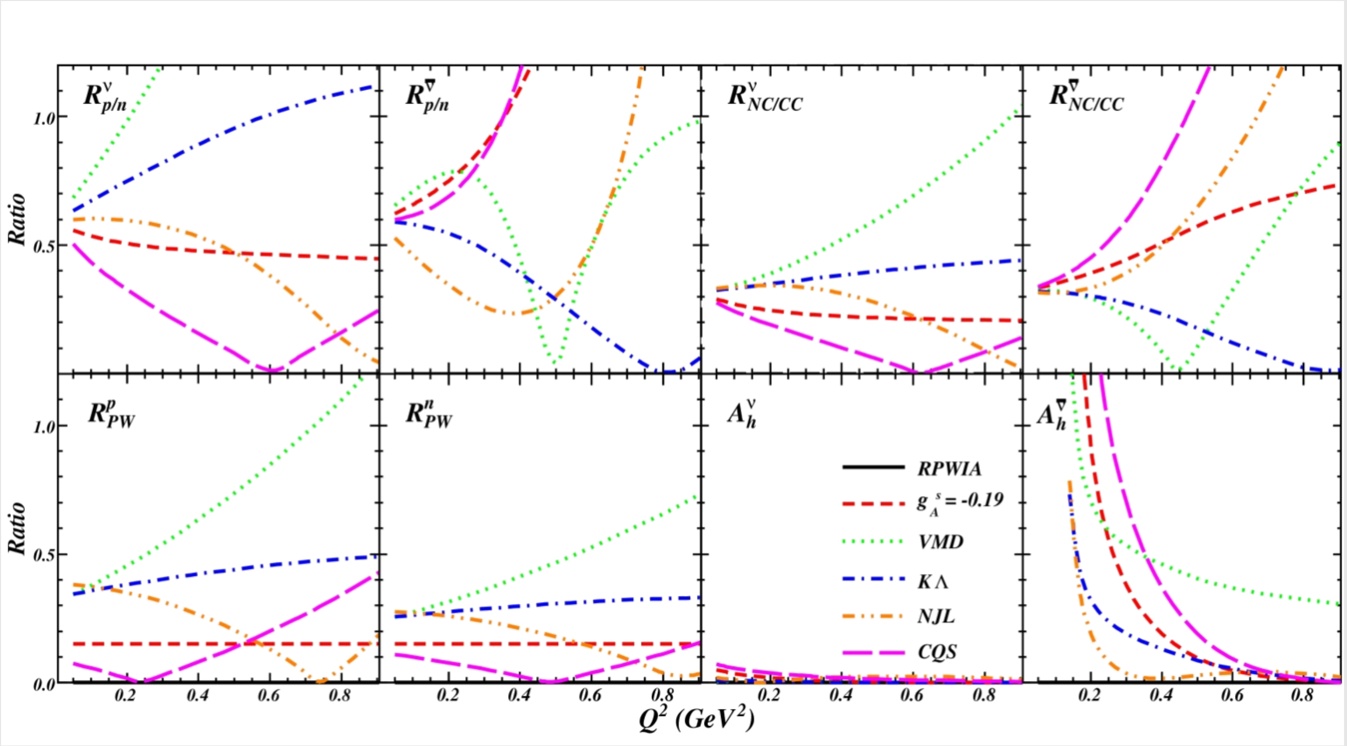

N.J., P. Vancraeyveld, P. Lava, J. Ryckebusch, PRC76, 055501 (2007).

Influence of strangeness on neutrino cross sections

- Generally : net strangeness effect vanishes for isoscalar targets
- close to particle knockout threshold the influence becomes larger due to binding energy differences between protons and neutrons
- differential cross sections differ, energy of reaction products can be very different

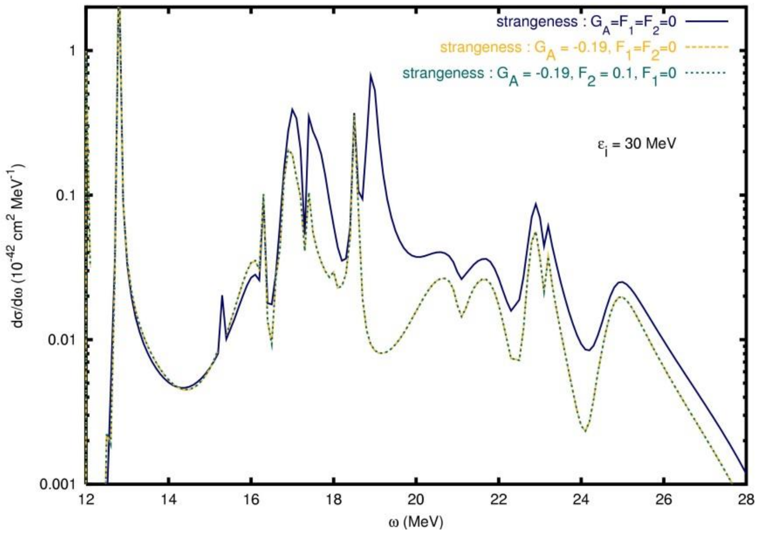

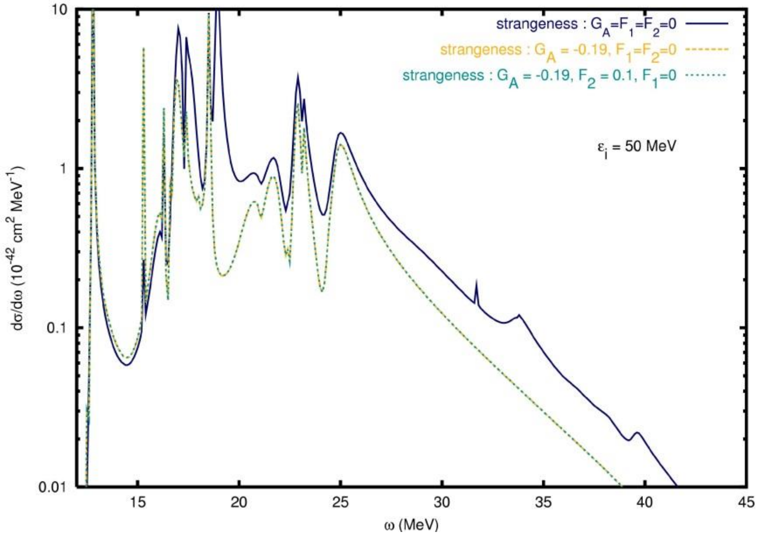

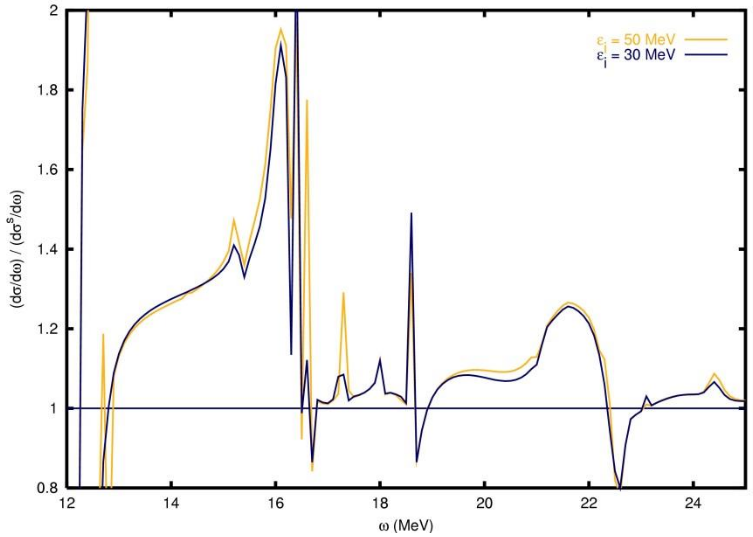

Influence of strangeness on p/n neutrino cross sections

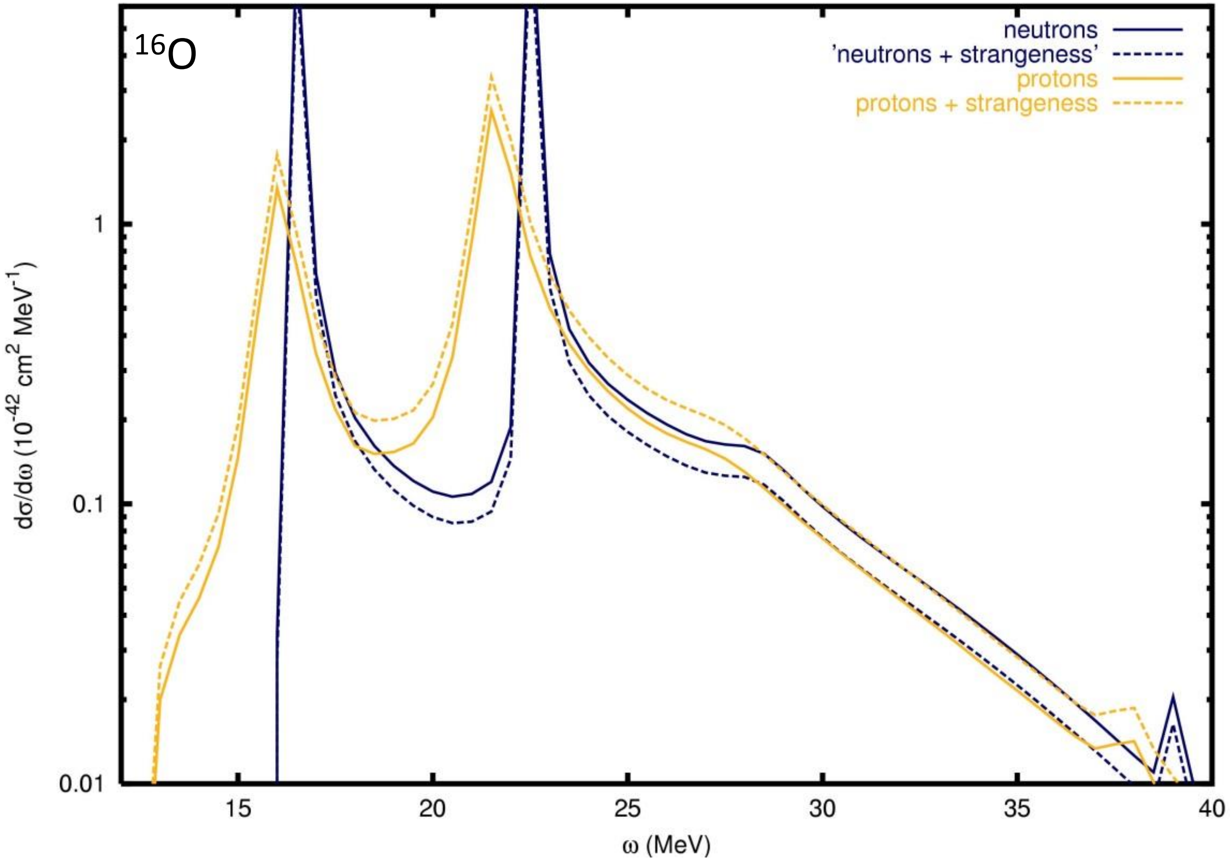

- differences up to 20%
- opposite effect for protons and neutrons

Electron vs muon neutrino CC cross sections

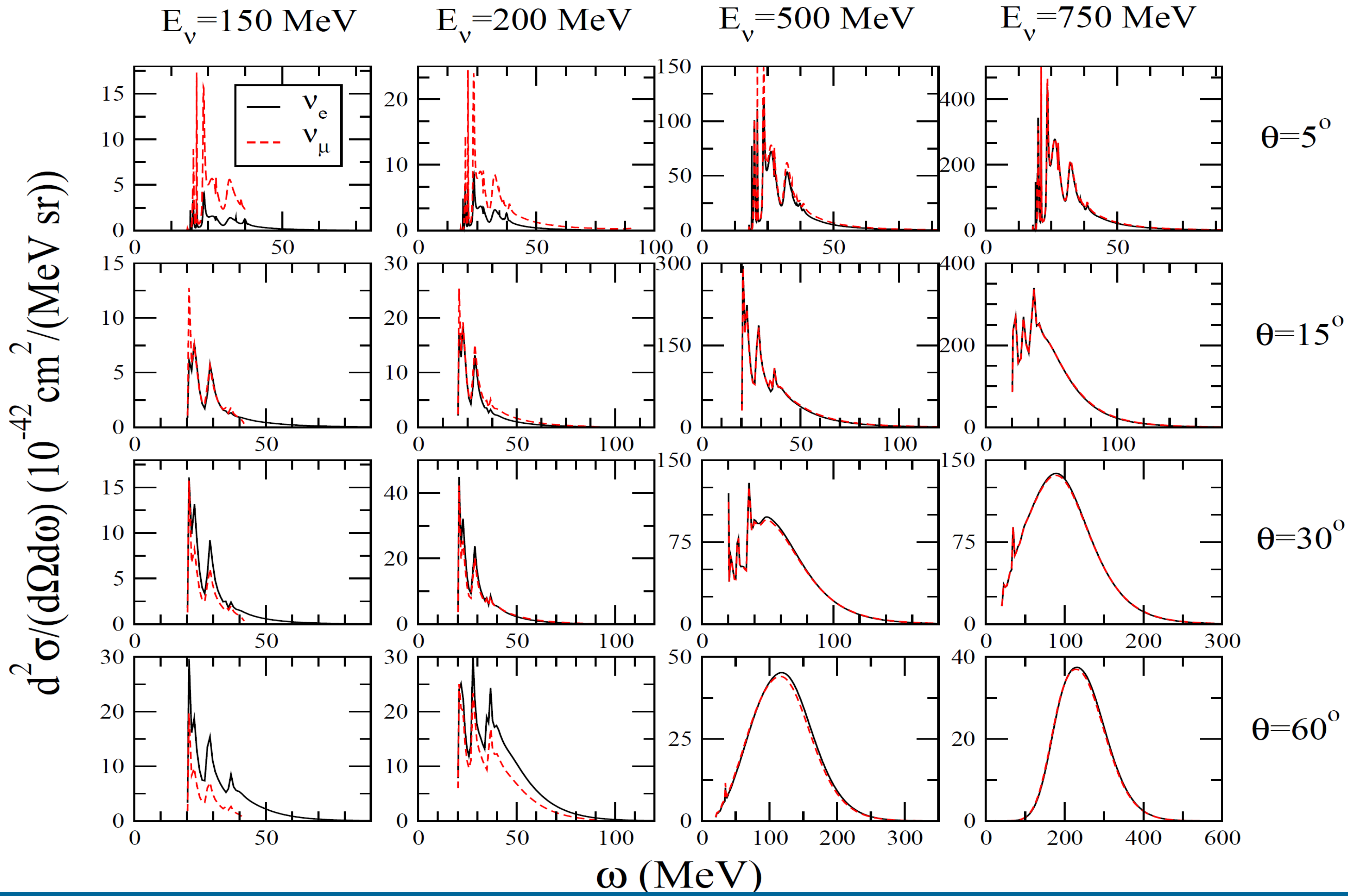

Electron vs muon neutrino CC cross sections

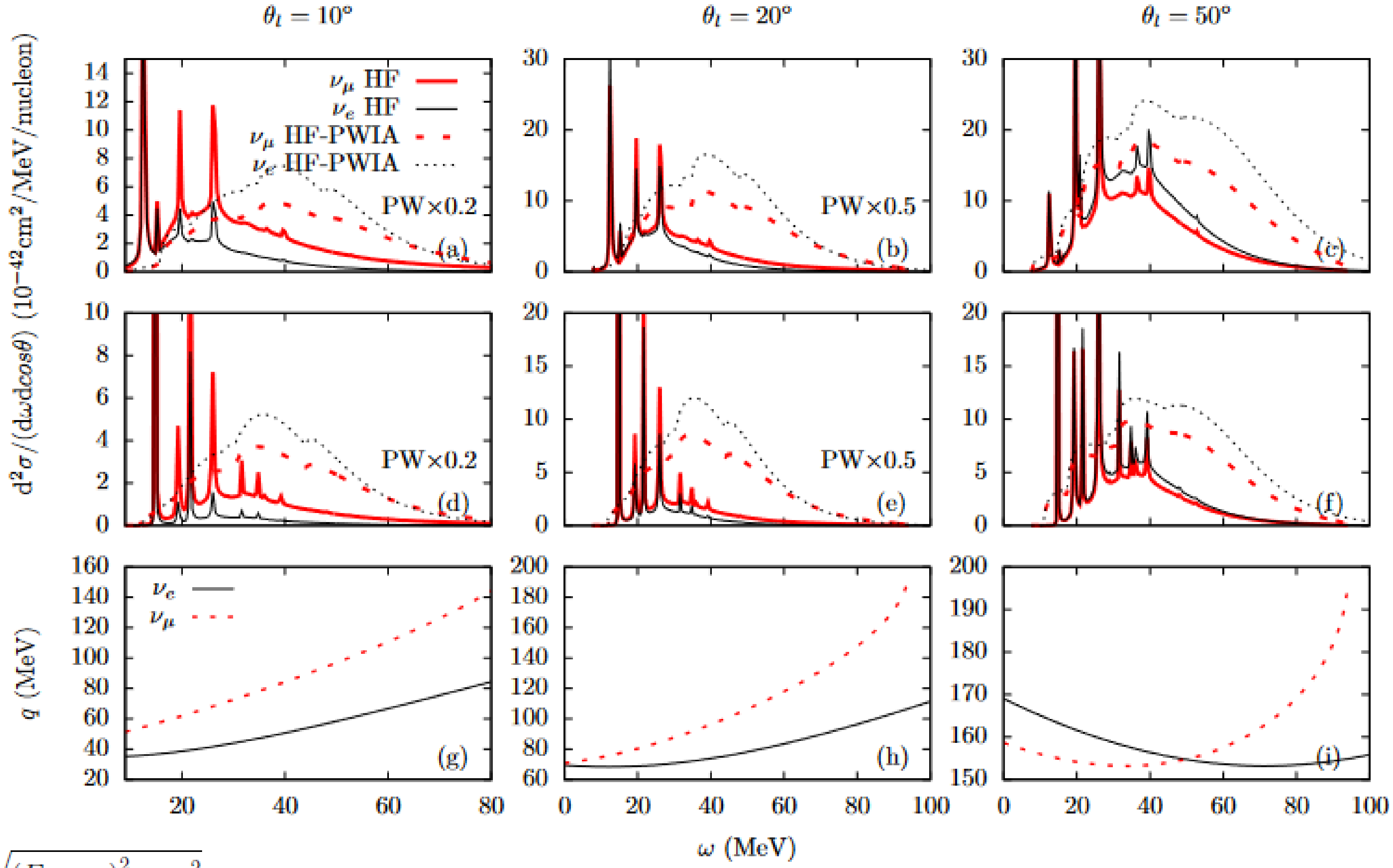

$$q = \sqrt{E_\nu^2 + P_l^2 - 2\cos\theta_l E_\nu P_l} \approx E_\nu - \sqrt{(E_\nu - \omega)^2 - m_l^2}.$$

A. Nikolakopoulos, N.J, N. Van Dessel, K. Niewczas, R. Gonzalez-Jimenez, J.M. Udias, V. Pandey, Phys. Rev. Lett. 123, 052501 (2019)

Coherent Scattering

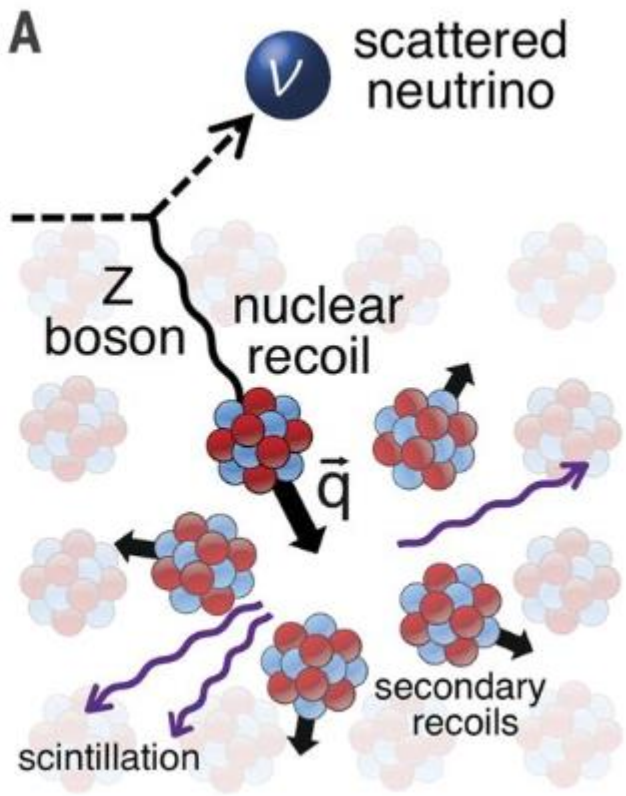

Science, September 2017 : **The First Observation of Coherent Elastic Neutrino Nucleus Scattering**

Coherent Scattering

Coherent cross section as a function of nuclear recoil energy :

$$\frac{d\sigma}{dT} = \frac{G_F^2}{\pi} M_A \left(1 - \frac{T}{E_i} - \frac{M_A T}{2E_i^2}\right) \frac{Q_W^2}{4} F_W^2(Q^2),$$

Mainly sensitive to neutron distributions

$$F(Q^2) = \frac{4\pi}{Q_W} \int \left((1 - 4\sin^2\theta_W)\rho_p(r) - \rho_n(r)\right) \frac{\sin(qr)}{qr} r^2 dr,$$

$$F_W(Q^2) = \frac{1}{Q_W} \left[(1 - 4\sin^2\theta_W)\, f_p(\vec{q}) F_p(Q^2) \;\; - f_n(\vec{q}) F_n(Q^2)\right]$$

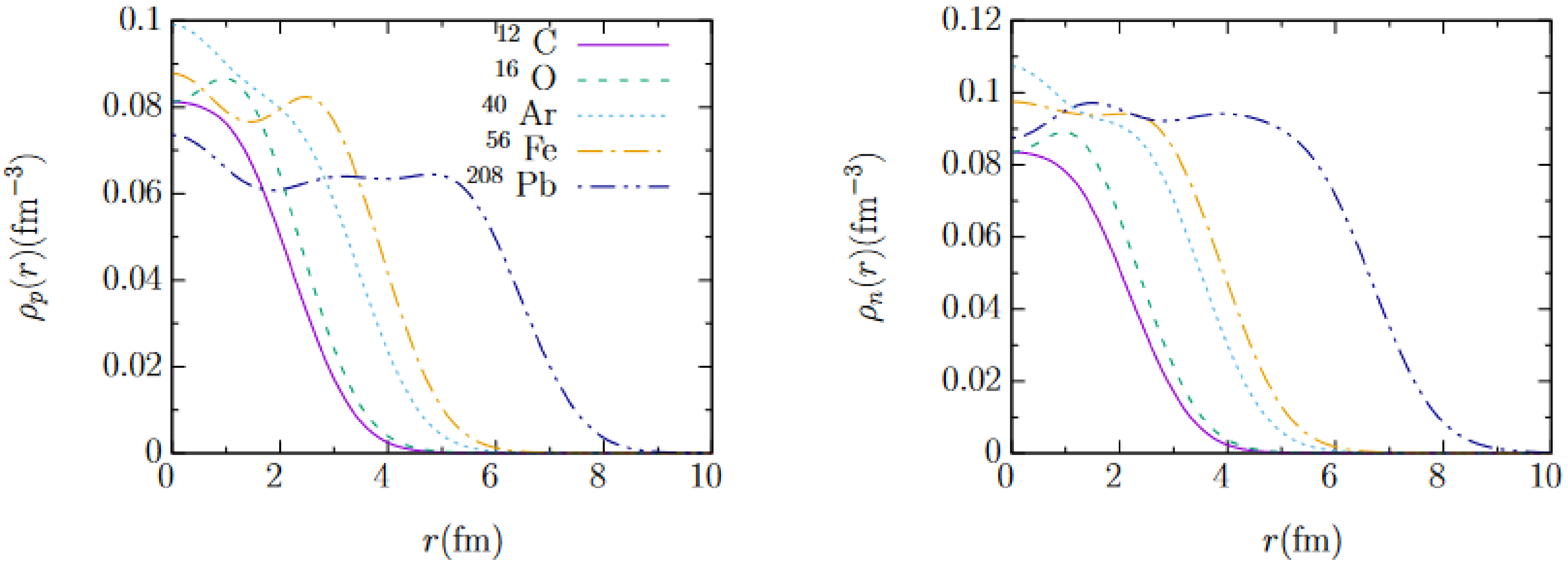

Coherent Scattering

Weak form factor : Model comparison

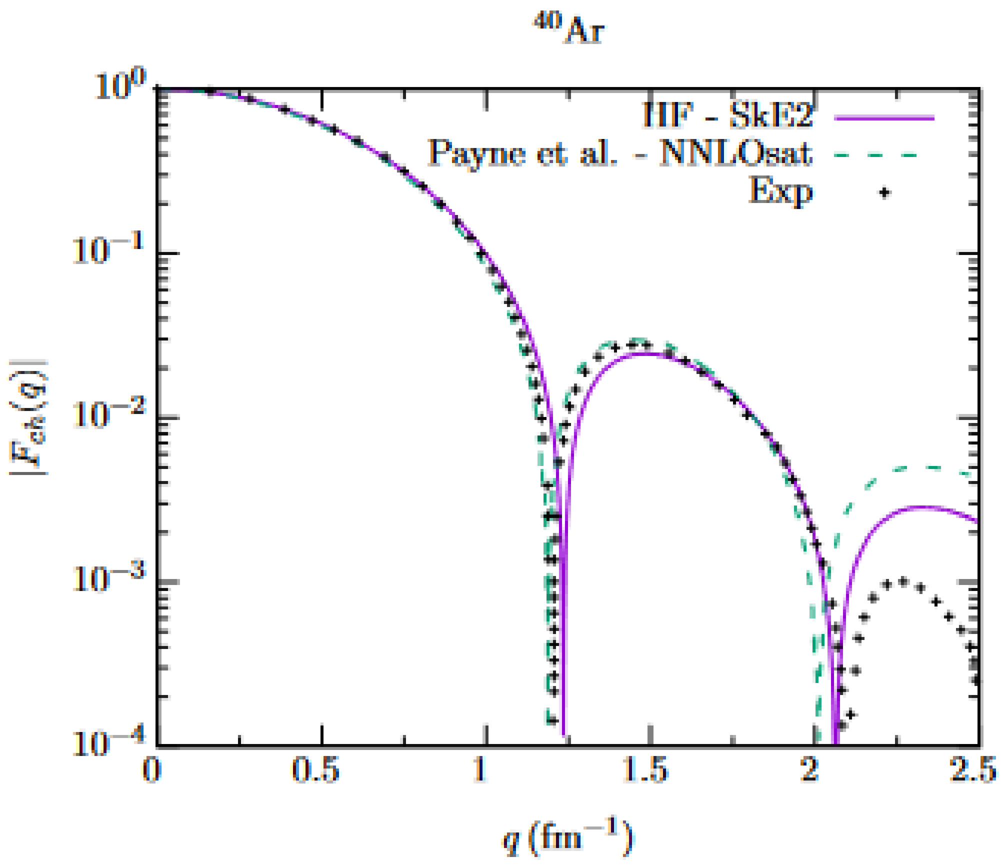

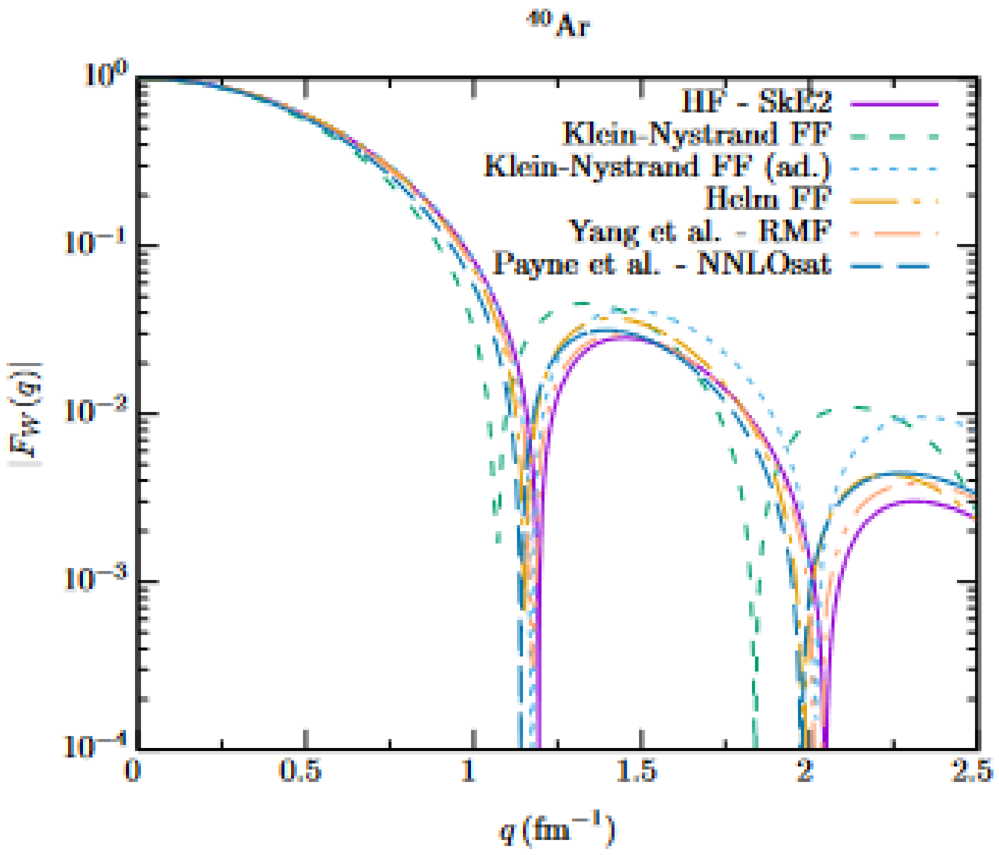

N. Van Dessel, V. Pandey, NJ, Universe 9, 5 (2023)

Coherent Scattering

Weak form factor : Model comparison

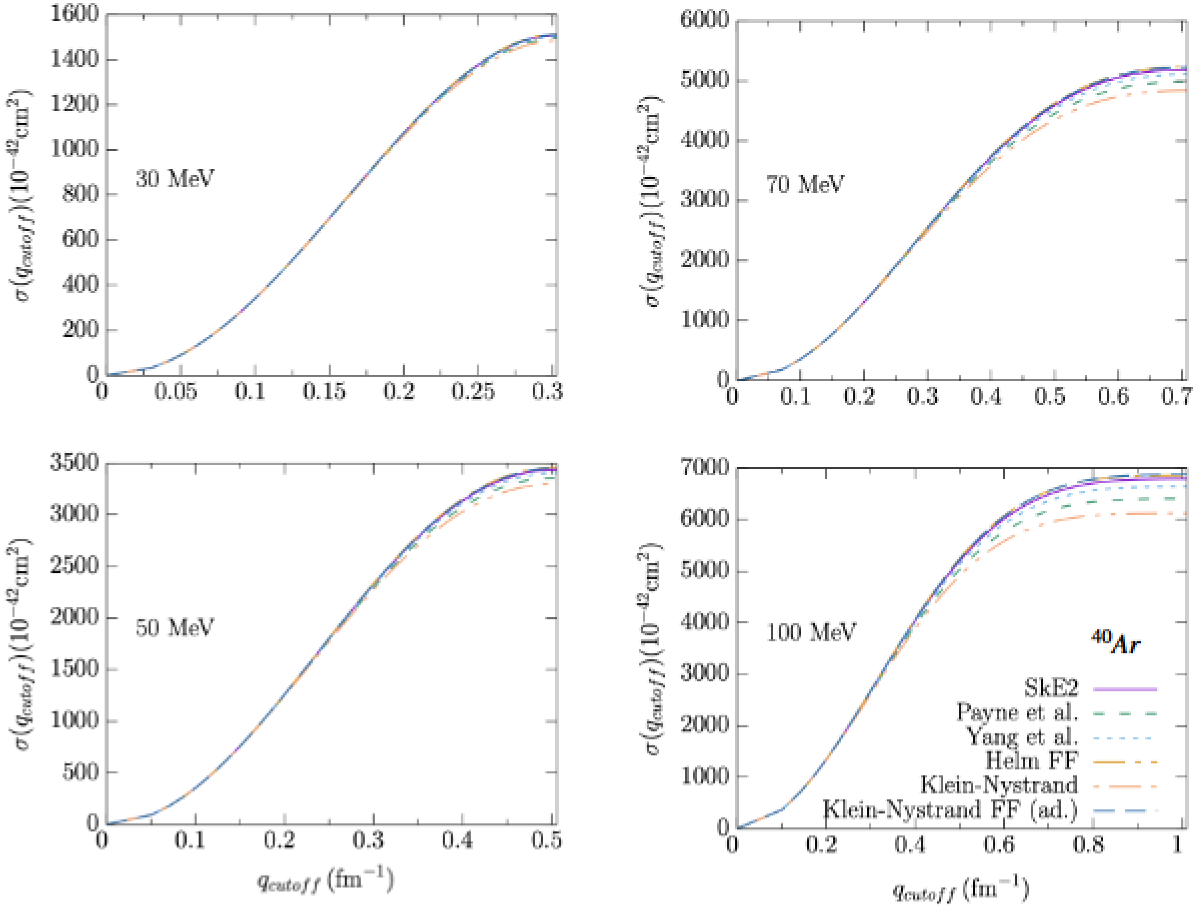

Coherent Scattering

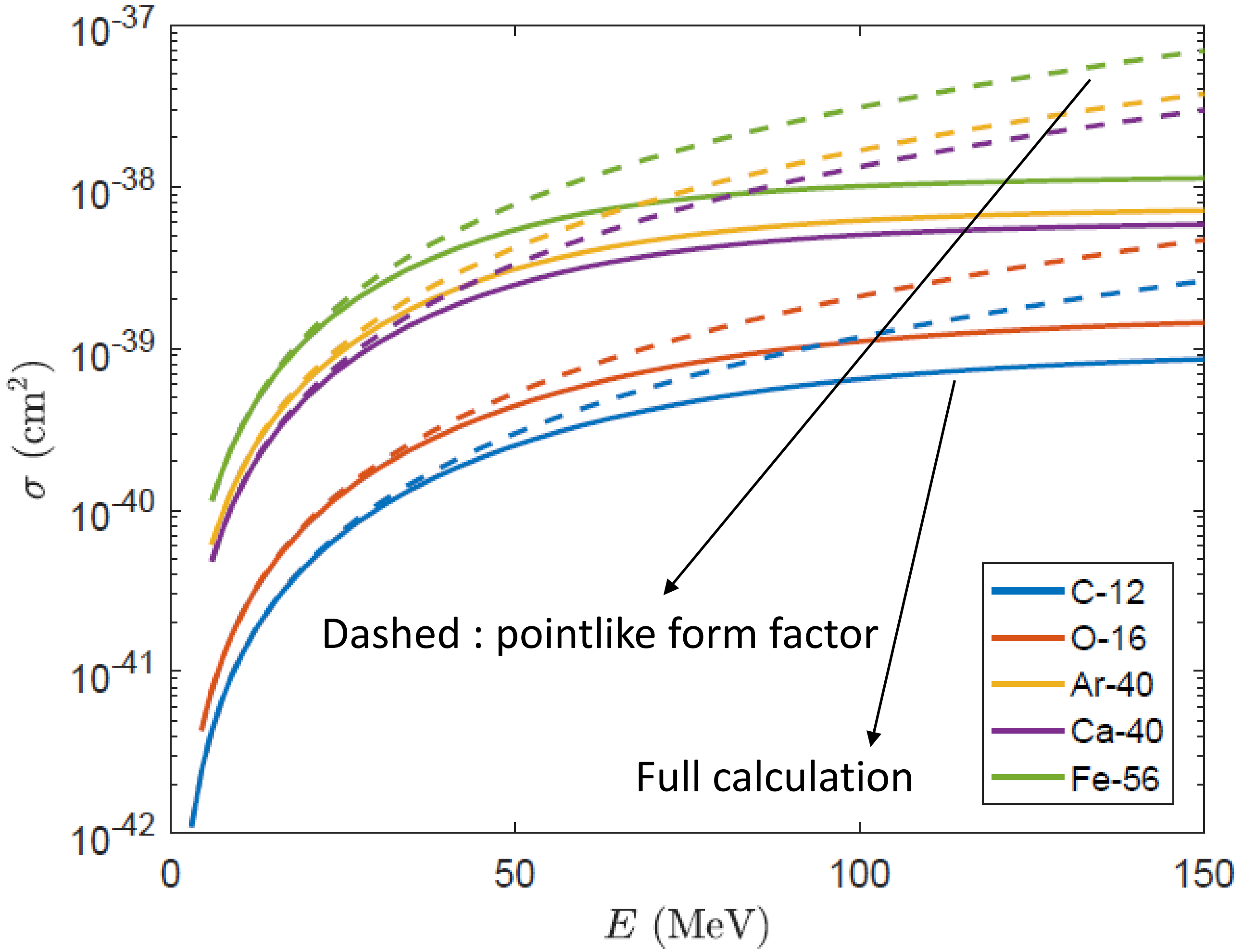

Coherent Scattering

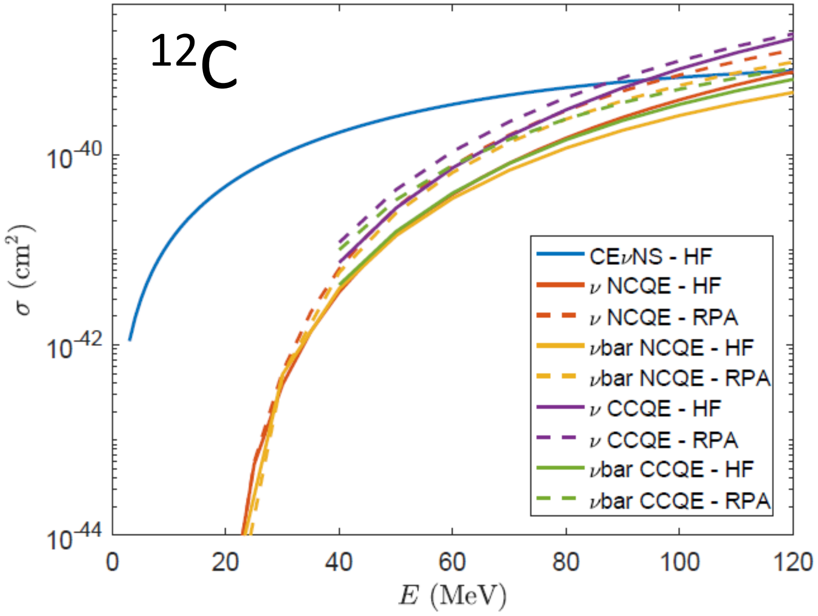

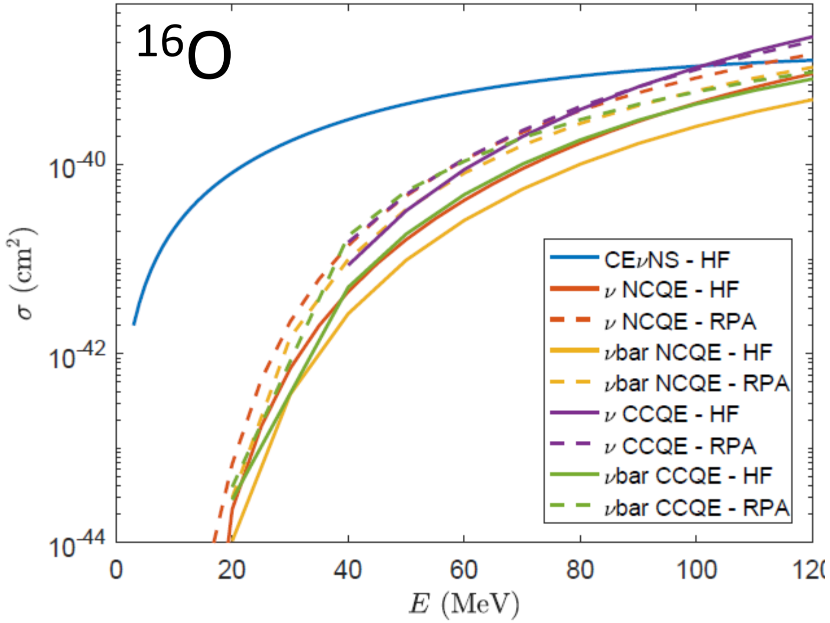

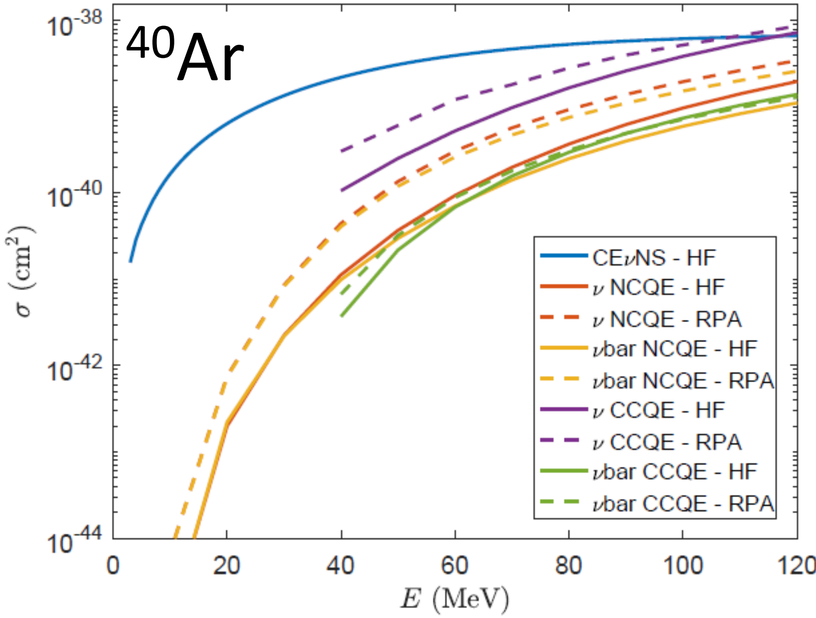

- Strong mass dependence of coherent cross section
- Coherent process stronger than inelastic over a large kinematic range

Summary & Outlook

Neutrino-nucleus scattering at low energies provides a very rich source of information about the weak interaction and nuclear structure effects, of interest for weak particle, nuclear as well as astrophysics !